

CHEAPER AND MORE DURABLE PROTON
EXCHANGE MEMBRANE

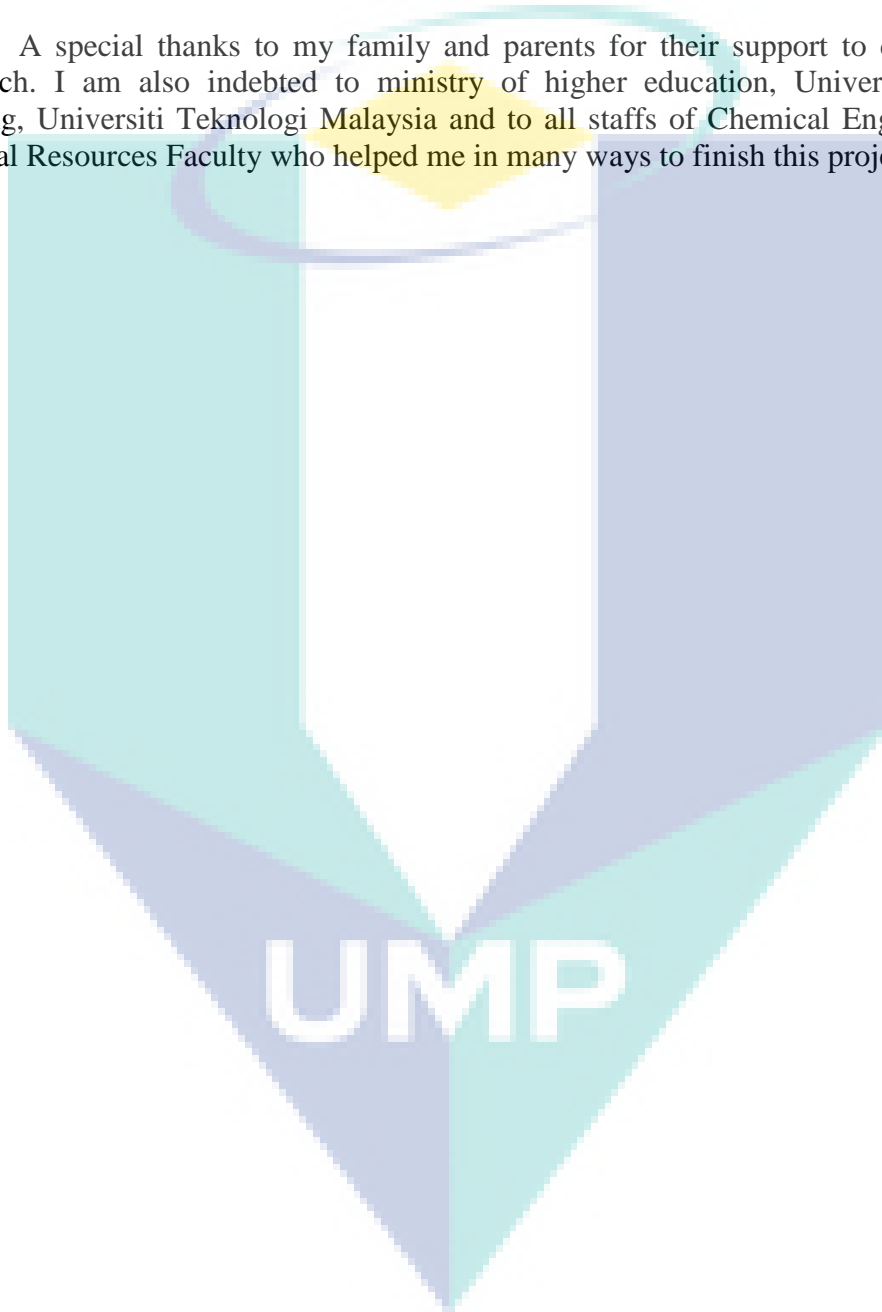


UNIVERSITI MALAYSIA PAHANG

ACKNOWLEDGEMENTS

I would like to express my gratitude to Prof. Dr. Arshad Ahmad who give me the chance to be part of the LRGS team member. My special appreciation and thanks to my Master student, Umarul Imran Amran for his effort and contribution throughout the duration of this research grant.

A special thanks to my family and parents for their support to complete this research. I am also indebted to ministry of higher education, Universiti Malaysia Pahang, Universiti Teknologi Malaysia and to all staffs of Chemical Engineering and Natural Resources Faculty who helped me in many ways to finish this project.



ABSTRAK

Permintaan bahan api fosil semakin meningkat dari tahun ke tahun tetapi sumber bahan api fosil berkurangan. Pada masa kini, para penyelidik cuba mencari sumber alternatif baru bagi mengurangkan kebergantungan terhadap bahan api fosil. Hidrogen merupakan salah satu bahan api alternatif yang menarik untuk dikaji. Tujuan kajian ini adalah untuk menilai terhadap kesan alam sekitar dan ekonomi bagi dua laluan proses penghasilan hidrogen iaitu metana (Kes1) dan etanol (Kes 2). Proses simulasi telah dijalankan dalam kajian ini dengan menggunakan perisian Aspen Plus versi 8.6. Reaksi stim reformasi metana dan etanol disimulasi berasaskan kepada tindakbalas kinetik. Data kinetik telah diperolehi melalui kajian literatur. Tindakbalas dilakukan dalam perisian Aspen Plus dengan menggunakan blok RPlug dengan menyusun kembali model kinetik Langmuir-Hinselwood-Watson (LHHW) dan model kinetik *power-law*. Pada masa yang sama, penulenan bagi hidrogen turut menggunakan kaedah simulasi. Pengesahsahihan data telah menunjukkan keputusan yang hampir sama dalam literatur. Selain itu juga, analisis sensitiviti juga telah dijalankan untuk melihat kesan beberapa parameter seperti suhu, tekanan, berat pemangkin dan nisbah masukan ke dalam rektor untuk kedua-dua kajian kes. Selepas itu, penilaian terhadap alam sekitar dan ekonomi telah dibuat. Data yang diperolehi telah digunakan untuk membuat perbandingan antara kedua-dua kajian kes. Penilaian kitaran hayat (LCA) telah digunakan dalam kajian ini untuk menilai kesan alam sekitar menggunakan perisian GaBi menggunakan kaedah ReCiPe untuk menilai impak alam sekitar bagi semua proses yang terlibat dalam kajian ini. Unit berfungsi bagi LCA dalam kajian ini adalah 1 kg untuk hidrogen. Secara keseluruhannya, 16 kategori impak telah dikaji dan hanya 3 menunjukkan kategori yang banyak memberi impak iaitu perubahan iklim, pengurangan fosil dan pengurangan air. Perbebasan gas rumah hijau tinggi untuk kes 2 iaitu 30.84 kg CO₂ eq. berbanding dengan kes 1 iaitu 9.44 kg CO₂ eq. Manakala, pengurangan fosil tinggi kes 2 iaitu 12.54 kg oil eq. berbanding kes 1 sebanyak 4.044 kg oil eq. Kes 2 juga menyebabkan penyusutan sumber air yang tinggi sebanyak 23.35 m³ eq berbanding kes 1 sebanyak 4.01 m³ eq. Penilaian ekonomi terhadap kedua-dua kajian kes telah dibuat. Kos modal untuk penghasilan hidrogen bagi kes 1 adalah kurang berbanding dengan kes 2 dengan perbezaan 7.92%. Manakala, kos utiliti untuk kes 1 lebih rendah berbanding kes 2 dengan perbezaan sebanyak 12.81%. Secara keseluruhannya, kes 1 iaitu hidrogen daripada metana adalah lebih mesra alam dan lebih jimat dalam kos CAPEX dan OPEX berbanding kes 2 walaupun daripada sumber tenaga yang boleh diperbaharui iaitu etanol.

ABSTRACT

The demand for fossil fuel increased year by year but the sources of fossil fuel is decreasing. Nowadays, researchers are looking at alternative energy sources to reduce the dependency on fossil fuel. Hydrogen is an interesting energy source alternative to be studied. The aim of this study is to perform environmental and economic assessment for two hydrogen production pathways namely from methane (Case 1) and ethanol (Case 2). Rigorous simulation of both processes was done using Aspen Plus version 8.6. The reaction of steam reforming from methane and ethanol were kinetic based simulation. The kinetic data was obtained from the literature. The reactions were modelled using RPlug blocks with rearranged Langmuir-Hinselwood-Hougen-Watson (LHHW) kinetic model and power law kinetic model. The purification of hydrogen was based on rigorous model in the simulation. The validation results show good agreement with results found in the literature. In addition, sensitivity analysis was carried out observing the effect of several parameters such as temperature, pressure, catalyst weight and feed ratio to the reactor performance for both cases. After that, environment and economic assessment were performed. The data obtained were used for comparison purposes. The environment assessment was based on life cycle assessment (LCA) to evaluate the environmental impact of all processes involved in hydrogen production using GaBi software based on ReCiPe method. The LCA functional unit used for both case studies was 1 kg of hydrogen. Overall, 16 categories impact assessment were carried out and only three were highly significant namely climate change, fossil depletion and water depletion. Case 2 shows high impact on climate change with 30.84 kg CO₂ eq compared to Case 1 with 9.44 kg CO₂ eq. On the other hand, Case 2 shows higher fossil fuel resource depletion with 12.54 kg oil eq compared to Case 1 with 4.044 kg oil eq. Furthermore, Case 2 also has a higher water resources depletion of 23.35 m³ eq. compared to Case 1 which is only 4.01 m³ eq. The capital cost for Case 1 is 7.92% less compared to Case 2. Meanwhile, the total utilities cost for Case 1 is 12.81% less compared to Case 2. In conclusion, the hydrogen production from methane, Case 1, is environmental friendlier and less costing in term of CAPEX and OPEX than Case 2.

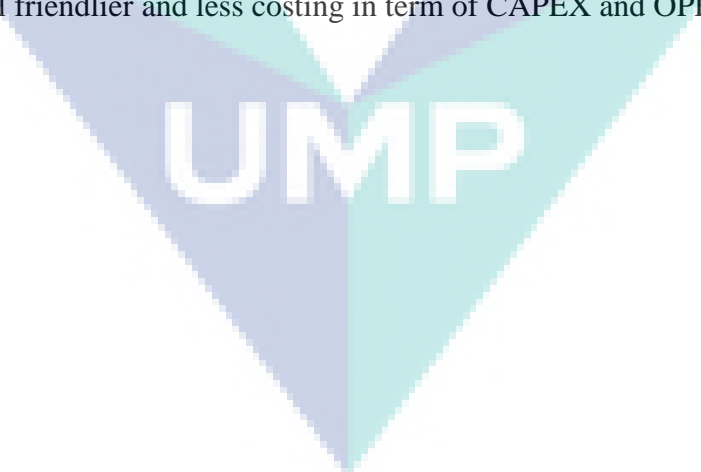
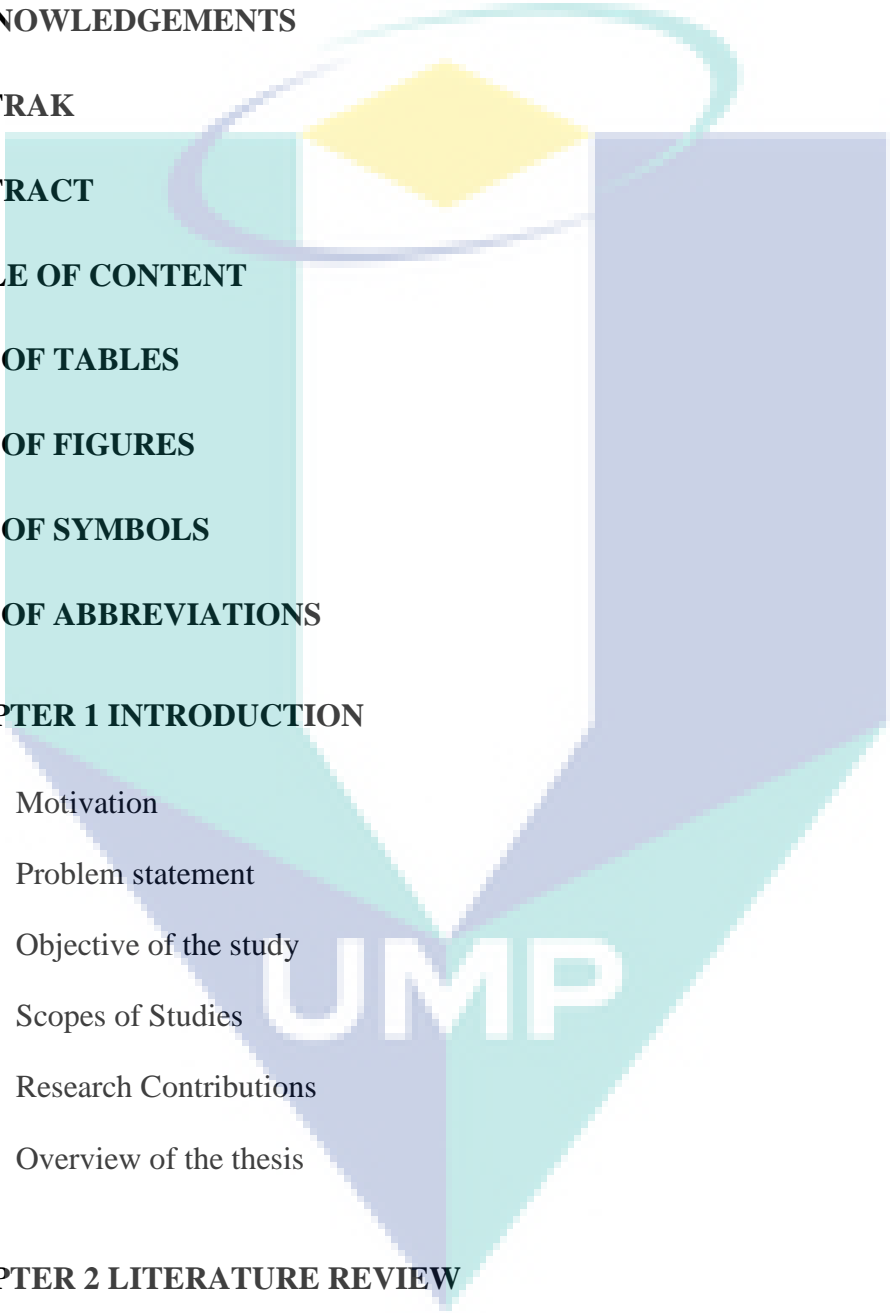
The logo for UMP (Universitas Muhammadiyah Palembang) is a large, stylized letter 'U' composed of several overlapping triangles in shades of blue and teal. The letters 'UMP' are written in a bold, white, sans-serif font across the center of the 'U'.

TABLE OF CONTENT



DECLARATION	
TITLE PAGE	
ACKNOWLEDGEMENTS	iii
ABSTRAK	iv
ABSTRACT	v
TABLE OF CONTENT	vi
LIST OF TABLES	ix
LIST OF FIGURES	x
LIST OF SYMBOLS	xii
LIST OF ABBREVIATIONS	xiii
CHAPTER 1 INTRODUCTION	1
1.1 Motivation	1
1.2 Problem statement	4
1.3 Objective of the study	4
1.4 Scopes of Studies	4
1.5 Research Contributions	5
1.6 Overview of the thesis	5
CHAPTER 2 LITERATURE REVIEW	7
2.1 Overview	7
2.2 Hydrogen as Energy Resource	7
2.2.1 Hydrogen from Methane	8

2.2.2	Hydrogen from Ethanol	13
2.3	Environmental and Economic Assessment	17
2.3.1	Life cycle analysis (LCA)	18
2.3.2	Economic feasibility	23
2.4	Concluding Remarks	25
CHAPTER 3 RESEARCH FRAMEWORK & PROCESS MODELLING		26
3.1	Research Framework	26
3.2	Process Description	28
3.2.1	Hydrogen production from methane (Case 1)	29
3.2.2	Hydrogen production from ethanol (Case 2).	30
3.3	Process Simulation	32
3.3.1	Reactor Modelling	34
3.3.2	Separation model	50
3.3.3	Overall Flowsheet Simulation Results	53
3.3.4	Concluding Remarks	56
CHAPTER 4 ENVIRONMENTAL AND ECONOMIC ANALYSIS		58
4.1	Introduction	58
4.2	LCA Goal and Scope	58
4.2.1	Case 1 system boundaries	58
4.2.2	Case 2 system boundaries	60
4.3	Life Cycle Inventory (LCI)	60
4.4	Life cycle impact assessment	62
4.5	Life Cycle Results Interpretation	62
4.5.1	Hydrogen Production from Methane (Case 1)	62

4.5.2	Hydrogen Production from Ethanol (Case 2)	66
4.6	Comparison Between Hydrogen Production from Methane (Case 1) and Hydrogen Production from Ethanol (Case 2).	69
4.6.1	Concluding Remarks	73
4.7	Economic Assessment	73
4.7.1	Economic Analysis of Case 1	74
4.7.2	Economic analysis of Case 2	75
4.7.3	Economic Comparison	76
4.7.4	Concluding Remarks	77
CHAPTER 5 CONCLUSION		78
5.1	Conclusion	78
5.2	Recommendation for future works	79
REFERENCES		80
APPENDIX A-1 STREAM SUMMARY FROM ASPEN PLUS FOR CASE 1		88
APPENDIX A-2 MODEL SUMMARY FROM ASPEN PLUS FOR CASE 1		90
APPENDIX B-1 STREAM SUMMARY FROM ASPEN PLUS FOR CASE 2		94
APPENDIX B-2 MODEL SUMMARY FROM ASPEN PLUS FOR CASE 2		96
APPENDIX C-1 DETAILS FROM THE GABI FOR CASE 1		100
APPENDIX C-2 DETAILS FROM GABI FOR CASE 2		102
APPENDIX D-1 CAPCOST DETAILS FOR CASE 1		104
APPENDIX D-2 CAPCOST DETAILS FOR CASE 2		105
APPENDIX E-1 LIST OF PUBLICATIONS AND CONFERENCES		106

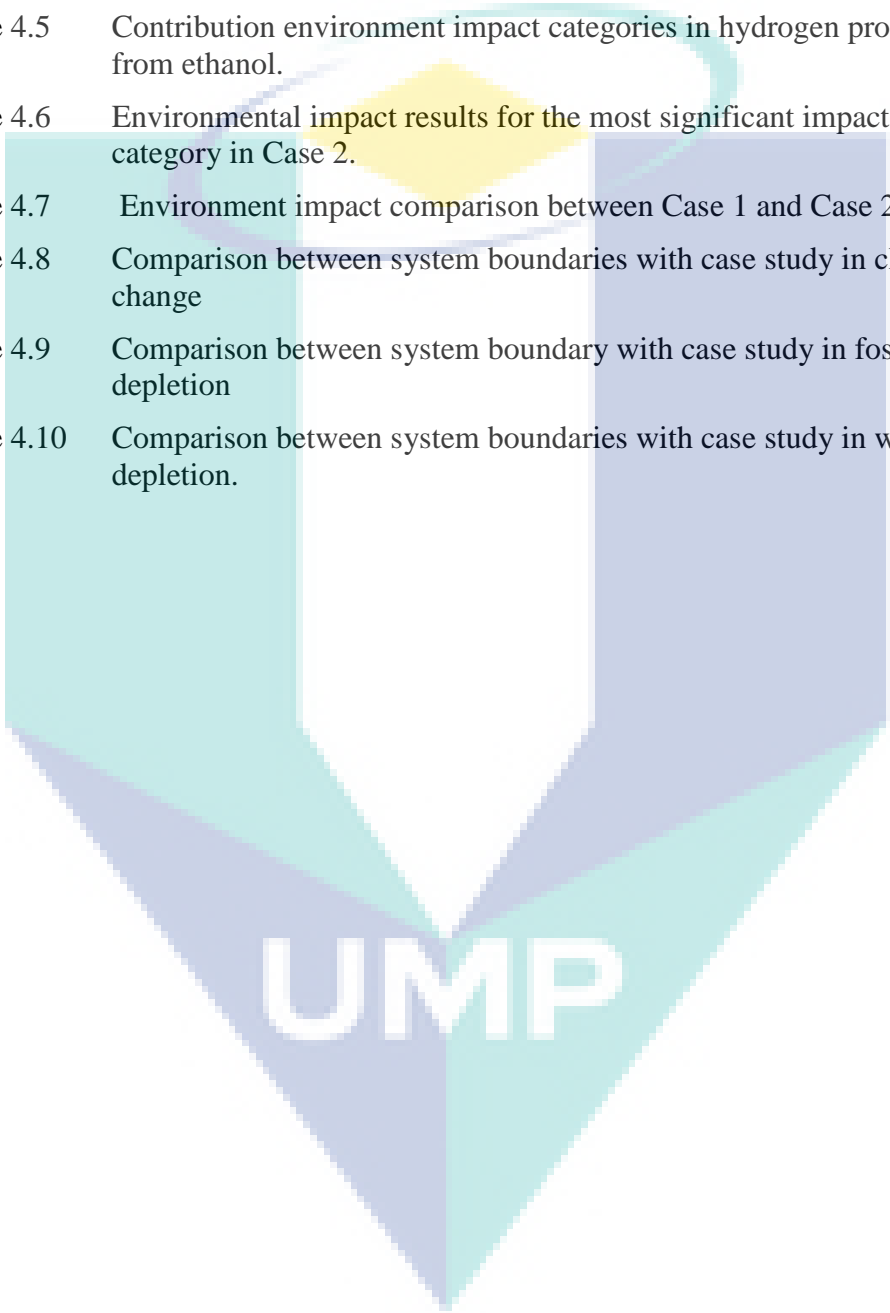
LIST OF TABLES

Table 1.1	Hydrogen consumption in the world	2
Table 2.1	Kinetic parameter for MSR.	10
Table 2.2	The kinetic parameter for WGS	11
Table 2.3	The elements in LCIA	21
Table 3.1	Summaries for Case 1	33
Table 3.2	Summaries for Case 2	34
Table 3.3	Kinetic parameter methane steam reforming	36
Table 3.4	Summaries for operating condition for validation	36
Table 3.5	Kinetic parameter for water gas shift	45
Table 3.6	Kinetic parameters for the kinetic reactions in absorber and stripper	51
Table 3.7	Summaries of design and operating condition for validation	52
Table 3.8	Comparison of Li et al. (2016) and simulation results	52
Table 3.9	Summaries results for the simulation	54
Table 3.10	Summary stream table for hydrogen production for Case 1	54
Table 3.11	Summaries of results for simulation.	55
Table 3.12	Summaries stream results for mole flow rate	56
Table 4.1	Main inventory data for the Case 1	61
Table 4.2	Main inventory data for Case 2	61
Table 4.3	Impact categories for each subsystems for case 1	64
Table 4.4	Impact categories for each subsystems for case 2	67
Table 4.5	The utilities cost per unit (Turton et al., 2013)	74
Table 4.6	The summary of capital cost for the hydrogen production from methane	74
Table 4.7	Summary utilities for hydrogen production from methane	75
Table 4.8	Summary capital cost for hydrogen production from ethanol	75
Table 4.9	Summary utilities used in hydrogen production from ethanol	76
Table 4.10	The comparison of the capital cost between Case 1 and Case 2	76
Table 4.11	The comparison utilities cost for Case 1 and Case 2	77

LIST OF FIGURES

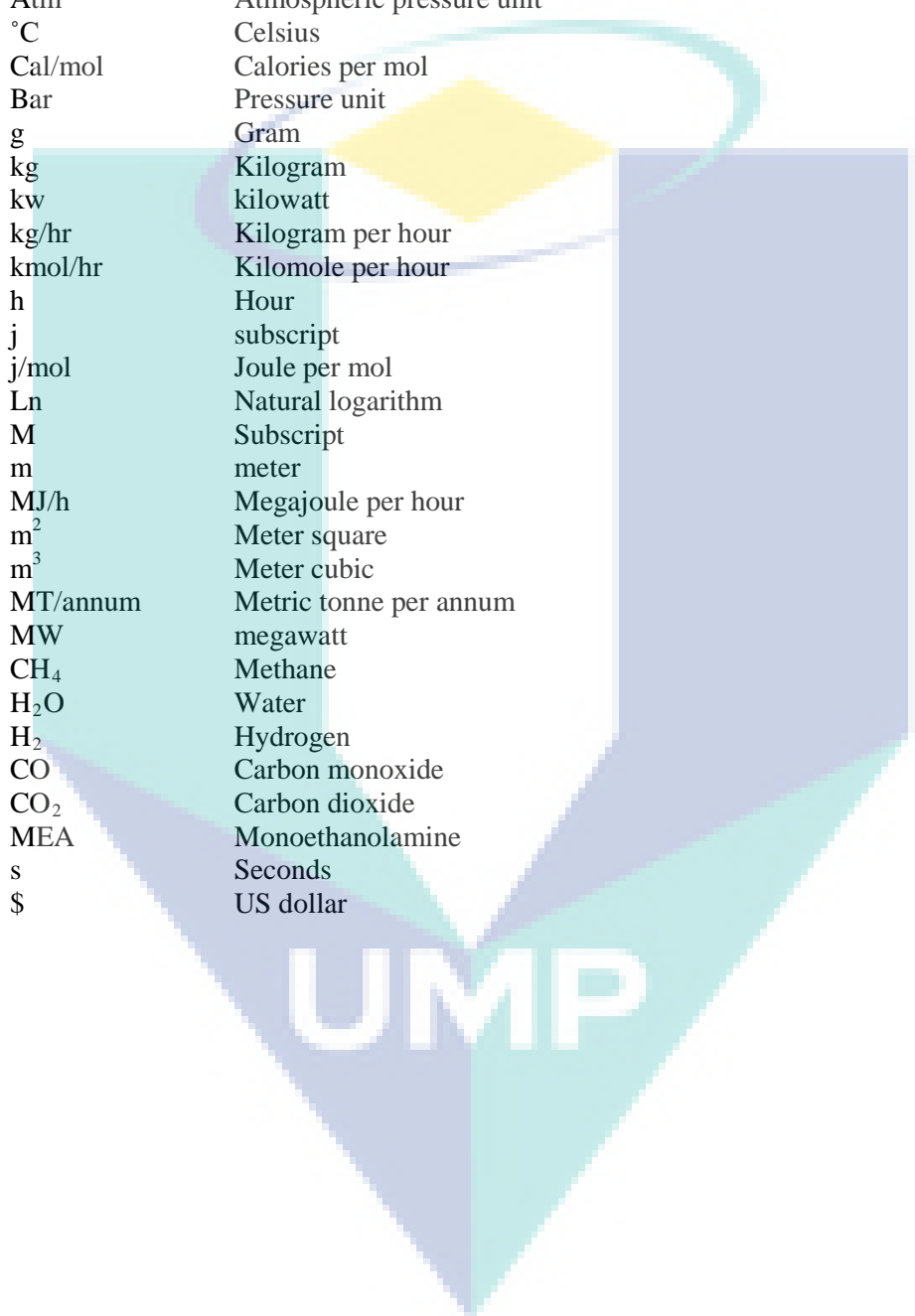
Figure 2.1	The simulation of methane steam reforming from Boyano et al. (2012)	12
Figure 2.2	The conventional methane steam reforming from Antzara et al. (2014)	13
Figure 2.3	Process flow for ethanol reforming from Gutiérrez-Guerra et al. (2015).	16
Figure 2.4	Schematic ethanol reforming from Rossetti et al. (2015b)	17
Figure 2.5	LCA Framework	19
Figure 3.1	Research framework	28
Figure 3.2	Process flow diagram of hydrogen production from methane.	30
Figure 3.3	Simplified process flow for hydrogen production from ethanol	32
Figure 3.4	Aspen Plus modelling of case 1	33
Figure 3.5	Aspen Plus modelling of case 2	33
Figure 3.6	The methane conversion effect on length of the reactor (a) from Singh et al (2014) (b) simulation using Aspen Plus	37
Figure 3.7	Weight of catalyst for MSR effect on molar flowrate of hydrogen	38
Figure 3.8	Temperature of MSR on molar flowrate of hydrogen.	39
Figure 3.9	The pressure of MSR on molar flow rate of hydrogen	39
Figure 3.10	Steam feed ratio on conversion of methane	40
Figure 3.11	The effect of molar ratio of steam to ethanol (a) from previous study (b) from simulation using Aspen Plus.	42
Figure 3.12	Catalyst weight effect on molar flowrate of hydrogen	43
Figure 3.13	Temperature of ethanol reforming on molar flowrate of hydrogen	44
Figure 3.14	The effect of pressure on molar flowrate of hydrogen.	44
Figure 3.15	The steam ratio feed to ethanol effect on conversion of hydrogen	45
Figure 3.16	Partial pressure of water effect on conversion of carbon monoxide (a) previous study (b) from simulation.	47
Figure 3.17	Sensitivity analysis of catalyst weight on molar flowrate of carbon monoxide	47
Figure 3.18	Sensitivity analysis of temperature on the molar flowrate of carbon monoxide.	48
Figure 3.19	Sensitivity analysis of pressure on molar flowrate of carbon monoxide	49
Figure 3.20	Sensitivity analysis of ratio steam to ethanol on the conversion of carbon monoxide.	49
Figure 3.21	The simulation flowsheet for CO ₂ removal	52

Figure 4.1	System boundaries for Case 1.	59
Figure 4.2	System boundaries for Case 2.	60
Figure 4.3	Contribution environment impact categories in hydrogen production from methane.	65
Figure 4.4	Environmental impact results for the most significant impact category in case 1.	65
Figure 4.5	Contribution environment impact categories in hydrogen production from ethanol.	68
Figure 4.6	Environmental impact results for the most significant impact category in Case 2.	68
Figure 4.7	Environment impact comparison between Case 1 and Case 2	70
Figure 4.8	Comparison between system boundaries with case study in climate change	71
Figure 4.9	Comparison between system boundary with case study in fossil depletion	72
Figure 4.10	Comparison between system boundaries with case study in water depletion.	73



UMP

LIST OF SYMBOLS



A	Subscript
B	Subscript
C	Subscript
D	Subscript
Atm	Atmospheric pressure unit
°C	Celsius
Cal/mol	Calories per mol
Bar	Pressure unit
g	Gram
kg	Kilogram
kw	kilowatt
kg/hr	Kilogram per hour
kmol/hr	Kilomole per hour
h	Hour
j	subscript
j/mol	Joule per mol
Ln	Natural logarithm
M	Subscript
m	meter
MJ/h	Megajoule per hour
m ²	Meter square
m ³	Meter cubic
MT/annum	Metric tonne per annum
MW	megawatt
CH ₄	Methane
H ₂ O	Water
H ₂	Hydrogen
CO	Carbon monoxide
CO ₂	Carbon dioxide
MEA	Monoethanolamine
s	Seconds
\$	US dollar

LIST OF ABBREVIATIONS

COMBRET	Combustion chamber
CAPEX	Capital Expenditure
CEPCI	Chemical Engineering plant cost index
C_p	Purchased cost
C_{TM}	Total module cost
C_{BM}	Base cost condition
C_{GR}	Grassroot cost
ESR	Ethanol steam reforming
Exp	Exponential
E-101	Heat exchanger 1 for Case 1
E-102	Heat exchanger 2 for Case 1
E-103	Heat exchanger 3 for Case 1
E-104	Heat exchanger 4 for Case 1
E-105	Heat exchanger 5 for Case 1
E-106	Heat exchanger 6 for Case 1
E-107	Reboiler stripper for Case 1
E-201	Heat exchanger 1 for Case 2
E-202	Heat exchanger 2 for Case 2
E-203	Heat exchanger 3 for Case 2
E-204	Heat exchanger 4 for Case 2
E-205	Heat exchanger 5 for Case 2
E-206	Heat exchanger 6 for Case 2
E-207	Reboiler stripper for Case 2
$^{\circ}E$	Enthalpy
ENTRL-RK	Electrolyte non-random two liquid model redlich kwong
Eq.	Equivalent
FU	Functional unit
GHG	Greenhouse gas
GWP	Global warming potential
HWGS	High temperature water gas shift
LWGS	Low temperature water gas shift
k	Pre-exponential factor
k_1	Rate constant of MSR
k_2	Rate constant of WGS
K	Adsorption equilibrium
K_1	Adsorption equilibrium for CO
K_2	Adsorption equilibrium for H ₂ O
K_3	Adsorption equilibrium for CO ₂
K_4	Adsorption equilibrium for H ₂
LCA	Life cycle assessment
LHHW	Langmuir-Hinshelwood Hougen Watson
MSR	Methane steam reforming
N	Number of components
OPEX	Operating expenditure
P	Partial pressure
P_{CH_4}	Partial pressure for CH ₄
P_{H_2O}	Partial pressure for H ₂ O
P_{H_2}	Partial pressure for H ₂
P_{CO}	Partial pressure for CO
P_{eth}	Partial pressure for ethanol
PFD	Process flow diagram
PSA	Pressure swing adsorption

R	Universal gas constant
R-101	Methane/Ethanol steam reforming reactor for Case 1
R-102	High temperature water gas shift reactor for Case 1
R-103	Low temperature water gas shift reactor for Case 1
R-201	Methane/Ethanol steam reforming reactor for Case 2
R-202	High temperature water gas shift reactor for Case 2
R-203	Low temperature water gas shift reactor for Case 2
RADFRAC	Rigorous distillation/separation column
RKSMHV2	RedlichKwong Soave Modified huron Vidal mixing rule
SB1	System boundary 1
SB2	System boundary 2
SB3	System boundary 3
SB4	System boundary 4
SB5	System boundary 5
SB1-1	System boundary 1 for Case 1
SB1-2	System boundary 2 for Case 1
SB1-3	System boundary 3 for Case 1
SB1-4	System boundary 4 for Case 1
SB1-5	System boundary 5 for Case 1
SB2-1	System boundary 1 for Case 2
SB2-2	System boundary 2 for Case 2
SB2-3	System boundary 3 for Case 2
SB2-4	System boundary 4 for Case 2
SB2-5	System boundary 5 for Case 2
T	Absolute temperature
T_0	Reference temperature
T-101	Absorption column for Case 1
T-102	Stripper tower for Case 1
T-201	Absorption column for Case 2
T-202	Stripper tower for Case 2
WGS	Water gas shift
x_i	Mole fraction of component
y_i	Activity coefficient of component

UMP

CHAPTER 1

INTRODUCTION

1.1 Motivation

The world energy demand currently depends on fossil fuel as a source. While the population of human increase more than 2% thus increasing energy demand, fossil fuel sources depleted yearly. It is estimated that 25% of the world population consumes 75% of the world energy supply (Dincer, 2000). Today, global demand towards energy consumes more than 85 million barrels of oil and 104 trillion cubic feet of natural gas per day and this consequently release a lot of greenhouse gas to the atmosphere (Haseli et al., 2008).

In the light of this, a new source of energy is needed as an alternative to fossil fuel. The new energy resource however need to be sustainable with minimal impact to the environment. It is found that of the promising new source of energy is hydrogen. Hydrogen energy is one of the most sustainable energy carrier to reduce the dependence on fossil fuels. Hydrogen is abundant with high reactivity chemically and can be found in water, fossil fuels and other living thing such as animals and plants. In addition, the energy content for hydrogen; 120 MJ/kg, is three times higher compared to gasoline with 44 MJ/kg. This shows that hydrogen is highly efficient in solving energy crisis (Kadier et al., 2014).

Hydrogen gas is a chemical element that contain two atoms and the molecular weight is one for each atom. Hydrogen gas is colourless, odourless, tasteless and non-toxic. When hydrogen burns with oxygen, it releases heat and produces water. Two moles of hydrogen react with one mole of oxygen will produce two moles of water. That means the burning hydrogen does not produce carbon emission thus using hydrogen as energy resource would reduce the carbon monoxide and other greenhouse

gas. Furthermore, hydrogen can be produced from a renewable source to reduce dependence on fossil fuel.

Hydrogen gas is considered as a secondary fuel and needs to be synthesized from primary fuel sources. Typically, hydrogen is produced from natural gas, coal and other renewable sources such as solar and wind energy. In the United States, hydrogen is produced at more than 8 million tons and mostly from fossil fuel (Koroneos, 2004). Furthermore, 97% of hydrogen production was synthesized from methane steam reforming (MSR) of natural gas. In the industry, MSR process is preferred because of its economic advantage and matured technology (Holladay et al., 2009).

The hydrogen economy has been introduced in 1960 and in 1970. Prior to that, the scientist and engineer were a dependence on fossil fuels as world energy and the international Association of Hydrogen Energy (IAHE) was introduced by 1974 with the purpose to develop and use hydrogen economy for the future generations (Dincer et al., 2012). In the hydrogen economy, sustainable energy sources such as the wind, solar, biomass and nuclear were used to produce hydrogen from water or other sources and to use hydrogen as an energy carrier. With studies on alternative sources to produce hydrogen, it can reduce dependence on fossil fuels as fuel sources.

Today, world consumption of hydrogen is about 450 billion m³ and mostly used as raw material for other chemicals such as ammonia and methanol production. Table 1 shows that, 61% of hydrogen is used for ammonia production and followed by oil refineries with 23%. However, few is used in the energy industry (Abbasi et al., 2011).

Table 1.1 Hydrogen consumption in the world

Category	Hydrogen consumed	
	Billion m ³	Share (%)
Ammonia producer	273.7	61
Oil refineries	105.4	23
Methanol Producers	40.5	9
Others	13.6	3
Merchant users	16.1	4
Total	449.3	100

Source: Abbasi and Abbasi (2011)

In order to reduce the effect on climate change, air pollution and faster depletion of crude oil caused by fossil fuel, the development of alternative energy

source substantially cut the fossil fuel dependence and reduce the carbon emission to atmosphere (Energy, 2015). The fossil fuel mostly used in transportation sector caused the increasing demand on fossil fuel and give negative impact to environment. With hydrogen as fuel offer various potential such as zero carbon emissions, increasing vehicle performance and fuel efficiency (Hwang et al., 2008; Hwang et al., 2005; Hwang, 2013). With the lack of dependence on the fossil fuel in transportation sector could improve drastically in air quality, carbon emission and energy consumption and energy security (Migliardini et al., 2011). The hydrogen can be produced from different feedstock, either renewable source such as ethanol or non-renewable sources such as methane. Non-renewable sources however, produce carbon and released into the air thus contribute to air pollution. Consequently, the production of hydrogen from different pathway i.e renewable source need to be studied for better option and comparison.

Process modelling techniques have emerged as an important tool to study and analyse chemical processes. A nearly realistic process models are becoming essential for the optimal synthesis and design of chemical processes since it provide systematic approach to process development and feasibility study (Li et al., 2016). Process modelling have been used to determine the hydrogen cost, price of competing fuels, hydrogen purity, development of technologies, the emission of greenhouse gas and revising the energy security regulation (Balat, 2008; Ball et al., 2009). Hydrogen price is mostly influenced by production technology, cost of raw materials, schedule waste production and the cost of utilities.

In this work, process modelling is used to provide the necessary data needed to perform the environmental impact and economic analysis assessment of renewable and non-renewable sources of hydrogen production. This assessment is important to raise public awareness on sustainability issues. Moreover, such quantitative sustainability assessment techniques can help decision makers to understand the environmental and economic impacts quantitatively which is required to mitigate undesired impacts and ensure the sustainability of new project to attract the community, government and investor interest and support (Cambero et al., 2014).

1.2 Problem statement

Energy resources are needed to satisfy the human needs. However, the overwhelming reliance on fossil fuels makes the hydrocarbon based energy source unsustainable and could lead to energy crisis in the future (Dincer, 2000). Furthermore, energy source from hydrocarbon caused serious environmental problem especially the release of greenhouse gas such as carbon monoxide and carbon dioxide to the atmosphere (Haseli et al., 2008). Hydrogen is an interesting alternative source to reduce the dependency on fossil fuels and the demand is growing. Currently, hydrogen is mainly produced from methane. However, methane feedstock availability is reduced year by year. On the other hand, ethanol is a good alternative hydrogen production since the feedstock for producing ethanol i.e. biomass of agriculture wastes are abundant and renewable. However, the questions raised, is bio-based feedstock more environmental friendly or more economical than fossil based option. Therefore, there is a need to perform sustainability assessment and compare both methane and ethanol based hydrogen production.

1.3 Objective of the study

The main objective of this research study is to perform environmental and economic feasibility assessment and comparison of simulated methane and ethanol based hydrogen production. The case studies are model in Aspen Plus. Life cycle analysis (LCA) is used for environment assessment whereas economic assessment involve capital cost and operating cost.

1.4 Scopes of Studies

In order to meet the objective below are the research scopes:-

- I. To model and validate hydrogen production using Aspen Plus via methane steam reforming and ethanol steam reforming. The model development involved rigorous modelling approach using kinetic based reactions and RADFRAC block.
- II. To perform equipment sizing and calculate the economic potential namely capital cost and operating cost of each production route.

- III. To model and perform Life Cycle Assessment (LCA) based environmental analysis using GaBi software.
- IV. To perform environmental and economic comparisons of both production routes.

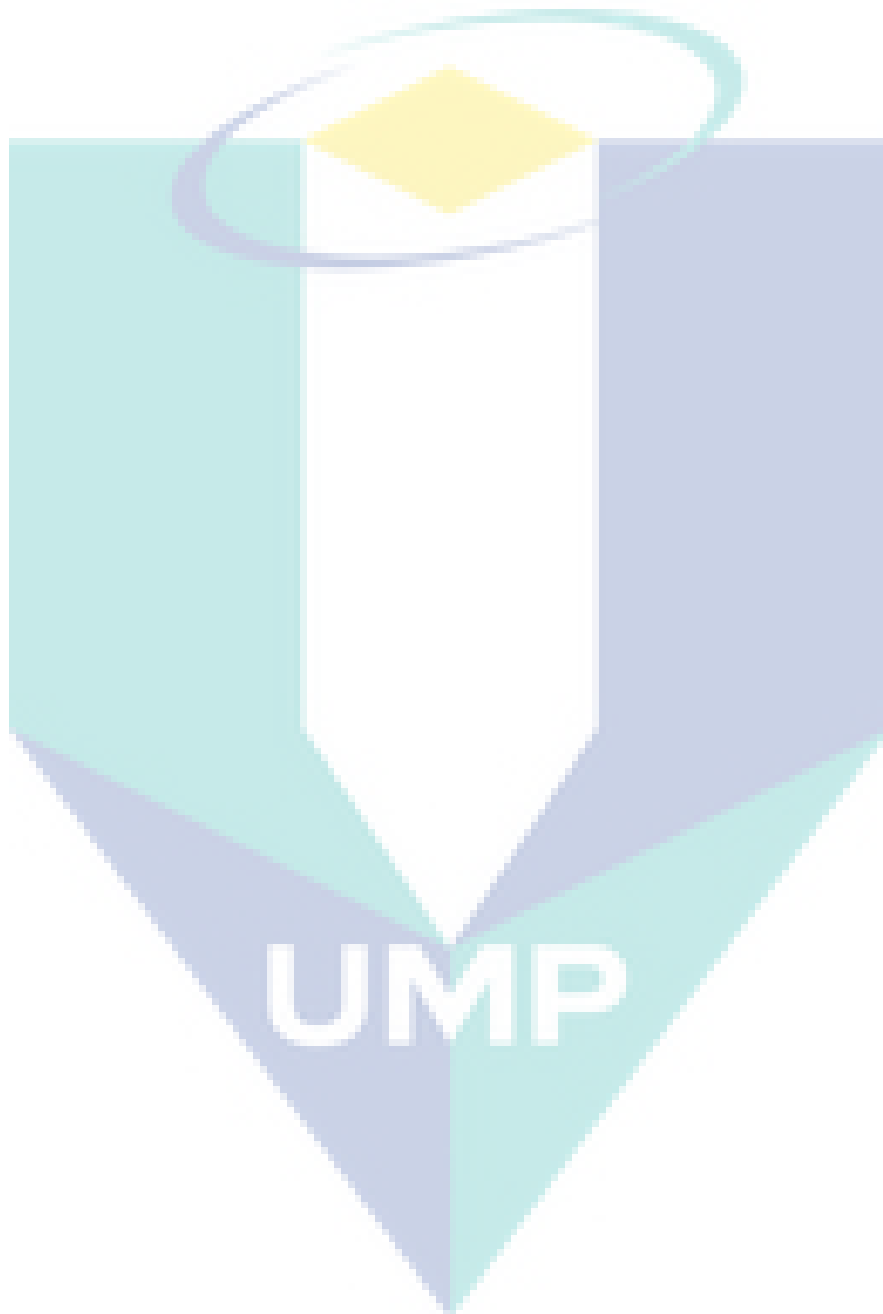
1.5 Research Contributions

This research will benefit researchers and policy makers to improve current process of producing hydrogen. In this study, hydrogen production from methane and from ethanol were simulated using rigorous modelling approach method in Aspen Plus. The reforming and water shift gas reactor were modelled using kinetic based block (R-Plug) whereas the separation processes; absorption and stripper for carbon dioxide removal, were modelled using RadFrac. Such rigorous modelling approach are more accurate and precise compared to the common stoichiometry and gibbs energy method. Apart from that, this research also contributes to the depth analysis and insights of both environment and economic assessment and comparison which have not been done extensively. The environment assessment was performed using Life Cycle Assessment (LCA) which give details insight into the impact to the environment. The economic analysis involve capital cost calculation of each unit operations whereas operating cost calculation involve utilities particularly steam and water consumption. Overall, this study will help researchers and policy makers to make decisions and improve environment quality and regulation.

1.6 Overview of the thesis

This thesis contains five chapters. The first chapter presents the motivation, objective and scope of the research. Second chapter provides the literature review related to the hydrogen production from methane and ethanol, environmental assessment and economic analysis which include the kinetic parameters of modelling work by another researcher. Other than that, the environmental assessment and economic analysis method were reviewed including related work carried out by previous researcher. Chapter 3 explained the process modelling for both case studies. Focus is given on the explanation of the steps for modelling the process including reactor and separation block in aspen plus. Furthermore, simulation results were also included in this chapter. Life cycle assessment (LCA) is discussed in Chapter 4 which

include life cycle goal and scope, life cycle inventory, impact assessment and result interpretations. In addition, Chapter 4 also include economic assessment and comparison for both case studies, in the final chapter, Chapter 5, all findings in this research work are concluded and some remarks for the further research.



CHAPTER 2

LITERATURE REVIEW

2.1 Overview

The purpose of this chapter is to review and discuss the process synthesis of hydrogen production methane and ethanol. Apart from that, this chapter also include review and discussions on environment and economic assessment of hydrogen production of both routes.

2.2 Hydrogen as Energy Resource

The global energy consumption is still dependent on hydrocarbon fuel although its resources is decreasing year by year and, in addition, these resources are closely linked with carbon emission as well as other pollutants (Rossetti et al., 2015a). Hydrogen is considered as one of the alternative energy sources for the future and as it can be stored and transported efficiently and burns cleanly with less pollutants and furthermore only produce water as by-product. Since the production of hydrogen from fossil fuels is unsustainable, a steady supply of renewable energy cannot be guaranteed and fortunately hydrogen can be produced from renewable feed materials (LeValley et al., 2014; Sobrino et al., 2010). Sustainability is the biggest issue as well as the driving force for sustainable development. A reliable tool to measure sustainability is a prerequisite for identifying non-sustainable processes, informing design-makers of the quality of products and monitoring impacts on the environment and social (Afgan et al., 2008).

The advantage of hydrogen as an energy resource include securing energy by reducing oil imports, sustainable by taking advantage of the renewable energy sources, less pollution and better urban air and finally economic viability by potentially shaping

the future global energy markets (Acar et al., 2014; Marbán et al., 2007; Saxena et al., 2008). As such, hydrogen attracts researchers to make it as an alternative fuel source of the future.

Hydrogen can be produced from different feedstocks, either renewable sources or non-renewable sources. Example of renewable source is from ethanol and non-renewable source is from methane. Hydrogen production can become economically if the renewable sources are fully utilized. Note that, hydrogen do not exist in free state in nature but always combined state with the other elements such as CH₄, C₂H₄OH and H₂O because hydrogen alone is highly reactive (Chaubey et al., 2013). Since, hydrogen is not free state in nature, it need to be extracted from the other compounds and the process used is non-contaminating environmentaly. If the hydrogen produced from hydrocarbon, it will produce carbon and released into the air. So, to claim hydrogen as a clean fuel is only true if the raw material is biomass and the energy consumed by the process is renewable (Mas et al., 2008).

2.2.1 Hydrogen from Methane

2.2.1.1 Process Description

The feed stream for this reaction route contained CH₄ and H₂O. It is preheated between 500°C to 1000°C in the heat exchanger before entering the methane steam reforming (MSR) reactor. The reaction for MSR is shown in the Equation 2.1 in which hydrogen and carbon monoxide is produced.



Since MSR reaction is reversible which means the reaction is limited by thermodynamics and strongly endothermic (Oliveira et al., 2010; Oshima et al., 2013). For this reason, the reforming reactor is operated at very high temperatures to impose strong limitations for the materials employed in the reactor and used large amount of energy for heating. This reaction can be performed between 1 bar to 25 bar usually in presence of nickel supported catalyst.

In order to reduce undesired CO and increase the H₂ yield in the production, the reformer products undergo two stage water gas shift (WGS) reactor operating at

temperature between 200-400 °C and 127-177 °C usually in presence of copper/zinc oxide/alumina catalyst (Basile et al., 2015; Boyano et al., 2012; Hla et al., 2015). In the WGS reactor, CO react with excess steam from the reformer to produce CO₂ and H₂. The reaction for WGS is shown in the Equation 2.2



Then, the outlet products from WGS is cooled down in the heat exchanger and undergone the separation of CO₂. Common methods to remove the CO₂ is absorption and desorption process with MEA solutions. Other than that, pressure-swing adsorption (PSA) can also be used (Simpson et al., 2007).

2.2.1.2 Reaction Kinetic for Methane Steam Reforming (MSR) and Water Gas Shift (WGS).

Methane steam reforming (MSR) require high temperature and pressure thus increase the operating cost. In order to reduce the high-energy transfer, minimize reaction time and increase hydrogen yield, catalyst used is normally nickel based catalyst. It was found, catalyst that contains 10% Ni have high conversion of methane to hydrogen with 95.7% at 700 °C (Bej et al., 2013). The MSR kinetic model have been developed by Chen et al. (2003) and Singh et al. (2014) following Langmuir-Hinshelwood Hougen-Watson (LHHW) kinetic rate equations, R_{MSR} based on the two main reactions (2.1) and (2.2).

For reaction 2.1 the rate expressions in shown in Equation 2.3

$$R_{MSR} = k_1 \left(\frac{P_{CH_4} P_{H_2O}}{P_{H_2}^{2.5}} - \frac{P_{CO} P_{H_2}^{0.5}}{K_1} \right) / DEN^2 \quad 2.3$$

Where P is partial pressure, k_1 is rate constant and K is adsorption equilibrium constant. The term DEN is given by,

$$DEN = 1 + K_{CO} P_{CO} + K_{H_2} P_{H_2} + K_{CH_4} P_{CH_4} + \frac{K_{H_2O} P_{H_2O}}{P_{H_2}} \quad 2.4$$

The kinetic parameter for methane steam reforming reaction rate equation is shown in Table 2.1. Rui et al. (2008) used this kinetic model in his simulation work and found good agreement with the experimental data. Note that for Aspen Plus simulation rate expressions in Equation 2.3 need to rearrange because of the negative order for the partial pressure of hydrogen giving the infinite reaction rates. Adding hydrogen to the reactor could help model convergence in simulation and avoid simulation becoming error during iteration. (Rui et al., 2008).

Table 2.1 Kinetic parameter for MSR.

Parameter	Pre-Exponential factor	Value
k_1	4.2248×10^{15} (mol atm ^{0.5} /g h)	240.1
K_{CH_4}	6.65×10^{-4} (atm ⁻¹)	-38280
K_{H_2O}	1.77×10^5 (atm ⁻¹)	88680
K_{H_2}	6.12×10^{-9} (atm ⁻¹)	-82900
K_{CO}	8.23×10^{-5} (atm ⁻¹)	-70650
K_1	7.846×10^{12} (atm ²)	220200

Source: Fernandes et al. (2006)

Water gas shift (WGS) reaction is commonly used in industrial to increase the yield of hydrogen after MSR reaction and also to reduce the amount of carbon monoxide. The reaction is exothermic and usually performed in two stages which is high temperature WGS and low temperature WGS operated at 200-400 °C and 127-177 respectively usually in presence of CuO/ZnO/Al₂O₃ catalyst (Basile et al., 2015; Boyano et al., 2012; Hla et al., 2015)

The rate of reaction expression for the reaction 2.2 was proposed by Mendes et al. (2010) and Amadeo et al. (1995) by using LHHW kinetic expression. The rate expression is as follows:

$$R_{WGS} = \frac{k_2 P_{CO} P_{H_2O} (1 - \beta)}{(1 + K_{CO} P_{CO} + K_{H_2O} P_{H_2O} + K_{CO_2} P_{CO_2} + K_{H_2} P_{H_2})^2} \quad 2.5$$

Where,

$$\beta = \frac{P_{CO_2} P_{H_2}}{P_{CO} P_{H_2O} K_e} \quad 2.6$$

The parameter for the constants in the rate Equations 2.5 and 2.6 were obtained from previous experiments by Amadeo and Laborde (1995) and Mendes et al. (2010). The constant values are shown in Table 2.2.

Table 2.2 The kinetic parameter for WGS

Parameter	Pre-Exponential factor	Value
k_2	0.92 (mmol g ⁻¹ s ⁻¹ atm ⁻²)	4080
K_{CO}	2.21	-910
K_{H_2O}	0.4	-1420
K_{CO_2}	0.0047	-24720
K_{H_2}	0.052	-14400

Source: Mendes et al. (2010)

2.2.1.3 Modelling work on hydrogen production from methane

From our literature review, works on modelling and simulation of hydrogen production from methane are few. Boyano et al. (2012) for example model a hydrogen production process by adding a combustion chamber before the MSR reactor. This is to provide heat required by the MSR reaction. The flowsheet is shown in Figure 2.1 and model in Aspen Plus. Methane from natural gas is compressed to 10 bar and heated at 700°C and mixed with water steam before entering the MSR reactor. The steam to methane feed ratio used is 3.6 and the conversion ratio is set to 83% of methane but for this process the combustion chamber (COMBRET) was added and simulated with 15% excess if air. Besides that, the MSR reaction can also be accomplished by reacting methane and steam at high temperature conditions at 627-927°C and at pressure 5-25 bar. Since the reaction is endothermic heat must be supplied to the reactor (Boyano et al., 2012). The reactions were simulated using a non kinetic based approach.

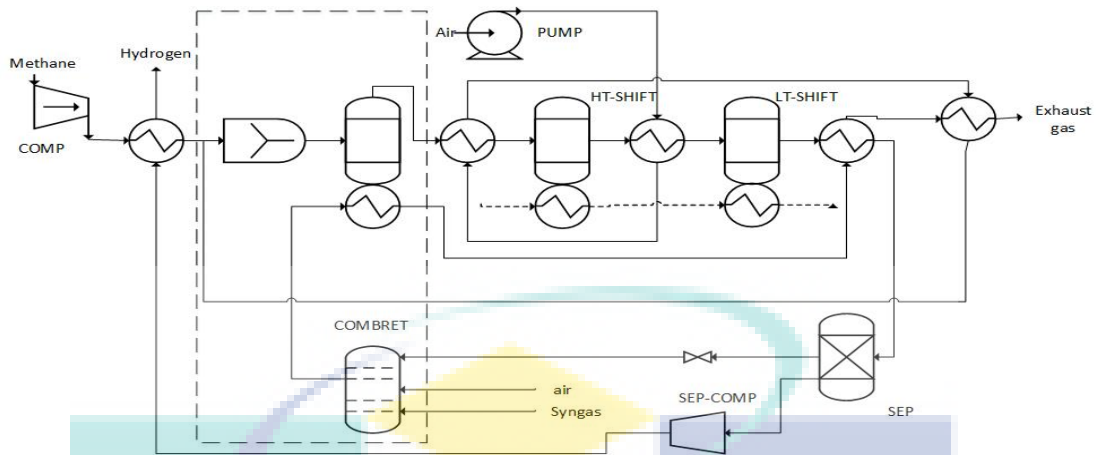


Figure 2.1 The simulation of methane steam reforming from Boyano et al. (2012)
 Source: Boyano et al. (2012).

In another work by Antzara et al. (2014), hydrogen process were modeled to analyse the thermodynamic effect of hydrogen production in situ with carbon dioxide capture. Modelling and simulation were done in Aspen Plus. The process flowsheet is shown in Figure 2.2. Feed stream 1 containing CH_4 and H_2O is preheated to 490°C . The preheating is performed in two heat exchangers in which HE2 utilizes the hot flue gases from methane combustion. Feed stream 3 then enters the MSR reactor (R1) to produce hydrogen and carbon monoxide. In order to convert undesired CO and increase the H_2 yield, the reformer products going through with two stages of WGS reactors namely R2 and R3 operating at 400°C and 210°C respectively. The product gas R1 is cooled down by HE3 before entering the high temperature WGS (R2). After that, the outlet product from high temperature WGS is cool down in by HE4 before entering the low temperature WGS (R3). The outlet products from R3 is then cooled and the unreacted steam is condensed and removed in the CO1 tower. In this work, the MSR and WGS reactions were modelled using the RGibbs reactor. Sensitivity analysis were also done for several parameters such as temperature, pressure, feed ratio, carbon capture efficiency and NiO/CaO ratio. Both simulation works imply non kinetic model based approach in simulating the MSR and WGS reactors namely RGibbs and RStoic block model. Although simplified models were easier to converge, a kinetic based model approach is needed to provide more insights and accurate behaviour of the process.

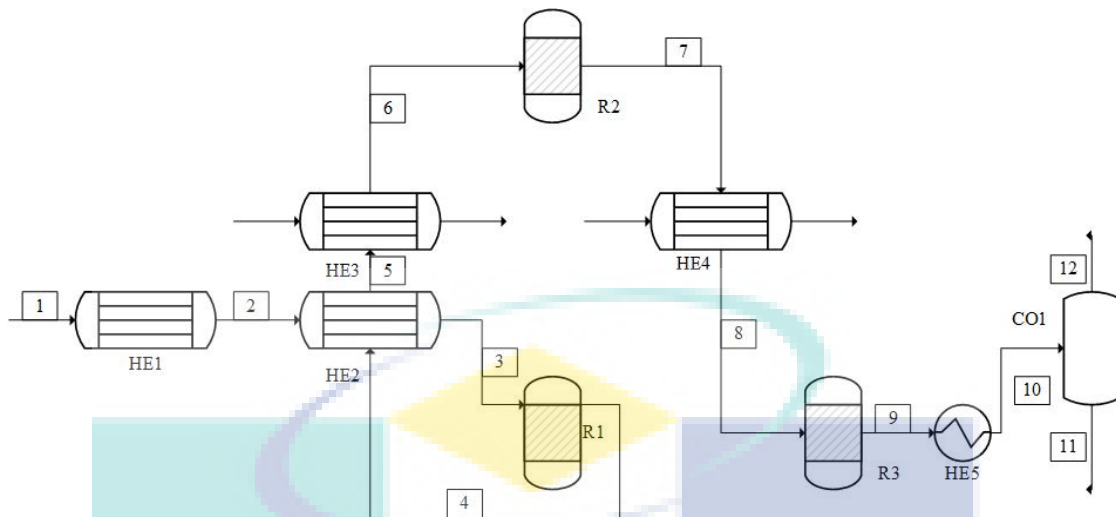


Figure 2.2 The conventional methane steam reforming from Antzara et al. (2014)
Source: Antzara et al. (2014)

Therefore, mostly work from literature used stoichiometry and Gibbs blocks in the reactions for methane steam reforming. So, the gap in simulation works from literature were using non-kinetic approach. In this study are using the kinetic block such as R-Plug in the simulation to study more details behaviour of the process. The operating conditions can be used from these literature review in this study.

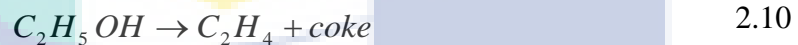
2.2.2 Hydrogen from Ethanol

2.2.2.1 Process Description

Ethanol is a promising alternative feedstock compared to methane because of its high hydrogen content, availability, non-toxicity and storage and handling safety and can be produced from renewable sources such as biomass sources, agroplantation waste and municipal solid waste (Mas et al., 2008). Ethanol produces three molecules of hydrogen and it is non-toxic liquid at room temperature and a stable compound. Furthermore, ethanol has an advantage of being nearly reduction carbon producing because carbon dioxide was consumed for biomass growth (Llera et al., 2012).

Production of high purity hydrogen by ESR is a complex process because it involve several reactions and separation steps. The reaction for ethanol steam reforming (ESR) for producing hydrogen is endothermic as shown in Equation 2.7. Ethanol can also undergo several reactions such as dehydrogenation (Equation 2.8), dehydration (Equation 2.9) and cracking (Equation 2.10) to produce side products such as carbon

dioxide, methane, carbon monoxide and coke (Contreras et al., 2014). Therefore, selectivity to hydrogen is affected by many undesired side reaction (Authayanun et al., 2015; Mas et al., 2008).



To avoid these undesired reaction, for example, acetaldehyde formation from ESR can undergo cracking process to form methane. To avoid this temperature is increased and excess water is added to the reaction (Bion et al., 2012; Vicente et al., 2014).

In ESR, this process also requires two more additional methods for reducing the concentration of CO which is WGS reaction or CO preferential oxidation (COPO) reaction that produce CO₂ and at the same time increase H₂ yield. To minimize the carbon formation and other side reactions such as acetaldehyde, the ratio of water to ethanol can be increased (Wurzler et al., 2016). Separation of high purity hydrogen requires several separation steps and the common method for CO₂ and H₂O removal are pressure swing adsorption (PSA) and condensation of remaining water (Gutiérrez-Guerra et al., 2015).

2.2.2.2 Reaction Kinetics for Ethanol Steam Reforming (ESR).

The production of hydrogen by ESR has been widely investigated. Many researchers investigated the catalyst to produce hydrogen from ethanol. Han et al. (2016) investigated a Ni/Al₂O₃ catalyst for hydrogen production from ethanol and concluded that Ni/Al₂O₃ catalyst can produced high hydrogen yield. The kinetic data used in this work, were based on previous experimental work by Han et al. (2016) and they had simplified in the form of power-law kinetic model. The kinetic model was proposed by Akande et al. (2006) in their studies. Akande et al. (2006) carried out the kinetic experiment in a packed bed tubular reactor to perform a kinetic modeling of the

production of hydrogen by catalytic reforming of crude over a Ni/Al₂O₃ catalyst. Mathure et al. (2007) used Ni/Mg/Al₂O₃ catalyst in their study and used the kinetic model proposed by Akande et al. (2006). The following model is the power-law model used in this simulation.

$$R_{EtOH} = 4.39 \times 10^2 \exp\left(-\frac{2.3 \times 10^4}{RT}\right) (P_{EtOH})^{0.711} (P_{H_2O})^{2.71} \quad 2.11$$

Where R is universal gas constant and T is temperature. The activation energy for this rate expression is 23 kJ/mol, the reaction order for the partial pressure, P of ethanol and water frequency factor was 0.711 and 2.71 respectively. The collision frequency factor was $4.39 \times 10^2 \text{ mol (min g-cat)(atm)}^{3.42}$ (Mathure et al., 2007). The highest conversion for this model obtained was above 95%. Therefore, it necessary to use as kinetic model in this simulation.

2.2.2.3 Modelling work on hydrogen production from ethanol

Gutiérrez-Guerra et al. (2015) simulated a catalytic ethanol steam reforming in Aspen HYSYS with the Peng-Robinson thermodynamic method. The process flowsheet is shown Figure 2.3. In the feed stream ethanol and water is mixed with molar ratio 6 and through a network of six integrated heat exchangers (HE-01 to HE-06) before entering the ESR reactor. The final temperature from HE-06 is 800 °C. Then, ESR reactor operates at 800 °C and the pressure of 1.8 atm. Fractional conversion is assumed 60%. The ESR reactor product stream then enters WGS to convert CO to CO₂ and H₂. As with hydrogen production from methane, two WGS reactors are needed which are high temperature WGS and low temperature WGS operate at 400 °C and 250 °C respectively. Then, remaining CO from low temperature WGS reactor is oxidized with excess air in a carbon monoxide preferential oxidation (COPROX) reactor 170 °C. The ESR reactor were model as fractional conversion reactor while WGS and COMPROX reactors were simulated as equilibrium reactors. To obtain the desired hydrogen purity, a membrane unit is used which operates at 300 °C. The operating conditions for the simulation used in Gutiérrez-Guerra et al. (2015) were based on by (Caravaca et al., 2013; de Lucas-Consuegra et al., 2014; Khila et al., 2013; Liguras et al., 2003; Montané et al., 2011).

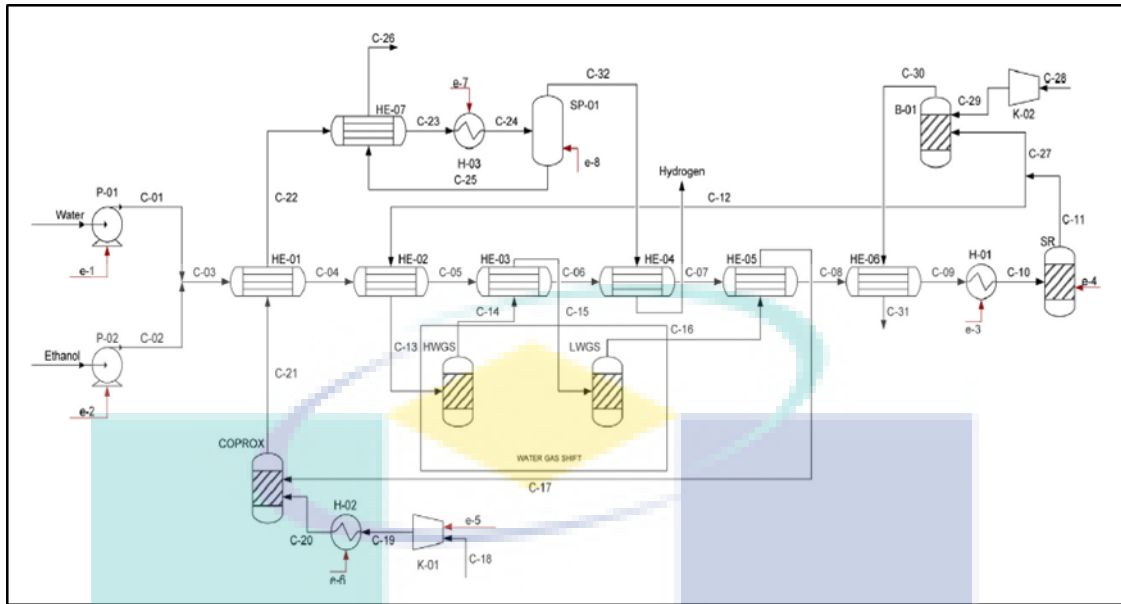


Figure 2.3 Process flow for ethanol reforming from Gutiérrez-Guerra et al. (2015).
Source : Gutiérrez-Guerra et al. (2015)

In another work, Rossetti et al. (2015b) simulated a hydrogen production process for modified combined heat and power (CHP) generation unit. In this work, Peng-Robinson thermodynamic method is used particularly suited to describe light gas mixture in wide temperature and pressure range. The process flowsheet is shown in Figure 2.4. The feed stream contained ethanol and water with molar ratio range between 5 to 14. The ESR reactor temperature is set at 750 °C. Using Ni/Al₂O₃ catalyst and operating temperature above 600 °C, coking can be negligible. ESR product stream then enters two WGS reactors namely high temperature and low temperature operated at 350 °C and 280 °C respectively. Methanation reaction in the reactor (COMET) is considered when methane is present the process due to the side reactions in the ESR reactor. Both WGS and methanation used Gibbs reactor model. As with hydrogen production from methane, simulation work on hydrogen production from ethanol mainly based on non-kinetic model. For comparable effort, there is a need to simulate this process based on kinetic model.

economic feasibility depends on the capital expenditure (CAPEX) and operating expenditure (OPEX). CAPEX is a fund used to purchase equipments or services to setup and expand the company abilities to generate profits. CAPEX is needed before deciding to build any plant especially when the technology is new or immature. OPEX on the other hand, involves the ongoing cost to run the plant such as utilities, maintenance, salary etc. In this work, CAPEX and OPEX is used for the economic feasibility study and comparison of both case studies.

2.3.1 Life cycle analysis (LCA)

Life cycle assessment (LCA) is a method for assessing various environmental aspects associated with the development of a product and its potential impact throughout a products life from raw material, processing, manufacturing, use and disposal or end of life (ISO14040, 2006). LCA allows for characterization of the consequences of possible public policy options or scientific alterations and development of novel sustainable energy resources and technologies (Dufour et al., 2011). Apart from that, LCA can be used to evaluate the process and product impacts towards the environment as well as helping manufactures and customer to select an environmentally friendlier option.

2.3.1.1 LCA Framework

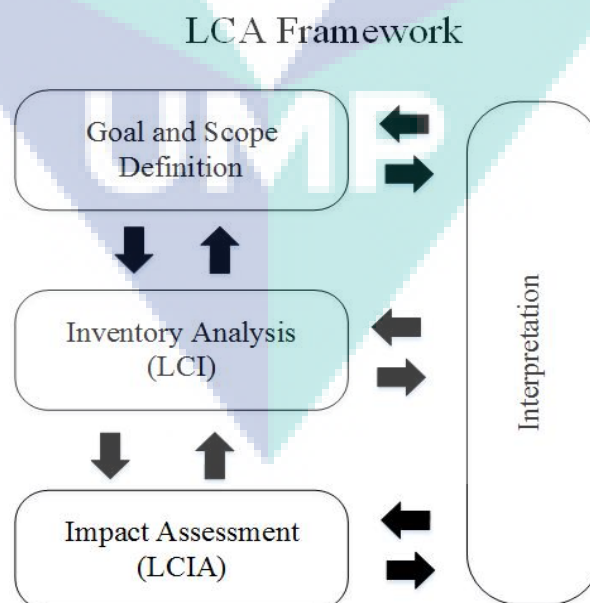


Figure 2.5 LCA Framework

Figure 2.5 shows the LCA framework according to ISO 14044/44 which consist of four life cycle phases. Primary phase in LCA is to clarify the goal and scope definition. In defining the goal of the LCA study, it is required to clearly report the reason for carrying out the study, the intended application and audience, the intention to use the results in comparative assertions and to disclose them to the public (ISO14040, 2006). With respect to scope definition, it is required to clearly detail the product system to be studied, functions of the product system, functional unit, references flow, system boundary, allocation procedures, assumption, requirement on data and its quality, limitation and impact categories. In principle, system boundary involve selection of analysis such as gate-to-gate, cradle-to-gate or cradle-to-cradle. System boundary also define the processes and elementary flows to include in the LCA study where mass, energy and environmental relevance have been established by, as cut-off criteria used to study (ISO14040, 2006).

Perticularly for boundary selection between different systems in first phase in LCA study, a few methods have been reported and as follows (raynolds et al., 2000; Suh et al., 2004):

- Define the contents of the system either by process tree system, technological or social-economic whole system.
- Consider only the significant life cycle stream in the study. This method is to avoid the boundaries to be repeatedly selected, nor does the selection of similar boundaries in the same system.
- Set a percentage of the total mass, generally more than 5 % of the unit process in the system. Cut-off ratio happened when the percentage is below 5% and it is eliminate any input below than that. This method does not consider the impact of an input its system from entire LCA.
- Use alternative cut-off criteria by taking weight, energy, toxicity and price into accounts in defining the contribution of an input to the system as negligible, small or large issues regarding unrepeatable boundaries remain unsolved.

The second phase for LCA study is life cycle inventory analysis (LCI) which involve clarification on data sources and principles to use for quantitative computation. The purpose of developing the LCI is to calculate the quantities of input and outputs involved in delivering a specific functional unit of the product system under study (Rebitzer et al., 2004). The sources of primary data for the inputs are energy, raw material, ancillary materials and other physical inputs. Meanwhile, the sources of data for output mostly come from product, co-product, emission, waste and other environmental aspects. The input like water, emissions CO₂, preparation of chemical and electricity used in the different production stage are included in analysis. The upstream impacts of inputs production were based on database from Ecoinvent or GaBi (Ye et al., 2018). The inputs and outputs also can be obtained from simulation tools such Aspen Plus (Galera et al., 2015; Susmozas et al., 2016).

There are several steps of the various issues that can be analyzed in an inventory analysis:

- Data collection. It is procedures to quatify relevant inputs and outputs of a product system. These inputs and outputs may include the use of resources and releases to air, water and land associated with the system.
- Refining system boudaries. The system boudaries are definde as a part of the scope definition procedure but the system boundaries can be refined by decisions of exclusion life stages or sub-systems, exclusion of material flows or inclusion of new unit processes shown to significant.
- Calculation procedures. No formal calculation demands exist for calculation in LCA except the described for allocation procedures. The calculation can be done by using software or other applications such as Excel.
- Validation of data has to be conducted during the data collection process in order to improve the overall data quality.
- Relating of data to specific system. The fundamental inputs and outputs data are often delivered from industry in arbitrary units such as energy

consumption as MJ/ watt or emissions to sewage system as mg metal/ liter wastewater.

- Allocation and recycling. When performing a LCA of complex system, it is difficult to manage all the impacts and outputs inside the system boundaries. The difficulties can be solved by expanding the system boundaries to include all the inputs and outputs or by allocating the relevant environment impacts to studied system.

The third phase of the LCA study is life cycle impact assessment (LCIA). This phase provide indicators and basis for analysing the potential contribution of the resource extractions and waste/emission in an inventory to a number of potential impacts. In consistency with the defined goal and scope and based on the LCI results, three steps are taken for LCIA. First is the selection of relevent impact categories and characterisation model. Second is classification of LCI results to appropriate impact categories and thirdy is the characterisation or calculation of category indicator results. To ease the tasks, a commercial LCA software such as Simapro and GaBi can be used, as currently practised by many LCA reseachers (Ling-Chin et al., 2016).In LCIA containing two main issues, which are mandatory elements and optional elements. The mandatory elements is consist of selection of impact categories and category indicators, assignment of LCI results (classification) and characterization. On the other hand, optional elements contains normalization, grouping, weighing and data quality analysis. The Table 2.3 is shows the description of elements in LCIA.

Table 2.3 The elements in LCIA

LCIA-Mandatory Elements	
Impact Categories	Class representing environmental issues of concern to which LCI results may be assigned.
Classification	Assignment of LCI results.
Characterization	Calculation of category indicator results
LCIA-Optional Elements	
Normalization	Calculation of the magnitude of category indicator relative to reference information.
Grouping	Sorting and possibly ranking of the impact categories.
Weighting	Convert and possibly aggregating indicator results across impact categories using numerical factors based on values-choice.
Data quality analysis	Better understanding the reliability of the collection of indicator results, the LCA profile.

The life cycle interpretation occurs at every stage in the LCA study. When the results from LCI and LCIA are interpreted, significant issues shall be identified, uncertainties inherited in the study shall be addressed via uncertainty analysis and sensitivity analysis. The purpose for interpretation step is to reach conclusions and recommendations for the report of the LCA study or LCI study. This stage is important to improve the reporting and transparency of the study. This is important for the LCA final report.

2.3.1.2 Previous work on LCA on hydrogen production

Giraldi et al. (2015) used LCA to analyse the environment burden of hydrogen production while applying high temperature electrolysis in the process. The system function is the production of hydrogen using electricity and heat from nuclear power with functional unit of 1 kg of hydrogen. The study however, focused on emissions of greenhouse gases and the result shows the emission value at 416 g of CO₂ eq kg H₂. Verma et al. (2015) conducted the LCA for hydrogen production from underground coal gasification with and without carbon capture. The study focused on the global warming impact and greenhouse gas emission. The calculated global warming impact and greenhouse gas emission is 0.91 kg CO₂ eq and 18 kg CO₂ kg eq respectively.

In 2015, Authayanun et al. (2015) conducted LCA for bio-ethanol reforming and proton exchange membrane fuel cell (PEMFC) integrated process fueled by cassava based bio-ethanol and methane as co-reactant. In their study, methane was added to enhance the hydrogen fraction and efficiency of bio-ethanol reformer. The LCA is used to understand the environmental effect of each PEMFC system and to determine the steps needed for its improvement. Their LCA analysis shows that mixed bio-ethanol and methane reforming integrated with PEMFC system (BM-PEMFC) is more overall environmental impact than dehydrated bio-ethanol reforming with PEMFC system (DE-PEMFC). However, the global warming potential (GWP) and photochemical oxidant formation (POFP) impacts of the BM-PEMFC system remain high.

In another study, (Galera & Ortiz, 2015) used LCA to assess the environmental impact of supercritical water reforming of glycerol for hydrogen production. Aspen Plus was used as simulator to solve the mass and energy balance. Their finding shows that the process give a low carbon emission in the greenhouse gas inventory. Christoforou et

al. (2016) investigate the environmental impact of torrefaction process through the application LCA using GaBi software according to the CML2001 methodology. They conclude the important of the drying phase of the whole torrefaction system and the potential improvement of olive husk process in terms of energy consumption (Christoforou & Fokaidis, 2016).

In conclusion, the LCA had been used in a variety of case studing to assess the environment impact for the process. Based on literature, the LCA study mostly focussed on hydrogen production from renewable sources especially using electrolysis and membrane fuel cell. For LCA for hydrogen production from ethanol especially for ethanol steam reforming is less conducted. So, this is opportunity to fill that gap for conducting environment assessment on hydrogen production from ethanol by using LCA method with software GaBi.

2.3.2 Economic feasibility

CAPEX focused on capital cost estimation of major equipment in a process whereas OPEX focusses on cost of utilities used annually in a process. OPEX calculations involve data from cooling water, steam and electricity consumption during the operation of the plant. Richard Turton et al. (2013) developed a cost estimation tool (CAPCOST 2012) to evaluate the fixed capital cost from estimation of the purchased equipment cost by introducing the capacity, operating pressure and tempearture, heat transfer area needed and building material. The tool will calculate the bare module cost (C_{BM}) of equipment installed in a chemical process. C_{BM} consist of the purchase cost (C_P) of a piece of equipment multiplied by bare module factor (F_{BM}) as shown in Equation 2.12. When C_P were estimated for each piece of equipment based on capacity equation (Richard Turton et al., 2013).

$$C_{BM} = C_P F_{BM} \quad 2.12$$

The total module cost (C_{TM}) is defined as the sum of the bare module cost and contingency and fee costs. The C_{TM} is calculated by Equation 2.13 (Richard Turton et al., 2013). Values of 15% and 3% of the bare module cost are assumed for contingency cost and fees, respectively.

$$C_{TM} = 1.18 \sum_{i=1}^n C_{BM} \quad 2.13$$

The grassroots cost (C_{GR}) is the costs for the site development, auxiliary buildings and utilities. These terms are generally unaffected by cost of the materials of construction or operating pressure of the process. These costs are assumed to be equal to 50% of the bare module costs for the base case conditions. The C_{BM} is calculated by equation (Richard Turton et al., 2013).

$$C_{GR} = C_{TM} + 0.50 \sum_{i=1}^n C_{BM} \quad 2.14$$

2.3.2.1 Previous work on economic feasibility of hydrogen production

Roldan (2015) investigated the technical and economic feasibility of adapting an industrial steam reforming unit for production of hydrogen from ethanol. The configuration proposed involves the conversion of ethanol in the pre-reforming reactor. The economic analysis performed indicates that the high market price of pure ethanol makes the process far from viable and caused the production cost of almost double compared to conventional price of MSR units.

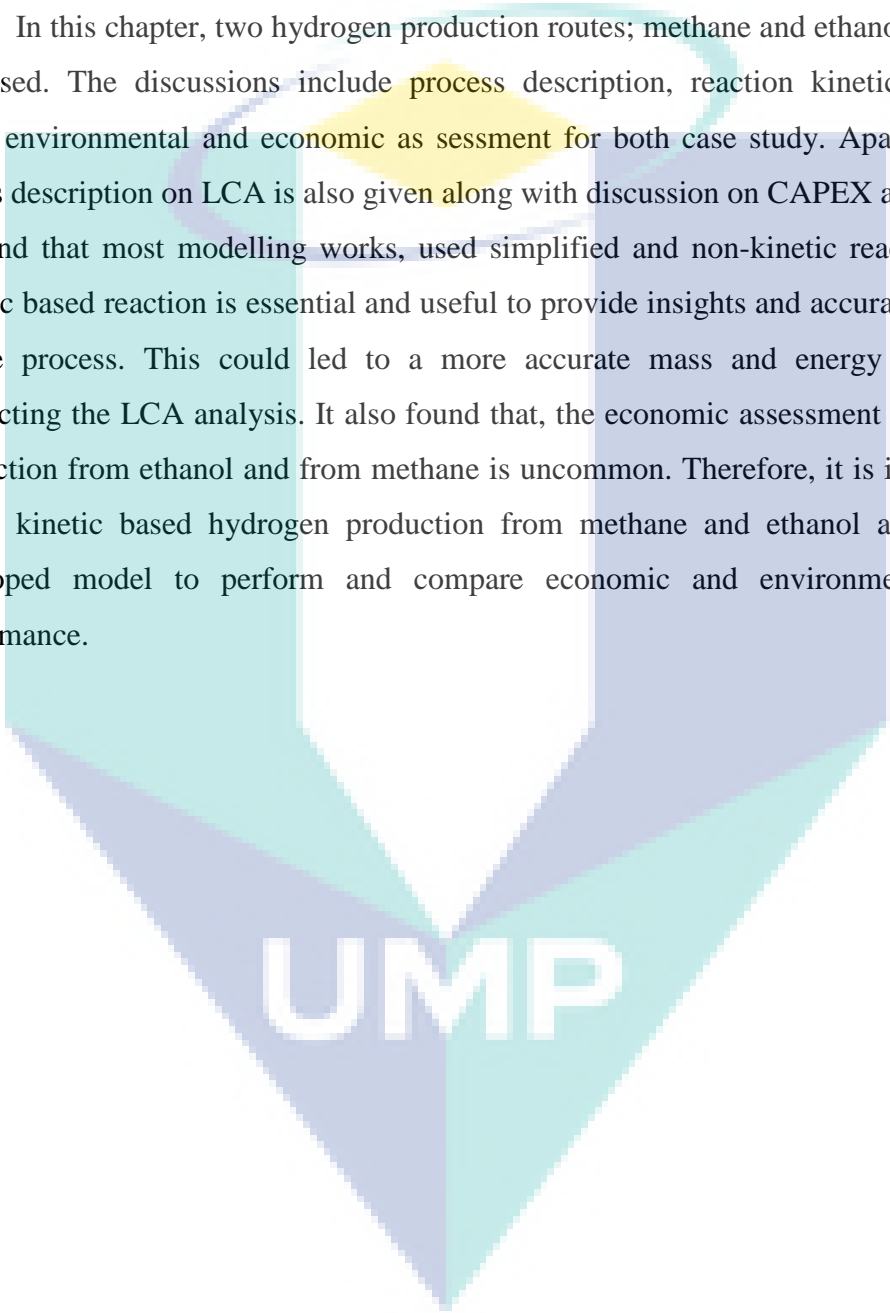
Braga et al. (2013) performed a technical, economical and ecological analysis of hydrogen production from biogas steam reforming. In their work, they used biogas in MSR as alternative for hydrogen production and claimed that it is able to decrease the negative environmental impact compared to natural gas. Economic analysis was performed to analyze the investment, operation and maintenance costs. Braga et al. (2013) concluded that hydrogen production cost decreases with the increase of payback period and the equivalent period of operation.

Muellerlanger et al. (2007) conducted an economical evaluation on selected hydrogen production processes based on natural gas steam reforming, coal and biomass gasification and water electrolysis. From an economic viewpoint steam reforming of natural gas is currently the most favourable hydrogen production method compared with other methods. Gasification of coal could be competitive even at present conditions.

but is only sensible if coupled with carbon capture. Hydrogen production from electrolysis is unlikely to be an economically competitive option mainly due to high electricity.

2.4 Concluding Remarks

In this chapter, two hydrogen production routes; methane and ethanol, have been discussed. The discussions include process description, reaction kinetic, modelling work, environmental and economic assessment for both case study. Apart from that, details description on LCA is also given along with discussion on CAPEX and OPEX. It is found that most modelling works, used simplified and non-kinetic reaction model. Kinetic based reaction is essential and useful to provide insights and accurate behaviour of the process. This could led to a more accurate mass and energy balance for conducting the LCA analysis. It also found that, the economic assessment on hydrogen production from ethanol and from methane is uncommon. Therefore, it is interesting to model kinetic based hydrogen production from methane and ethanol and used the developed model to perform and compare economic and environmental impact performance.

The logo for UIMP (University of Malaya Institute of Process Engineering) is a large, stylized 'V' shape. The left side of the 'V' is light blue, the right side is light purple, and the bottom point is a darker blue. The letters 'UIMP' are written in white, bold, sans-serif font across the bottom of the 'V'.

CHAPTER 3

RESEARCH FRAMEWORK & PROCESS MODELLING

3.1 Research Framework

The objective of this research is to perform LCA analysis and economic feasibility assessment and comparison for both methane (Case 1) and ethanol (Case 2) based hydrogen production. In achieving the objective several elements were involved. This include process modelling, model verification, LCA modelling, equipment sizing and costing which were performed using CAPCOST. Figure 3.1 shows the overall framework which summarize the works and platfroms involved. Generally the framework consists of four major elements which are:-

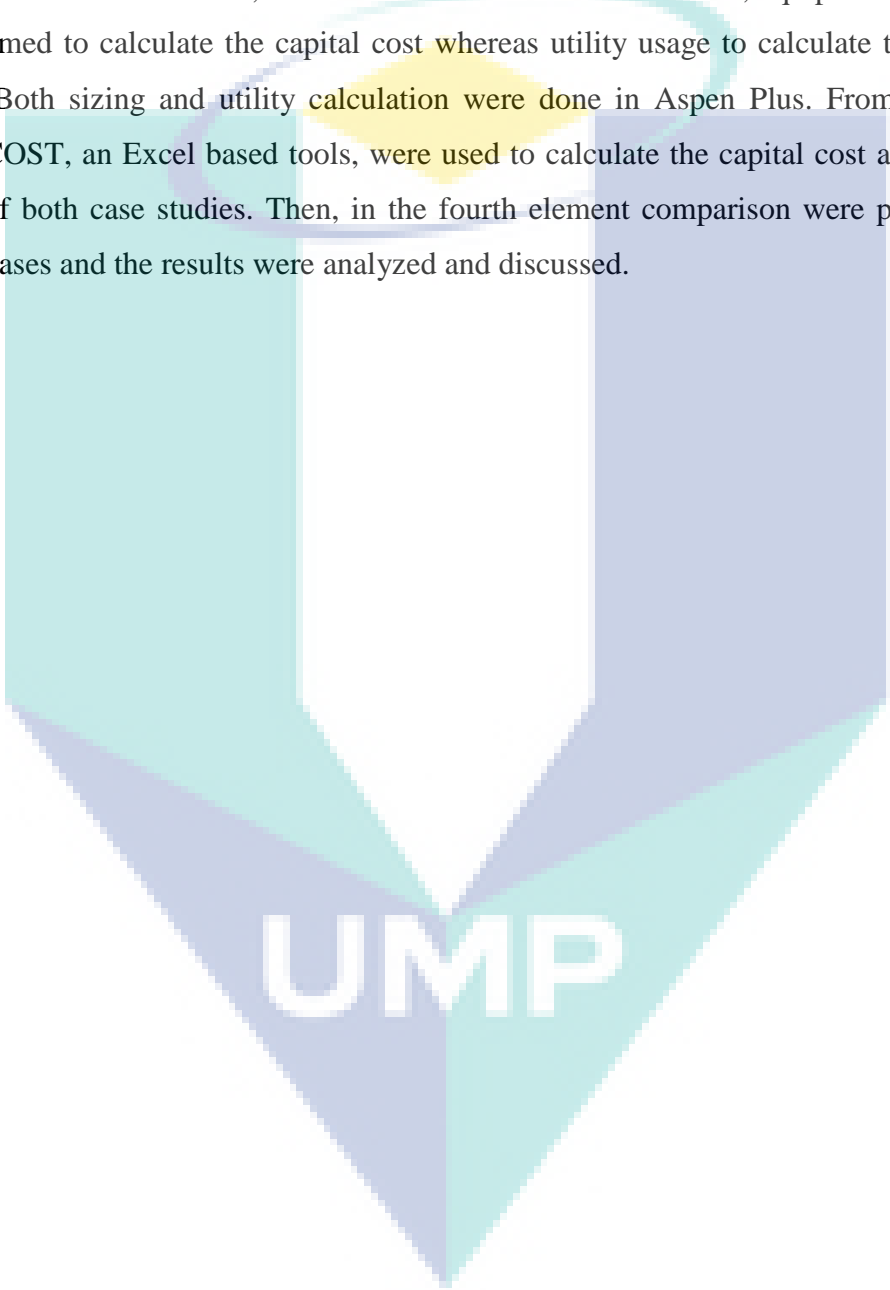
1. Process modelling
2. Life cycle assessment (LCA) analysis
3. Economic assessment
4. Case study comparison

Each of these elements involved several software and computational tools. In the process modelling element Aspen Plus were used for modelling of the reactors, CO₂ removal and the overall flowsheet of Case 1 and Case 2. Aspen Plus is also used for validation of the process models and to perform sensitivity analysis for determining the optimal operating condition. The simulations which contain mass and energy balance information of both procesess were then used for LCA assessment and economic assesement.

LCA assessment element consists of several procedures namely goal and scope definition, life cycle inventory analysis (LCI), life cycle impact assessment (LCIA) and interpretation of life cycle impact assessment. The LCA were performed using GaBi a

commercial software for conducting LCA. In the goal and scope, the objective and the boundary in the case is determined. In the LCI, the data is obtained from simulation results. Then, the data from simulation is assessed the impact on environment. This LCIA is consist 15 categories impact. From the LCIA, the results obtained is discussed.

On the other hand, in the economic assessment element, equipment sizing were performed to calculate the capital cost whereas utility usage to calculate the operating cost. Both sizing and utility calculation were done in Aspen Plus. From the results, CAPCOST, an Excel based tools, were used to calculate the capital cost and operating cost of both case studies. Then, in the fourth element comparison were performed on both cases and the results were analyzed and discussed.



UMP

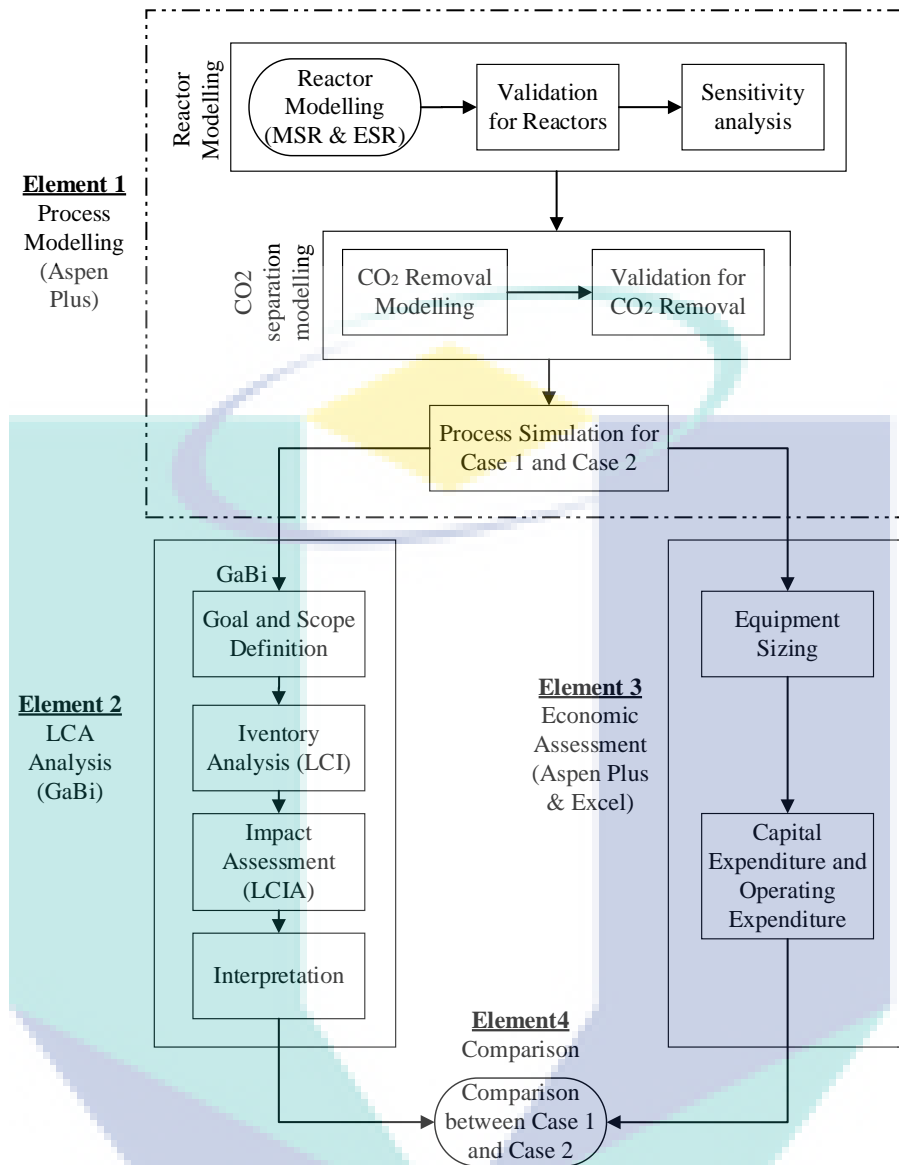


Figure 3.1 Research framework

3.2 Process Description

Apart from the framework this chapter also presents modelling of two different process for hydrogen production synthesis namely Case 1 as hydrogen production from methane and Case 2 as hydrogen production form ethanol. All models were developed in Aspen Plus 8.6. This chapter starts from general process flow diagram (PFD) of both processes followed by reactor modelling and its sensitivity analysis. Separation model for CO₂ removal were also included in the modelling work. The design capacity is to

produce 10000 MT/annum of hydrogen. A complete flowsheet of both processes and its results were presented and compared at latter part of this chapter.

3.2.1 Hydrogen production from methane (Case 1)

In Case 1 methane from natural gas is considered as the raw material. This process is illustrated in the Figure 3.2. The natural gas stream which consists of pure methane at 25 °C and 1 atm was mixed with steam at 1000 °C and 2 atm. Mass flow rate of methane and steam are 2550 kg/hr and 8000 kg/hr respectively (Boyano et al., 2012). The mixed gas are then heated to 700 °C by a heat exchanger (E-101) using hot flue gas . The mixed gas then entered the MSR (R-101) reactor which operates isothermally around 700 °C at 1 atm. In the reactor, methane reacts with steam to produce hydrogen and carbon monoxide using Ni-based catalyst. The reaction products namely hydrogen, carbon monoxide and excess steam are then cooled in the heat exchanger (E-102) until temperature reaches 400 °C. It is then mixed with steam before going through two WGS reactor; high temperature WGS (R-102) and low temperature WGS (R-103), to increase hydrogen yield and therefore reduce carbon monoxide in the stream. The high temperature WGS operates adiabatically at a pressure of 1 bar and temperature of 400 °C using comercial CuO/ZnO/Al₂O₃ catalyst. After the high temperature WGS reactor, the stream is cooled down to 210 °C using cooling water in the heat exchanger (E-103) before entering the low temperature WGS reactor. The low temperature WGS reactor operates adiabatically at pressure of 1 bar and temperature of 210 °C using comercial CuO/ZnO/Al₂O₃ catalyst (Amadeo & Laborde, 1995; Antzara et al., 2014). The products stream then cooled down to 40 °C in heat exchanger (E-104) using cooling water. After that, the stream is fed into a packed bed absorption tower (T-101) to remove carbon dioxide using monoethanolamine (MEA) solution at 40 °C at a pressure of 2 bar. The flow rate of MEA entering the tower is 7000 kmol/hr. The number of stages for the absorption tower is 20 filled with 4X Flexipac type packing. The carbon dioxide absorbed by MEA flows via RICH-OUT stream which then heated by heat exchanger (E-105) using high pressure steam before entering the stripping column. The top product stream is then cooled down in heat exchanger (E-106) before entering a flash column (V-101). In the flash column, hydrogen and water are separated in which 93 % of hydrogen mole flows at the top of the column whereby water flows at the bottom. For the stripping section (T-102), the number of stage in the stripper is 20 filled

with 4X Flexipac type packing equipped with reboiler and condenser. The reflux ratio for the stripper is 0.5 and the reboiler duty is 15 MW. The heat provided by the reboiler loosens the MEA-carbon dioxide interaction and thus breaks the bonds and therefore releasing the carbon dioxide via top of the tower. The MEA solution flows out at the bottom of the tower via stream LEAN-OUT.

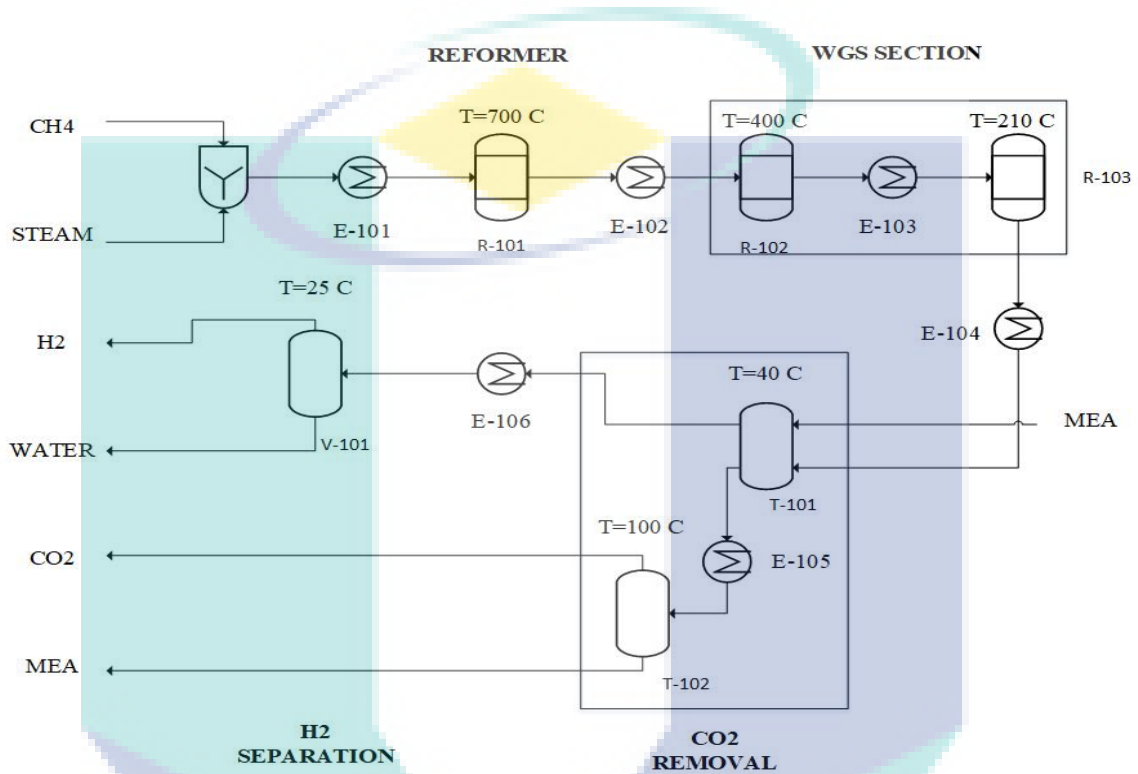


Figure 3.2 Process flow diagram of hydrogen production from methane.

3.2.2 Hydrogen production from ethanol (Case 2).

The process block diagram for Case 2 is illustrated in Figure 3.3. Pure ethanol is fed into the mixer with superheated steam. The ethanol fed flowrate is 4950 kg/hr at 25 °C and 1 atm whereas the steam flowrate is 11000 kg/hr at 1000 °C and 1 atm. The mixture is then heated to 800 °C in heat exchanger (E-201) using hot flue gas before entering ESR reactor. The reactor operates isothermally at temperature of 800 °C and pressure of 1 bar (Gutiérrez-Guerra et al., 2015; Mathure et al., 2007). The reactor used commercial nickel based catalyst and around 300 kg of catalyst are needed to produce high yield of hydrogen. The reaction products namely hydrogen, carbon monoxide, and excess steam are then cooled in heat exchanger (E-202) until temperature reaches 400 °C. It is then mixed with steam before going through two WGS reactor; high

temperature WGS (R-202) and low temperature WGS (R-203), to increase hydrogen yield and therefore reduce carbon monoxide in the stream. The high temperature WGS operates adiabatically at pressure of 1 bar and temperature of 400 °C using commercial CuO/ZnO/Al₂O₃ catalyst. After the high temperature WGS reactor, the stream is cooled down to 210 °C using cooling water in heat exchanger (E-203) before entering the LWGS reactor (R-103). The LWGS reactor operates adiabatically at pressure of 1 bar and temperature of 210 °C using commercial CuO/ZnO/Al₂O₃ catalyst (Amadeo & Laborde, 1995; Antzara et al., 2014). The products stream is then cooled down to 40 °C in heat exchanger (E-104) using cooling water. After the reaction process, the products gas enters an absorption tower to remove carbon dioxide therefore increase hydrogen purity. MEA solution is used to absorb carbon dioxide. The MEA molar flow rate is 13000 kmol/hr with temperature of 40 °C and pressure of 2 bar which flow at the top of the column. The absorption tower (T-201) has 20 stages equipped with structured packing Flexipac 4X with metal as material, the overall packing height section in each section is 0.5 m. The rich solvent leaving the absorber column at the bottom is pump through a heat exchanger (E-205) to be heated up to 112 °C before entering the stripping column. The stripper tower (T-202) has 20 stages including reboiler. Each stage is equipped with the structured packing Flexipac 250Y with metal as material. The height equivalent to theoretical plate used in this stripper is 0.5 m. The reflux ratio is set to 0.5 mole with the reboiler duty being 9000 kW at 112 °C. The released carbon dioxide goes to the top of the column whereas the MEA lean solvent flows out at the bottom of the stripper tower via LEANOUT stream. To achieve the high purity of hydrogen, water in the product stream need to be removed. The gas stream is cool down in the heat exchanger (E-206) at temperature of 25 °C by using cooling water. Then, the water is condensed and separated from the gas in the flash drum (V-201) and the water flows out via the bottom of the separator. The desired product goes to the top of separator to a storage tank at 93 % mole of purity.

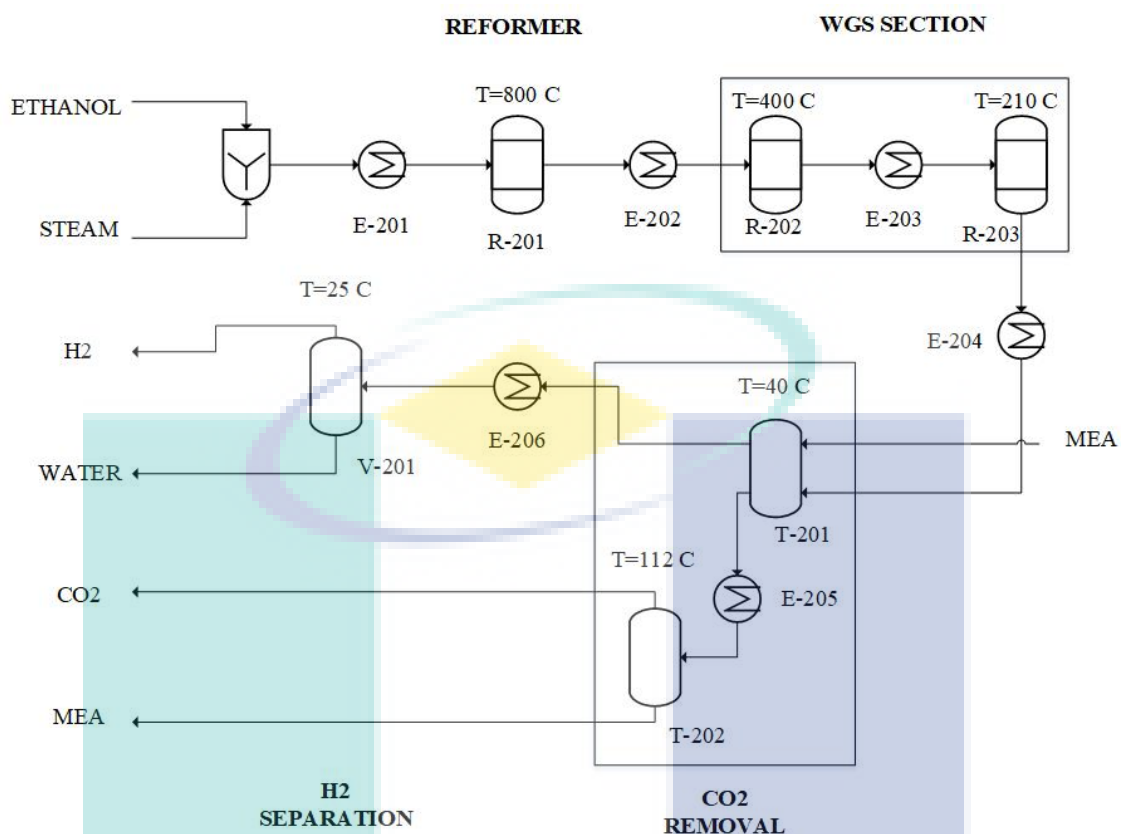


Figure 3.3 Simplified process flow for hydrogen production from ethanol

3.3 Process Simulation

Aspen Plus 8.6 were used to simulate both Case 1 and Case 2. Figure 3.4 and Figure 3.5 shows the process flowsheet developed in Aspen Plus which involves decomposition of the process into its constituent elements for individual study performance. Table 3.1 and Table 3.2 summaries the model blocks used in the flowsheet and its corresponding description. In this simulation, the global thermodynamic model used was ENRTL-RK model while RKSMHV2 model was adopted for MSR and WGS reactor RKSMHV2 (Hanaâ Er-rbib et al., 2014; H. Er-rbib et al., 2014). This thermodynamic model is used for mixtures of non-polar and polar compounds, in combination with light gaseous.

Reactions were model in RPLUG block using LHHW reaction kinetic model. Whereas RADFRAC block were used for the absorption tower and stripper. The absorption and stripper tower are rate-based to model the interaction between carbon dioxide with amine solution. Detail description of the modelling work will be presented

next. Table 3.1 and Table 3.2 are the summaries of the model in simulation for both case studies.

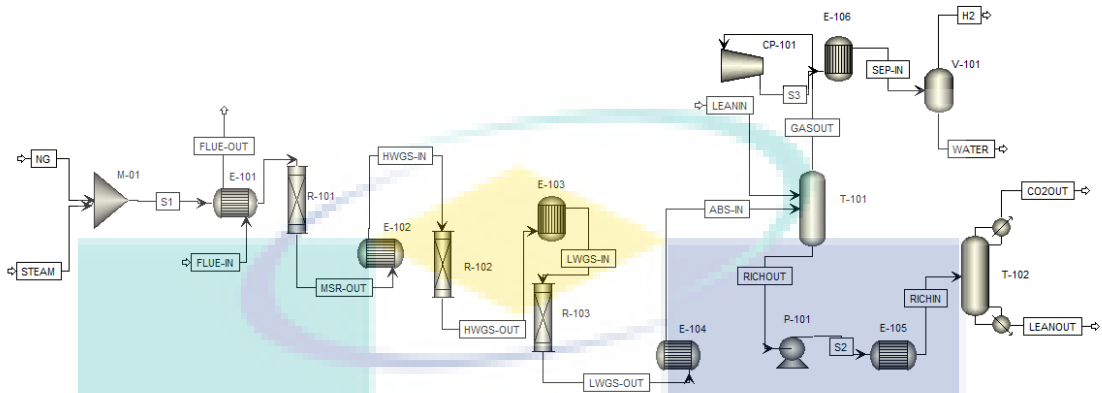


Figure 3.4 Aspen Plus modelling of case 1

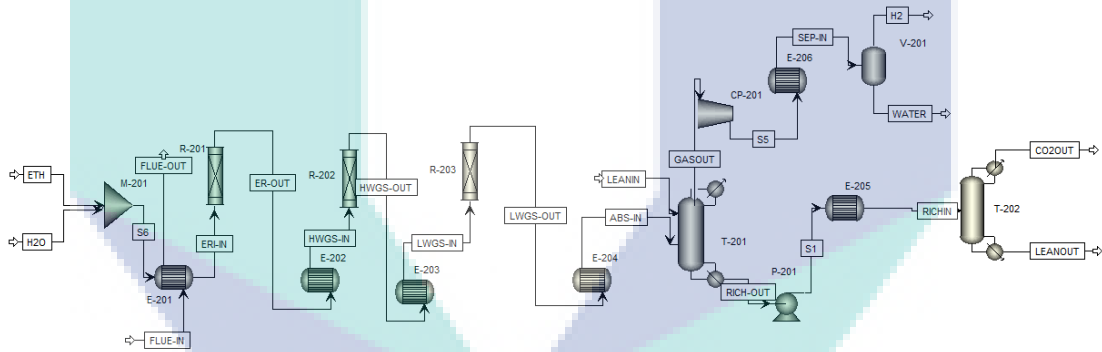


Figure 3.5 Aspen Plus modelling of case 2

Table 3.1 Summaries for Case 1

Id Block	Type Block	Description
M-101	Mixer	Feed methane and steam mixed
R-101	R-Plug	The MSR reaction take placed
R-102	R-Plug	High temperature WGS reaction take placed
R-103	R-Plug	Low temperature WGS reaction take placed
E-101	Heat-X	Supplied the heat to mixed gas until temperature of 700 °C
E-102	Heat-X	Cooled products gas from MSR until temperature of 400 °C
E-103	Heat-X	Cooled products gas from WGS until temperature of 210 °C
E-104	Heat-X	Cooled product gas from WGS until temperature of 40 °C
E-105	Heat-X	Heated the solvent from absorption at temperature of 100 °C
E-106	Heat-X	Cooled down product gas from absorption at temperature of 25 °C
T-101	RadFrac	Absorption tower for CO ₂ removal
T-102	RadFrac	Stripper tower
V-101	Flash2	Separation of water from gas

Table 3.2 Summaries for Case 2

Id Block	Type Block	Description
M-201	Mixer	Feed methane and steam mixed
R-201	R-Plug	The ESR reaction take placed
R-202	R-Plug	High temperature WGS reaction take placed
R-203	R-Plug	Low temperature WGS reaction take placed
E-201	Heat-X	Supplied the heat to mixed gas until temperature of 800°C
E-202	Heat-X	Cooled products gas from ESR until temperature of 400°C
E-203	Heat-X	Cooled products gas from WGS until temperature of 210°C
E-204	Heat-X	Cooled product gas from WGS until temperature of 40°C
E-205	Heat-X	Heated the solvent from absorption at temperature of 100°C
E-206	Heat-X	Cooled down product gas from absorption at temperature of 25°C
T-201	RadFrac	Absorption tower for CO ₂ removal
T-202	RadFrac	Stripper tower
V-201	Flash2	Separation of water from gas

3.3.1 Reactor Modelling

3.3.1.1 Reaction Kinetic, Validation and Sensitivity Analysis for Methane Steam Reforming (MSR)

Hydrogen production using MSR involves reaction between methane and steam to produce hydrogen and carbon monoxide. The reaction occurred in a catalytic fixed-bed reactor with molar ratio CH₄ to H₂O of 1:3. For fast reaction, Ni-based catalyst supported on alumina is commonly used in industry (Fernandes & Soares, 2006). The rate expression for the MSR reaction is based on LHHW reaction mechanism on nickel catalyst as Equation 2.3 in Chapter 2. The equation is as follows:

$$R_{MSR} = k_1 \left(\frac{P_{CH_4} P_{H_2O}}{P_{H_2}^{2.5}} - \frac{P_{CO} P_{H_2}^{0.5}}{K_1} \right) / DEN^2 \quad 3.1$$

However, the rate expression above cannot be used directly in Aspen Plus as the general equation for LHHW used as follows:

$$R = \frac{(kinetic\ factor)(driving\ force)}{adsorption\ term} \quad 3.2$$

Where,

$$\text{kinetic factor} = k \left(\frac{T}{T_0} \right)^n e^{-\left(\frac{E}{R} \right) \left(\frac{1}{T} - \frac{1}{T_0} \right)} \quad 3.3$$

$$\text{driving force} = K_1 \prod_{i=1}^N C_i^\alpha - K_2 \prod_{j=1}^N C_j^\beta \quad 3.4$$

$$\text{adsorption term} = \left[\sum_{i=1}^M K_1 \left(\prod_{j=1}^N C_j^M \right) \right]^m \quad 3.5$$

Where k is pre-exponential factor, T is absolute temperature, T_0 is reference temperature, n is temperature exponent, m is adsorption term exponent, E is activation energy, R is gas law constant, K is constant, N is number of components, M is number of terms in adsorption expression, C is component concentration, i and j are indices, α and β are exponent. Aspen Plus however, the pre-exponential constant, adsorption constant used the following equation instead:

$$K = A \exp\left(\frac{B}{T}\right) T^C \exp(DT) \quad 3.6$$

The equation above does not fit Equation 3.1 and need to be rearranged. Using natural logarithm (Ln) and some rearrangements, the newly rearranged equation is shown below:

$$R_{MSR} = \frac{k_1 K_1 \left[K_1 \frac{P_{CH_4} P_{CO}}{P_{H_2}^{2.5}} - P_{H_2}^{0.5} P_{CO} \right]}{DEN^2} \quad 3.7$$

The term DEN is given by,

$$DEN = 1 + K_{CO} P_{CO} + K_{H_2} P_{H_2} + K_{CH_4} P_{CH_4} + \frac{K_{H_2O} P_{H_2O}}{P_{H_2}} \quad 3.8$$

Table 3.3 shows the kinetic parameter used in Equation 3.7 and its corresponding natural log.

Table 3.3 Kinetic parameter methane steam reforming

Parameter	Ea or ΔH (J/mol)	Ln K
k ₁	240 100	12.39
K ₁	220200	29.69
K _{CH4}	-38280	-7.31
K _{H2O}	88680	12.08
K _{H2}	-82900	-9.70
K _{CO}	-70650	-941

Source: Singh et al. (2014)

To validate the model, the simulated MSR reaction in Aspen Plus were compared with experimental work by Singh et al. (2014). The modelled MSR reactor were based on the operating and design conditions shown in Table 3.4.

Table 3.4 Summaries for operating condition for validation

Parameter	Value
Feed CH ₄ , mol/s	1000
Ratio CH ₄ to H ₂ O	1:2
Temperature, C	700
Pressure, atm	29
Diameter, m	0.1
Length, m	10

Source: Singh et al. (2014)

Figure 3.6(a) shows that conversion of methane for conventional reactor by Singh et al. (2014). The figure shows that methane conversion increase rapidly at the first meter of the reactor length. After that, the conversion started to resolve. The same trend is also found in the simulated MSR reactor in Aspen Plus as shown in Figure 3.6 (b). The highest error was at 1 meter with 11.71 % while the smallest error is at 2 m with 0.53 %. Overall the mean error by using equation 3.9 was 3.27 % and therefore it can be concluded that the modelling approach for MSR is valid.

$$\text{Overall mean error} = \frac{\sum \left[\frac{x_{sim} - x_{lit}}{x_{lit}} \times 100 \right]}{n} \quad 3.9$$

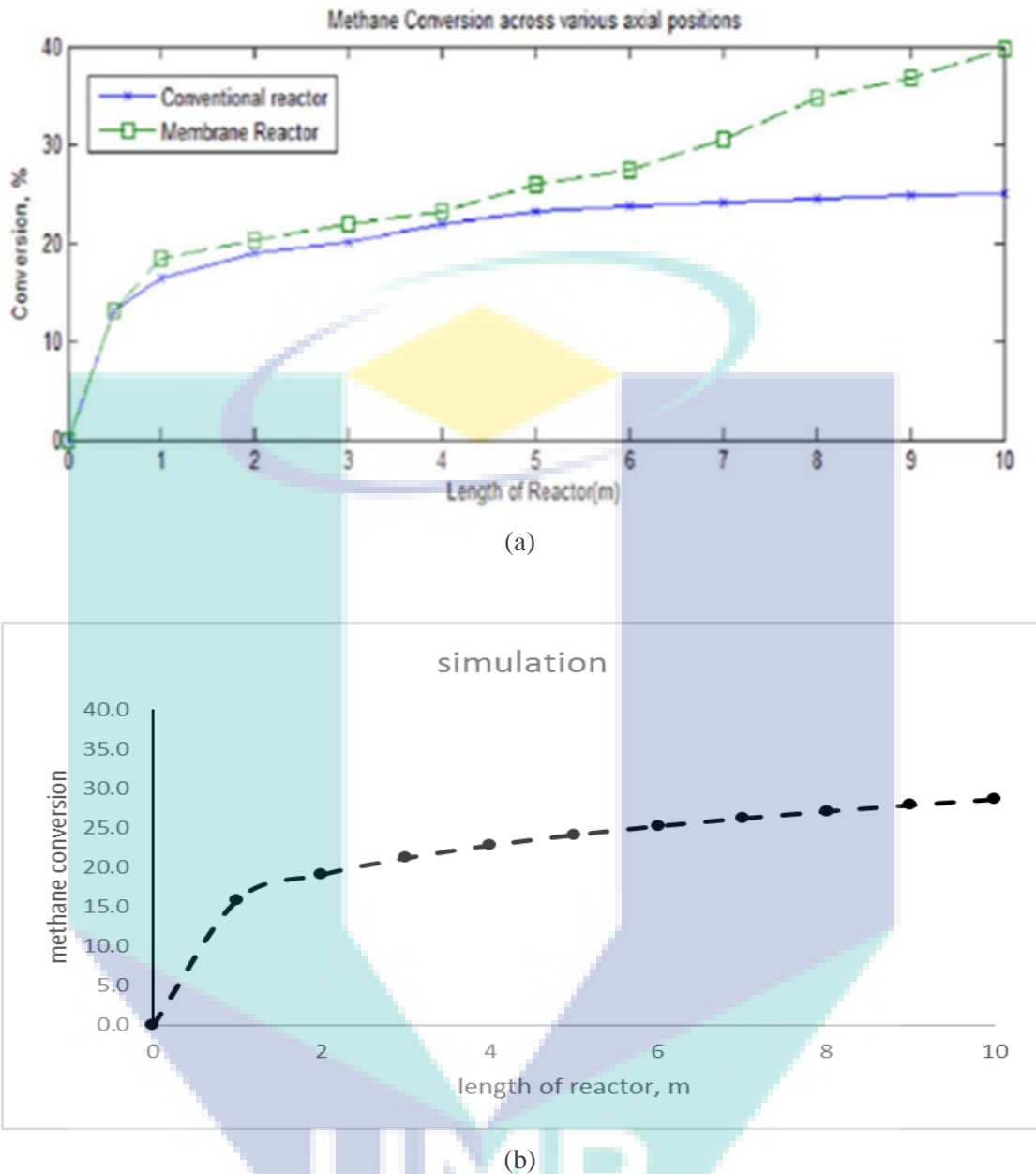


Figure 3.6 The methane conversion effect on length of the reactor (a) from Singh et al (2014) (b) simulation using Aspen Plus

Sensitivity analysis of the reactor performance was done by changing several operation variables namely catalyst weight, reactor temperature, pressure and steam to methane feed ratio into the reactor to observe and determine the suitable operating condition for MSR. For the sensitivity analysis, the manipulated variables were independently varied while the other design parameters remain unchanged. Figure 3.7 shows the sensitivity analysis results for variation in the catalyst weight to hydrogen molar flowrate. It shows that increasing the amount of catalyst in the reformer, increases

the hydrogen flow rate especially at the first 100 kg. However, after about 300 kg of catalyst the hydrogen flow rate starts to become constant. This is because methane totally reacted with steam and had achieved the maximum hydrogen production.

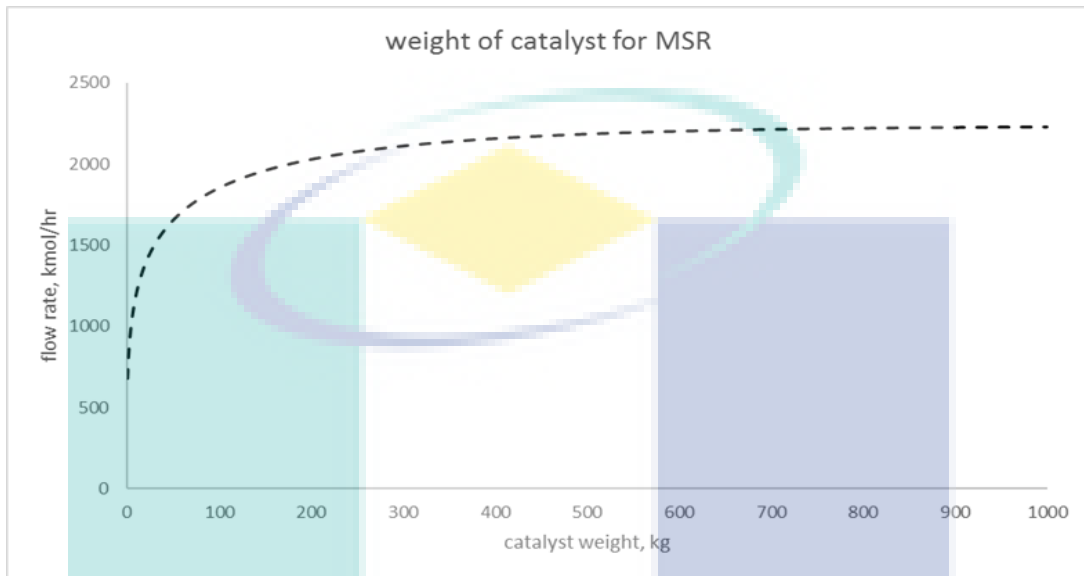


Figure 3.7 Weight of catalyst for MSR effect on molar flowrate of hydrogen

Figure 3.8 on the other hand, shows the response of the hydrogen molar flow rate to MSR reactor temperature increment. Hydrogen started to produce at temperature of 500 °C and increased drastically until the temperature of 700 °C. After that, hydrogen flow rate started to become constant. At this point, all the methane had been converted into hydrogen. This trend also shows that for MSR reaction, the hydrogen produced depends on a certain range of temperature between 500 °C to 700 °C. Increasing the reactor temperature leads to high reforming reaction rate and as a result improved methane conversion and increased the hydrogen yield.

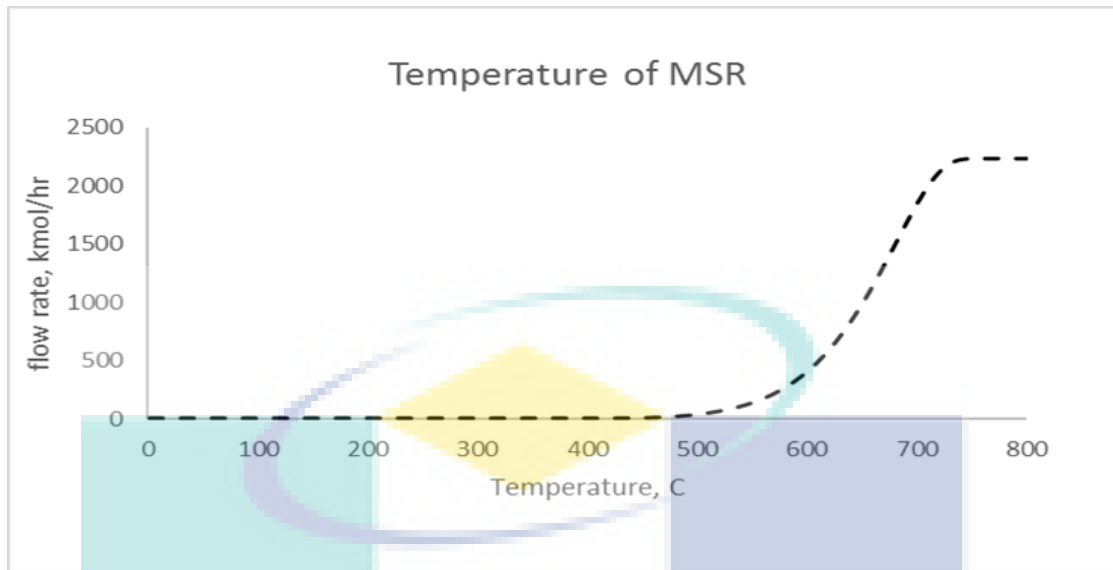


Figure 3.8 Temperature of MSR on molar flowrate of hydrogen.

Figure 3.9 shows the changing of reactor pressure in the reformer to hydrogen molar flowrate. From the results obtained, it is found that when pressure is increased, the hydrogen molar flow rate shows inverse response. The highest hydrogen produced is at 1 bar compared with the pressure of 30 bar. This inverse effect causes methane conversion and yield of the hydrogen to decrease. This phenomenon is called Le Chatelier's principle when the pressure increase has a negative effect on methane conversion (Antzara et al., 2014).

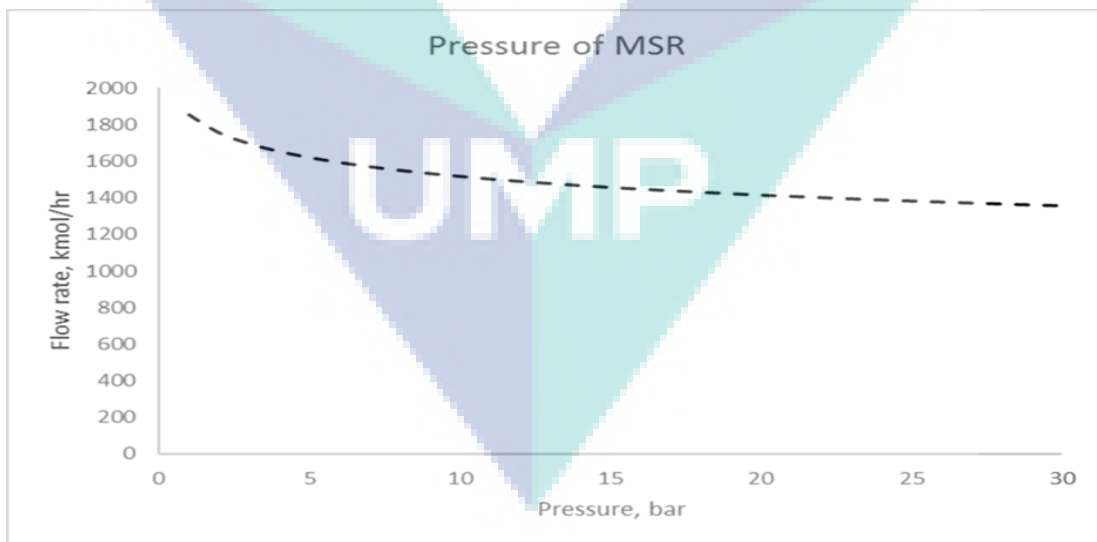


Figure 3.9 The pressure of MSR on molar flow rate of hydrogen

Figure 3.10 shows the effect the conversion of methane to hydrogen towards change in steam to methane feed ratio. When the steam feed flow rate is increased, the

percentage of methane conversion also increased. This shows that the feed ratio is important to ensure the reaction is pushed to the right side thus increase hydrogen flow rate. Moreover, when steam to methane ratio is increased, the energy requirement for the reformer reaction reduces due to the reduced flow rate of methane. Therefore, the methane conversion and hydrogen yield increased with increased in steam to methane ratio.

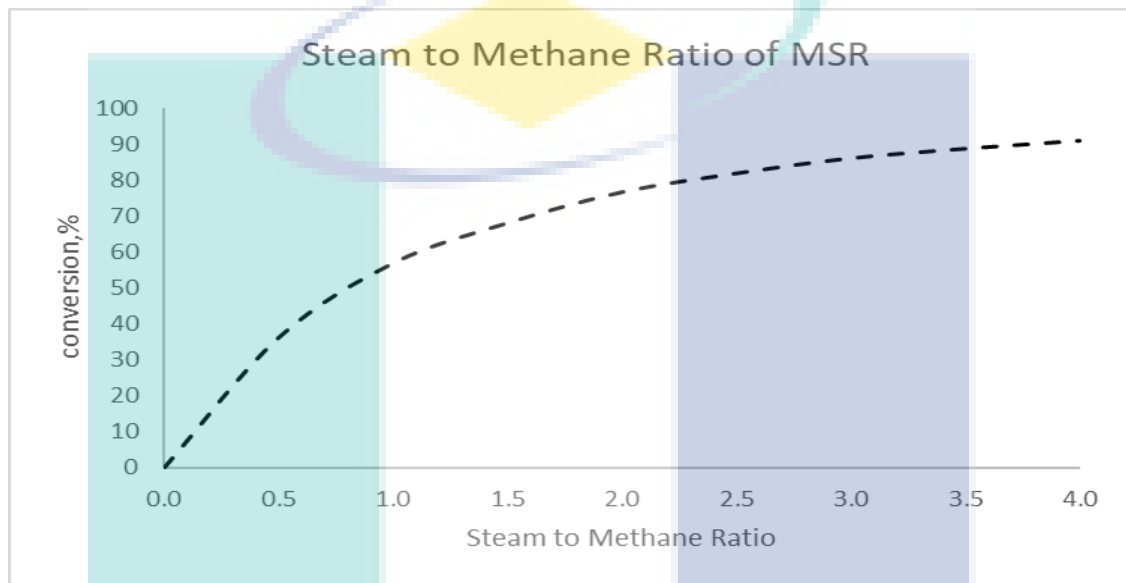


Figure 3.10 Steam feed ratio on conversion of methane

3.3.1.2 Reaction kinetic, validation and sensitivity analysis for Ethanol Steam Reforming (ESR).

ESR reaction can be represented by equation 3.10 and equation 3.11 is the kinetic expression for ESR as follows:-

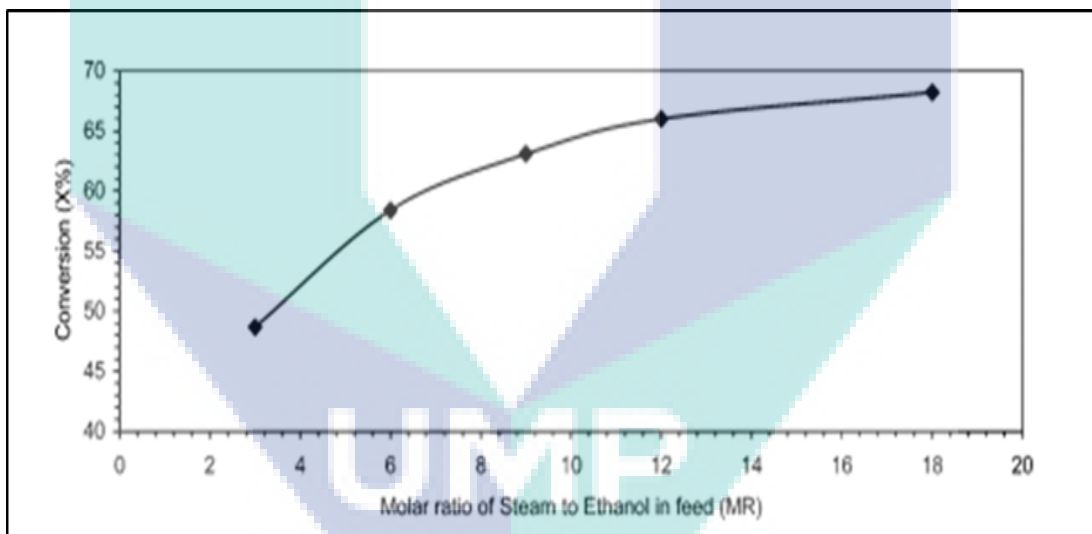


$$R_{EtOH} = 4.39 \times 10^2 \exp\left(-\frac{2.3 \times 10^4}{RT}\right) (P_{EtOH})^{0.711} (P_{H_2O})^{2.71} \quad 3.11$$

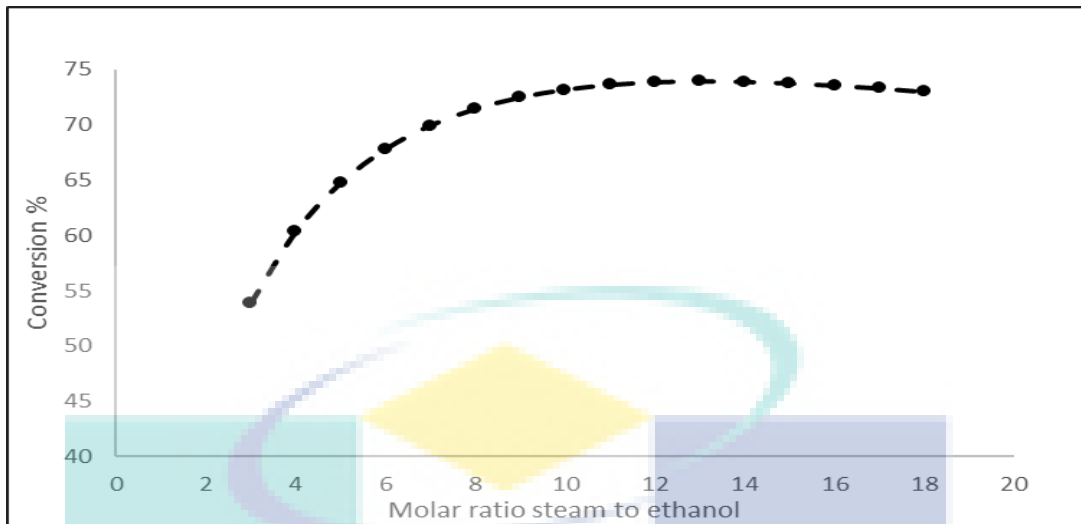
The kinetic model were in the form of simplistic power-law kinetic model by Mathure et al. (2007). However, as for MSR, the general power law model need to be rearranged to fit in Aspen plus kinetic model. The rearranged power law expression for ethanol steam reforming is describe in Equation.3.12.

$$R_{EtOH} = 7.3167 \times 10^5 \exp \frac{-2.3 \times 10^4 \text{ J/mol}}{RT} P_{eth}^{0.71} P_{H_2O}^{2.71}$$

The modelling based on Equation 3.12 was validated by previous study by Mathure et al. (2007) using the same design and operating conditions. The reactor diameter is 15 mm and the length is 40 mm whilst, the reactor temperature and pressure is 600 °C and 1 atm respectively. The mass of the catalyst is 35 g with the feed molar flow rate is 1 mol/min. Figure 3.11 (a) shows the results from Mathure et al. (2007) whereby the ethanol conversion is increased when the molar ratio of the steam in increased. The highest conversion is obtained at 18 molar ratio of steam to ethanol with conversion up to 69%. Figure 3.11 (b) on the other hand shows the results of the simulated model. The highest error was molar ratio at 6 with 14.9% and the smallest error was molar ratio at 18 with 7.3%. Then, the mean error for this validation was 12% of error.



(a)



(b)

Figure 3.11 The effect of molar ratio of steam to ethanol (a) from previous study (b) from simulation using Aspen Plus.

Source: Mathure et al (2007)

For the sensitivity analysis, the capacity of the reactor have increased at 10000 MTonne/annum. The purpose for this analysis, to observe and determined the suitable condition of the reactor. The sensitivity analysis for ESR reactor is to observe the output flow rate of hydrogen by manipulating the catalyst weight, reactor temperature, reactor pressure and steam to ethanol feed ratio. The simulation approach is the same as in MSR. Figure 3.12 shows the effect of increasing the amount of catalyst in the reformer. The graph shows that the molar flow rate of hydrogen is increased continuously when the amount of catalyst is increased. The maximum molar flow rate of hydrogen can be achieved is 2500 kmol/hr at 1000 kg of catalyst.

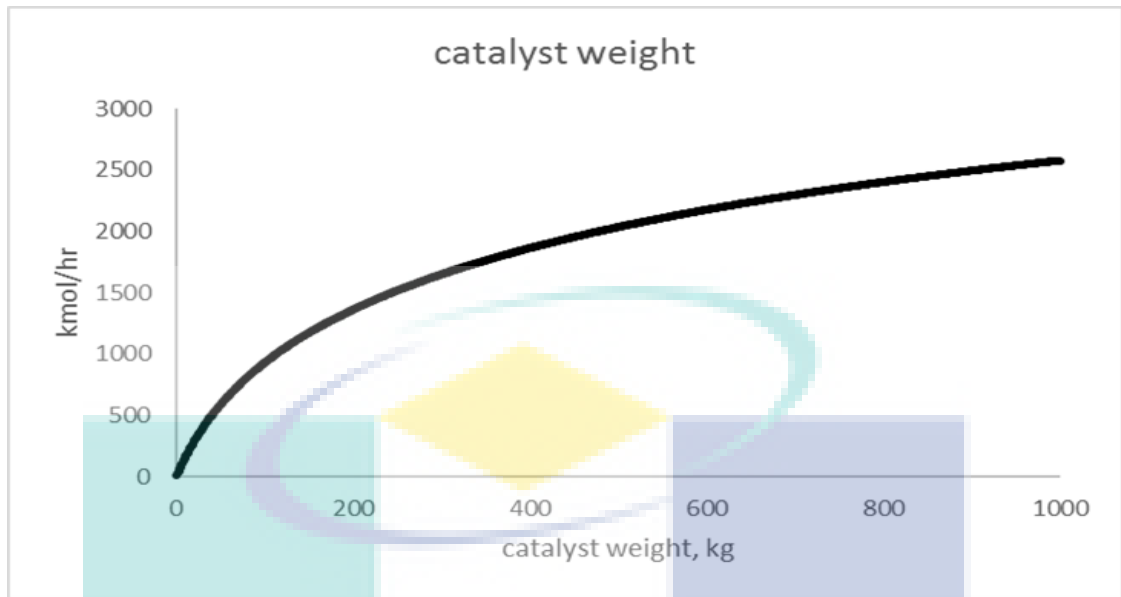


Figure 3.12 Catalyst weight effect on molar flowrate of hydrogen

The temperature effect on hydrogen molar flow rate of hydrogen is shown in Figure 3.13. From the result obtained, hydrogen flow rate started to increase at 600 C with the maximum flow rate is 1700 kmol/hr. After that, the molar flow rate started to decline a little from temperature of 600 C to 1000 C. On the other hand, Figure 3.14 illustrates the change of pressure in the reformer to hydrogen flow rate. From the results, it shows that the hydrogen flow rate increased rapidly when the pressure is increased from 1 bar to 3 bar. After that, the flow rate of hydrogen remain unchanged although the pressure is increased from 3 bar to 30 bar. The reason the hydrogen produced is unchanged from the pressure 3 bar to 30 bar because the ethanol is totally reacted with steam and had achieved the maximum yield of hydrogen.

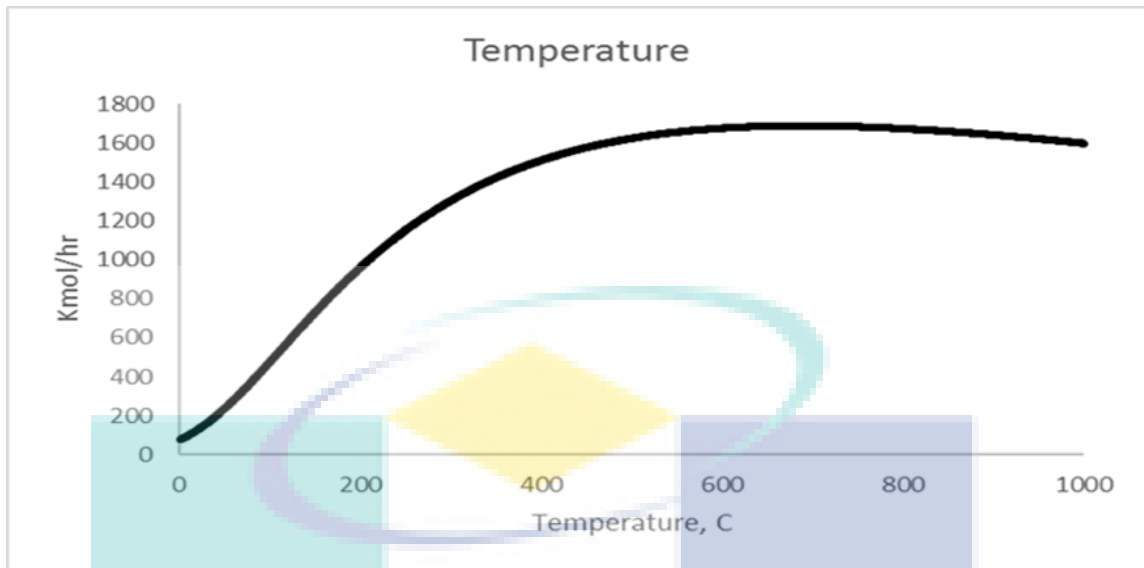


Figure 3.13 Temperature of ethanol reforming on molar flowrate of hydrogen

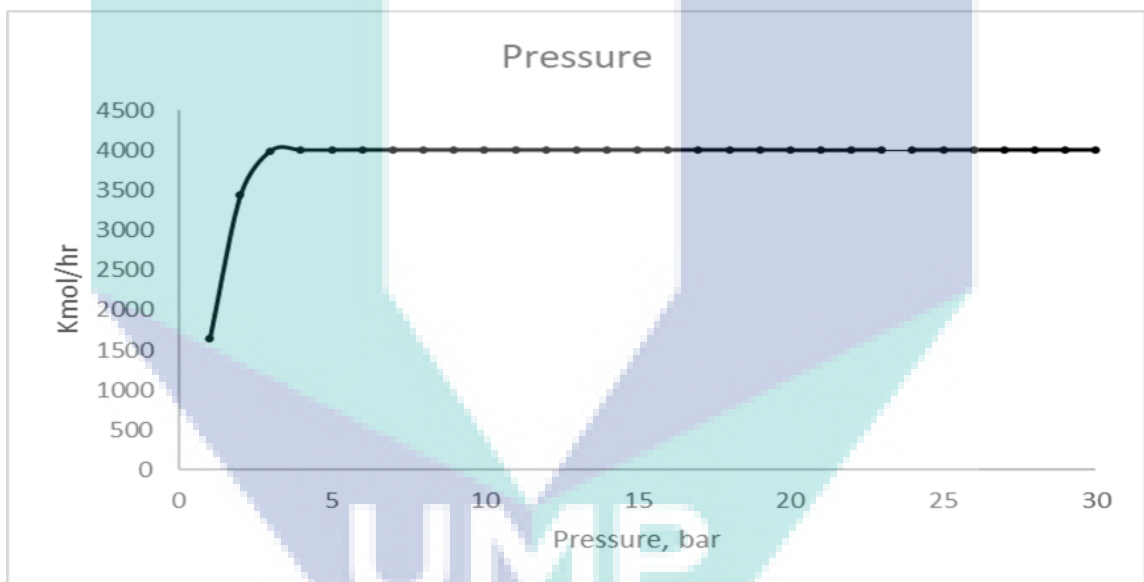


Figure 3.14 The effect of pressure on molar flowrate of hydrogen.

To analyse the effect of steam to ethanol feed ratio, the steam flow rate is increased while maintaining the flow rate of ethanol. Figure 3.15 illustrates that increase of hydrogen productivity is evident with the increasing water feed. Ethanol conversion is increased to 45% when the steam to ethanol feeding ratio is 4. Therefore, the use of diluted ethanol is an effective tool to improve hydrogen yield because to lower the impact of methanation and other side reaction such as acetaldehyde formation (Authayanun et al., 2015).

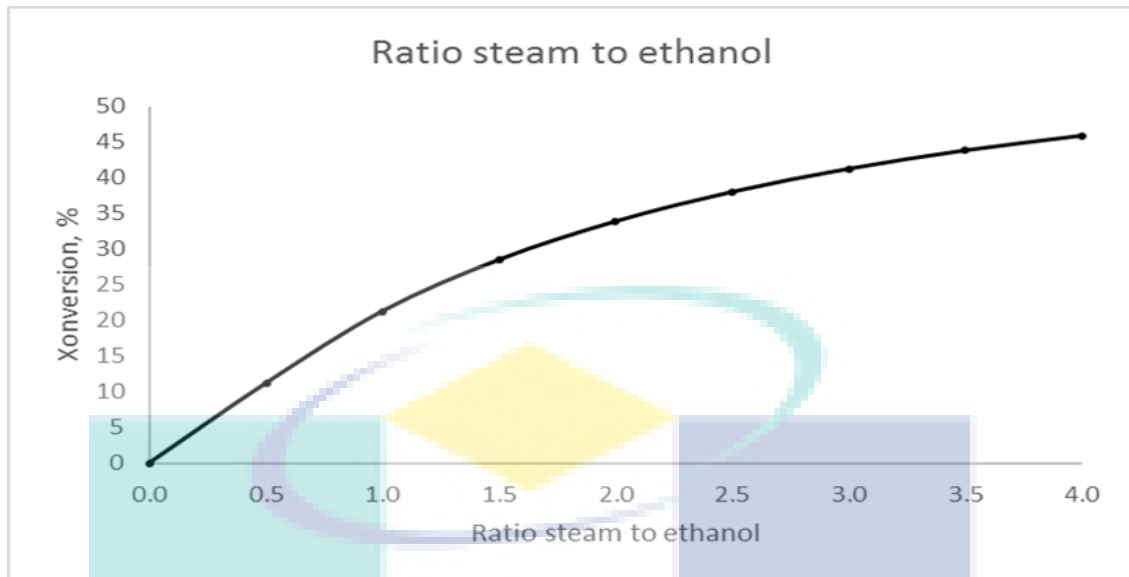


Figure 3.15 The steam ratio feed to ethanol effect on conversion of hydrogen

3.3.1.3 Reaction kinetic, validation and sensitivity analysis for water gas shift (WGS)

As for MSR and ESR reaction, the rate expression for WGS reaction also needs to be rearranged as shown in equation 3.8.

$$R_{WGS} = \pm \frac{k_2(P_{CO}P_{H_2O} - \frac{P_{CO_2}P_{H_2}}{K_e})}{(1 + K_1P_{CO} + K_2P_{H_2O} + K_3P_{CO_2} + K_4P_{H_2})^2} \quad 3.13$$

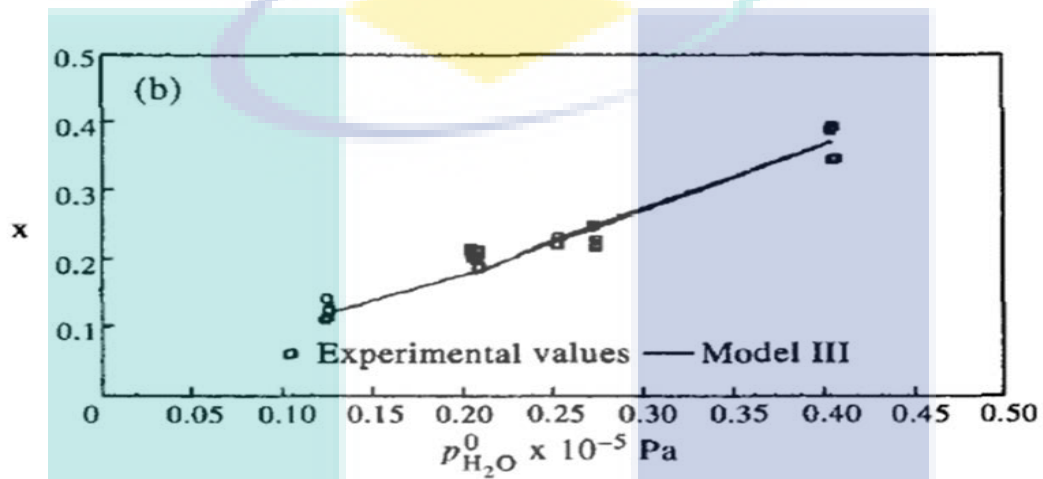
Table 3.5 Kinetic parameter for water gas shift

Parameter	Ea or ΔH (J/mol)	Ln K
k_2	4080	-
K_1	-910	0.79
K_2	-1420	-0.92
K_3	-24720	-5.36
K_4	-14400	-2.96

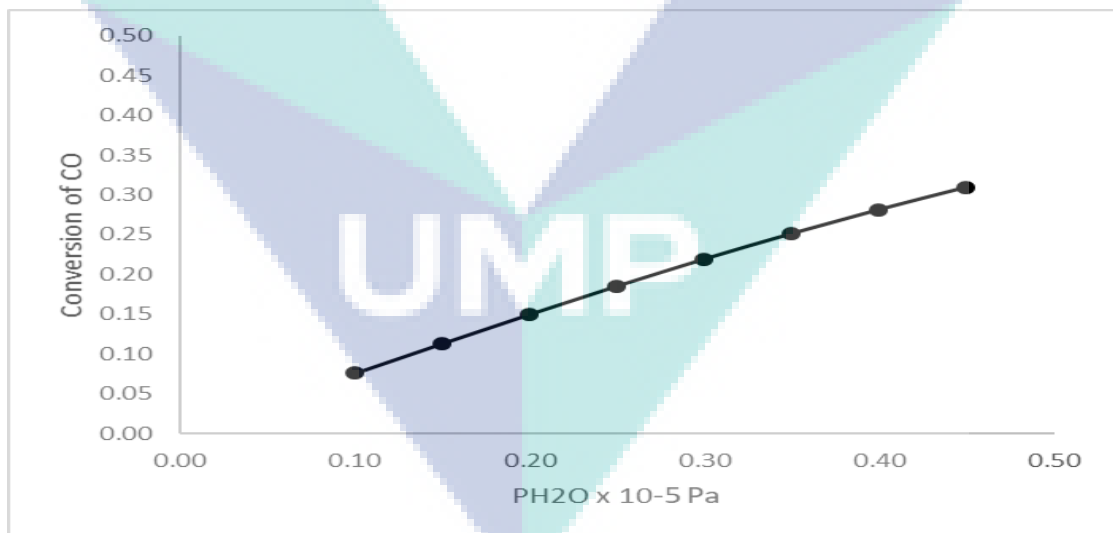
Source: Amadeo and Laborde (1995)

The parameter used in the model validation was based on the work by Amadeo (1995). Figure 3.16 (a) shows the experimental results by Amadeo (1995). It shows the relationship between the partial pressure of feed water into the reactor with the conversion of carbon monoxide. The RPLUG block model is set to have the same design parameters as in the experimental work which includes the operating condition,

catalyst specification and component flow rate. The hydrogen feed is 3.604 ml/s and carbon monoxide flow rate is 0.983 ml/s. The result from the simulation shows; refer to Figure 3.16(b), an agreement with the experimental data which indicate that with increased partial pressure of water the conversion of carbon monoxide to carbon dioxide will also increase. The highest error in this model was 21.70% at partial pressure of water at 0.30×10^{-5} Pa. For the lowest error was 2.75% at pressure of 0.15×10^{-5} Pa. The mean error for this validation was 13.87%.



(a)



(b)

Figure 3.16 Partial pressure of water effect on conversion of carbon monoxide (a) previous study (b) from simulation.

Source: Singh et al. (2014)

For sensitivity analysis several parameters were varied as with previous model namely catalyst weight, reactor temperature, reactor pressure and feed steam to carbon monoxide ration. The respond for carbon dioxide flow rate with different amount of catalyst is shown in Figure 3.17. The increment in catalyst weight is caused the increment the carbon dioxide produced. The results show that at 50 kg of catalyst produced 580 kmol/hr of carbon dioxide. Then, the carbon dioxide produced starts to be constant after 50 kg of catalyst. This is because the carbon monoxide is totally reacted with the steam to produce carbon dioxide.

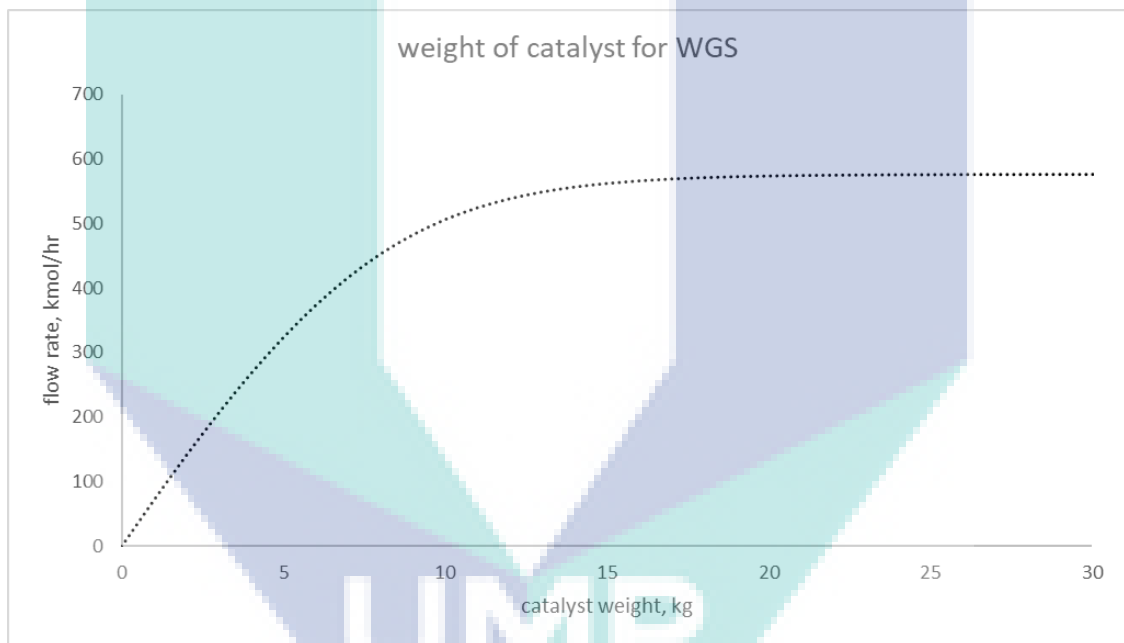


Figure 3.17 Sensitivity analysis of catalyst weight on molar flowrate of carbon monoxide

Figure 3.18 shows the effect of reactor temperature in which increase in temperature causes a dropped in carbon dioxide molar flow rate. The hydrogen molar flow rate gradually decreased from zero C until 1000 C. The WGS is intrinsically an exothermic reaction. So, based on Le Chatelier's principle that equilibrium constant decreases with increase in temperature thus lower down the conversion of carbon monoxide at the higher temperature (Chen et al., 2008).

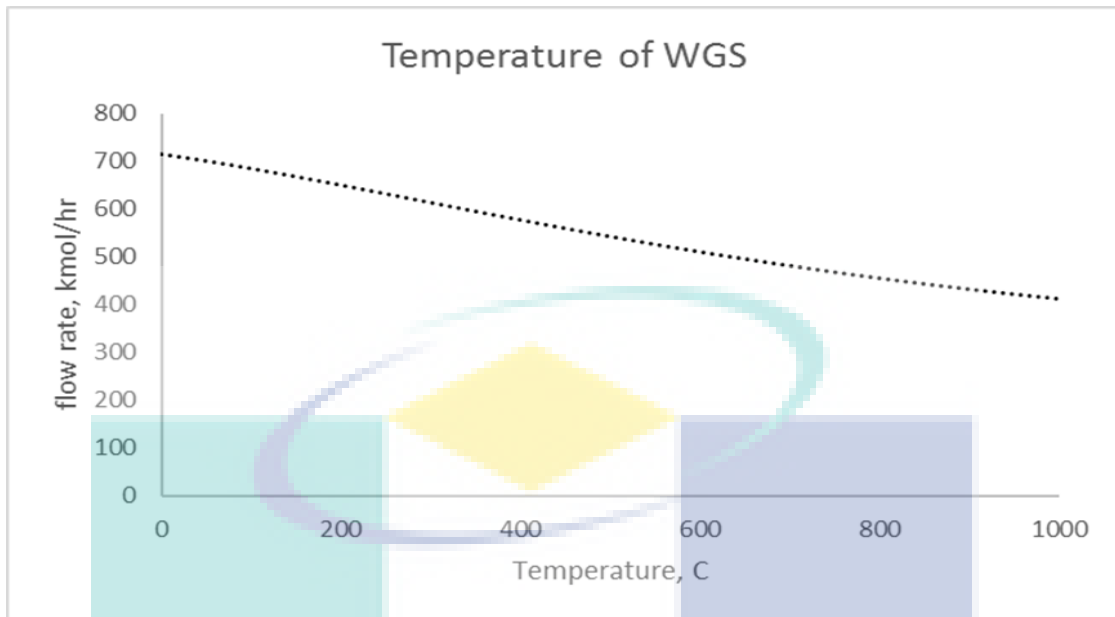


Figure 3.18 Sensitivity analysis of temperature on the molar flowrate of carbon monoxide.

Figure 3.19 on the other hand, shows the effect of reactor pressure. Carbon dioxide flow rate increased when pressure is increased. However, the increment is small and not significant in increasing the yield of carbon dioxide. The molar ratio of steam to carbon monoxide versus the carbon monoxide conversion to carbon dioxide is shown in Figure 3.20. The results show that, diluted carbon monoxide yield higher hydrogen and carbon dioxide flow rate. The maximum conversion can be achieved is 25% with feed molar ratio of 4. Higher value will have no significant effect on the conversion. This work is shown agreement by Haarlemmer (2015) with the pressure play as minor role in the reaction and to increase the conversion of CO by increasing the steam ratio.

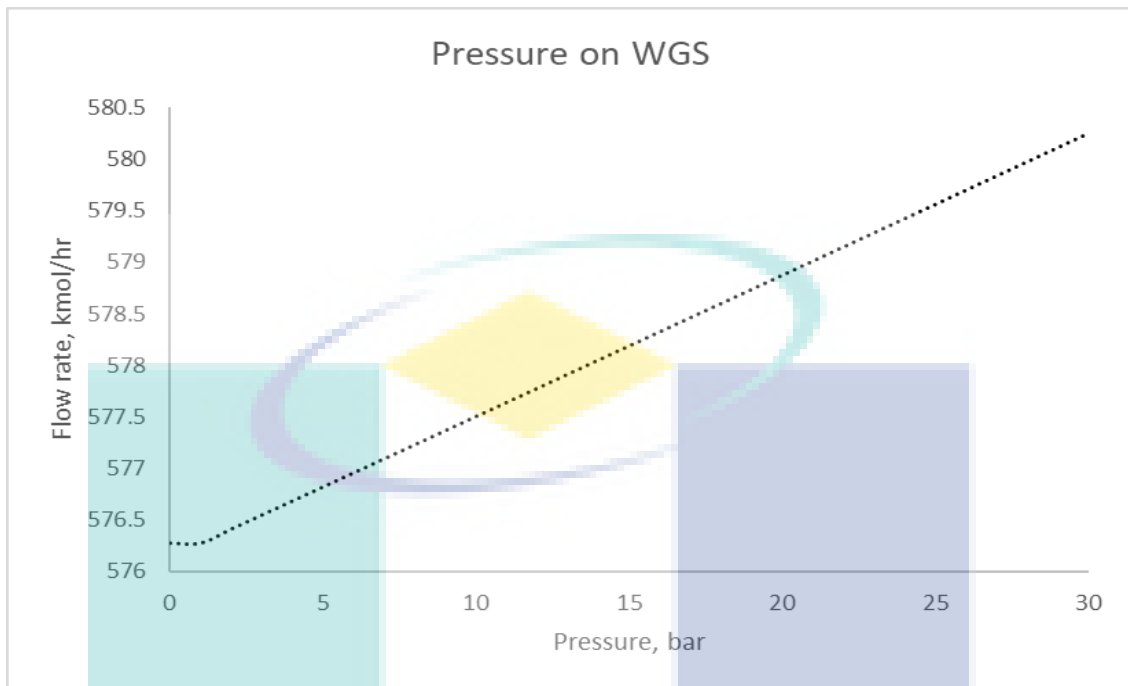


Figure 3.19 Sensitivity analysis of pressure on molar flowrate of carbon monoxide

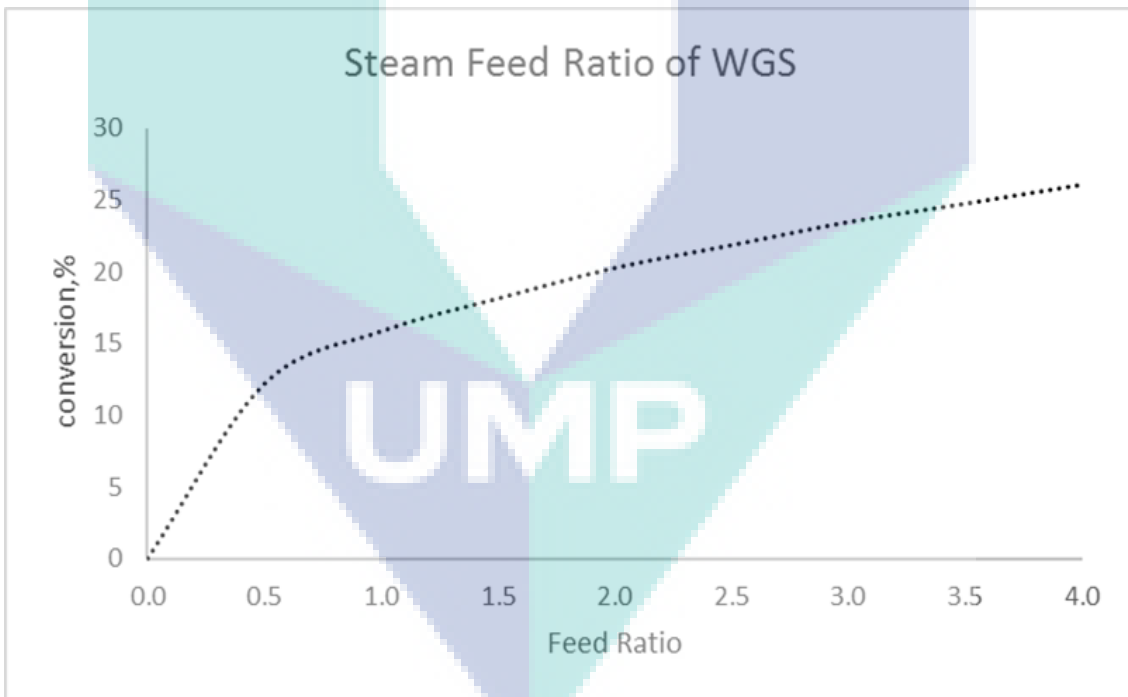


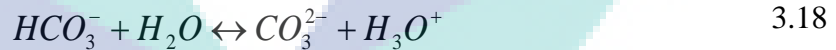
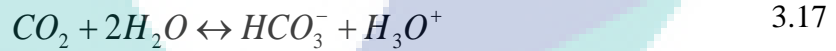
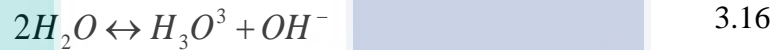
Figure 3.20 Sensitivity analysis of ratio steam to ethanol on the conversion of carbon monoxide.

3.3.2 Separation model

The purpose of separation is to increase the purity of hydrogen. In this work, absorption tower and stripper were used to separate carbon dioxide from the mixed gas to obtain high purity of hydrogen, >90 mol%. Aqueous monoethanolamine (MEA) were used as the solvent. Rigorous distillation model; RADFRAC, were used to model the absorption and stripping column.

3.3.2.1 Kinetic model

The rigorous model to the liquid and vapour flow in the absorption column were based on the calculation of heat transfer, mass transfer between the phases and chemical kinetics. A summary of the chemistry model is shown in Equation 3.14– 3.22 (Inc, 2014; Li et al., 2016).



In this model, it is assume NOx and SOx are neglected in the gas stream. In the separation model, the apparent (base) approach component was selected for electrolyte system. The electrolytes system has impacts on physical property calculations and phase equilibrium calculations. The electrolytes system is defined as one in which some of the molecular species dissociate partially or completely into ions in a liquid solvent and

some of the molecular species precipitate as salts. These dissociation and precipitation occurs fast enough that the reactions can be assume to be at chemical equilibrium. Reaction 3.14 - 3.18 is calculated from the standard Gibbs free energy change whereas reaction 3.16 - 3.22 used the following power law expression for the rate-controlled reaction.

$$r = k \left(\frac{T}{T_0} \right)^n \exp \left[\left(\frac{-E}{R} \right) \left(\frac{1}{T} - \frac{1}{T_0} \right) \right] \prod_{i=1}^N (x_i y_i)^{a_i} \quad 3.23$$

Where the r is rate of reaction, k is pre-exponential factor, T is absolute temperature, T_0 is reference temperature, n is temperature exponent, E is activation energy, R is universal gas constant, N is number of the components in the reaction, x_i is mole fraction of components i , y_i is activity coefficient of component i , a_i is the stoichiometric coefficient of component i in the reaction equation. The kinetic parameters for the reactions are shown in Table 3.6.

Table 3.6 Kinetic parameters for the kinetic reactions in absorber and stripper

Reaction No	k	E, (cal/mol)
3.19	1.33e17	13249
3.20	6.63e16	25656
3.21	3.02e14	9855.8
3.22 (for absorber)	5.52e23	16518
3.22 (for stripper)	6.50e27	22782

Source: Li et al. (2016)

3.3.2.2 Validation of CO₂ Removal

The flowsheet for CO₂ capture by MEA have been developed in Aspen Plus which include absorption column, stripping column and a heat exchanger between the two columns as shown in Figure 3.21. With regards to the convergence issue, it is assumed that the model have no recycle stream, no mark-up stream for amine and water washing section present in the systems. The model was validated with the work by Li et al. (2016) using the design and operating parameters listed in Table 3.7. The results of the simulated model are shown in Table 3.8. Errors were less than 6% except for O₂ in the GasOut stream with 14.37%. The mean error for this simulation was 2.53%.

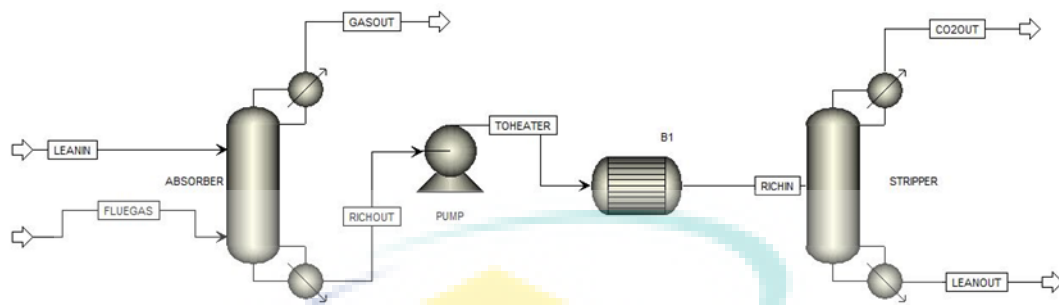


Figure 3.21 The simulation flowsheet for CO₂ removal

Table 3.7 Summaries of design and operating condition for validation

Equipment	Parameter	Value
Absorber	No of stage	20
	Pressure, bar	0.98
	Packed Height, m	4.2
	Section Diameter, m	0.125
	Size packing	250Y
	Type packing	Flexipac
Stripper	No of stage	20
	Distillate rate, kg/hr	6.93
	Reboiler duty	7.048 kW
	Pressure, bar	1.99
	F (kg/hr)	4.86
	Packed height, m	2.5
	Size packing	250Y
	Type of packing	Flexipac
	Section diameter,m	0.125

Table 3.8 Comparison of Li et al. (2016) and simulation results

Stream	Comp	Li et al. (2016)	Simulation	Error
GasOut	N ₂ (kg/kg)	0.798	0.7973	0.08
	O ₂ (kg/kg)	0.1085	0.0929	14.37
	H ₂ O (kg/kg)	0.0743	7.51E-02	1.07
	CO ₂ (kg/kg)	0.0191	0.0191	0.15
	F(kg/hr)	67.03	67.08	0.08
CO ₂ Out	H ₂ O	0.0043	4.32E-03	0.57
	CO ₂	0.9943	0.9943	0
	N ₂	0.0011	1.13E-03	3.13
	O ₂	0.0003	2.82E-04	5.88
	F (kg/hr)	4.86	4.86E+00	0.01

3.3.3 Overall Flowsheet Simulation Results

Based on the reaction and separation model that have been developed and validated, a full flowsheet for both process were simulated. Figure of the full flowsheets are shown in Figure 3.4 and Figure 3.5. This section summarizes the simulation result for Case 1 and Case 2. The results include summary of selected input output streams and the summary of the unit operation design parameters.

3.3.3.1 Case 1

Summary of the equipment is shown in Table 3.9 whereas Table 3.10 shows summary of the process streams and this result obtained from simulation. The former will be used for calculating the capital cost and operating cost. The natural gas contain pure methane (NG) was feed into the reformer at 158.7 kmol/hr. Methane then reacted with 444 kmol/hr of steam (STEAM) to produce 624.69 kmol/hr hydrogen (H₂). Furthermore, the solvent consumed is 301 kmol/hr for removal acid gas in the gas stream with the mole fraction MEA is 0.04 and the mole fraction for water is 0.90. In addition, with this amount of solvent can only recover up to 92% of CO₂ in the gas stream. It is only can absorbed 737.21 kmol/hr of CO₂ from the total CO₂ produced in the process. The CO₂ out from the stripper is high compared with total CO₂ produced from the reaction process. The reason behind this phenomenon occurred because it causing from the reaction between MEA with water such as reaction 3.22 that produced the CO₂. Meanwhile, the H₂ gas is flow out from the absorption tower with total mass flow rate of 624.69 kmol/h or 10000 MTA. The calculation for converting kmol/hr to MTA is shown in eq 3.24 and eq 3.25. The purity hydrogen can have collected is 93 % by mole fraction without doing optimisation.

$$\frac{624.69 \text{ kmol}}{\text{hr}} \times \frac{2.0159 \text{ kg}}{\text{kmol}} \times \frac{24 \text{ hr}}{1 \text{ day}} \times \frac{330 \text{ days}}{1 \text{ yr}} = \frac{9,973,755.56 \text{ kg}}{\text{yr}} \quad 3.24$$

$$\frac{9,973,755.56 \text{ kg}}{\text{yr}} \approx 10000 \text{ MTA} \quad 3.25$$

Table 3.9 Summaries results for the simulation

Block ID	Parameter	Value
E-101	Area of heat exchanger, m2	1.99
	Heat Duty, kW	2794.9
E-102	Area of heat exchanger, m2	6.33
	Heat Duty, kW	2794.9
E-103	Area of heat exchanger, m2	9.78
	Heat duty, kW	2595.22
E-104	Area of heat exchanger, m2	73.83
	Heat Duty, kW	2868.17
E-105	Area of heat exchanger, m2	68.27
	Heat duty, kW	8507.21
E-106	Area of heat exchanger, m2	133.7
	Heat duty, kW	2954.21
R-101	Residence time, s	10
	Heat duty, kW	9928.09
	Catalyst weight, kg	160
R-102	Residence time, s	8.5
	Heat duty, kW	-1.01E-09
	Catalyst weight, kg	430
R-103	Residence time, s	10
	Heat duty, kW	5.93E-09
	Catalyst weight, kg	300
T-101	No of stages	20
	Size of packing	4X
	Material	Metal
	Type of packing	Flexipac
	HETP, m	0.5
	Column diameter, m	1.47
T-102	No of stages	20
	Reflux ratio, mole	0.5
	Reboiler duty, kw	15000
	Size of packing	4Y
	Packing material	Metal
	Type of packing	Flexipac
V-101	HETP, m	0.4
	Vapour fraction	0.8461
	Heat duty, kW	172.29

Table 3.10 Summary stream table for hydrogen production for Case 1

Stream	NG	Steam	Leanin	H2	Water	CO2out	Leanout
Molar flowrate, kmol/hr							
MEA	0	0	301.84	1.49E-06	0.0026	0.016	285.23
H ₂ O	0	444.07	6119.71	21.38	121.54	737.21	5369.53
CO ₂	0	0	0.001	11.43	0.00126	121.52	0.093
CO	0	0	0	11.76	3.80E-5	0.0047	4.75E-27
H ₂	1.6	0	0	624.69	0.0017	0.26	4.75E-27
CH ₄	158.7	0	0	0	0	0	0

Comp								
MEA	0	0	0.04	2.23E-9	2.12E-5	1.81E-5	0.05	
H ₂ O	0	1	0.90	0.02	0.99	0.86	0.89	
CO ₂	0	0	1.47E-7	0.018	1.03E-5	0.14	1.53E-5	
CO	0	0	0	0.018	3.12E-7	5.53E-6	7.82E-31	
H ₂	0.01	0	0	0.93	1.36E-5	3.00E-4	7.82E-31	
CH ₄	0.99	0	0	0	0	0	0	

3.3.3.2 Case 2

The summaries result simulation for equipment in this case is shows in the Table 3.11 . Meanwile, Table 3.12 is the summaries streams results this case. These results also obtained from simulation using Aspen Plus.

Table 3.11 Summaries of results for simulation.

Block ID	Parameter	Value
E-201	Area of heat exchanger, m2	78.7
	Heat Duty, kW	3288.58
E-202	Area of heat exchanger, m2	10.62
	Heat Duty, kW	5260.58
E-203	Area of heat exchanger, m2	13.03
	Heat duty, kW	3615.94
E-204	Area of heat exchanger, m2	142.29
	Heat Duty, kW	5216.96
E-205	Area of heat exchanger, m2	124.69
	Heat duty, kW	17391.4
E-206	Area of heat exchanger, m2	68.11
	Heat duty, kW	1496.06
R-201	Residence time, s	10.8
	Heat duty, kW	8142.73
	Catalyst weight, kg	300
R-202	Residence time, s	5.86
	Heat duty, kW	-1.52E-07
	Catalyst weight, kg	250
R-203	Residence time, s	8.83
	Heat duty, kW	9.88E-08
	Catalyst weight, kg	430
T-201	No of stages	20
	Size of packing	4X
	Material	Metal
	Type of packing	Flexipac
	HETP, m	0.5
T-202	Column diameter, m	1.48
	No of stages	20
	Reflux ratio, mole	0.5
	Reboiler duty, kw	9000
	Size of packing	250Y
	Packing material	Metal

V-201	Type of packing	Flexipac
	HETP, m	0.5
	Vapour fraction	0.96
	Heat duty, kW	172.38

In the Table 3.12, the summaries of the stream table for hydrogen production in mole flowrate from ethanol by simulation using Aspen Plus 8.6. From the results obtained, the raw materials needed was 107.45 kmol/hr of ethanol and 610 kmol/hr of steam in producing hydrogen at 10000 Mtonne per annum. The solvent consumed 561.11 kmol/hr of MEA to remove acidic gas and the efficiency is 93%. The mole fraction for the MEA in Leanin stream is 0.90 of water and 0.04 of MEA. The CO₂ removed from the process is 167.89 kmol/hr. Meanwhile, the hydrogen separated from the water is 625.12 kmol/hr and the mole purity can be achieved at 93%. The mass flow rate of water separated in flash drum is 21.40 kmol/hr.

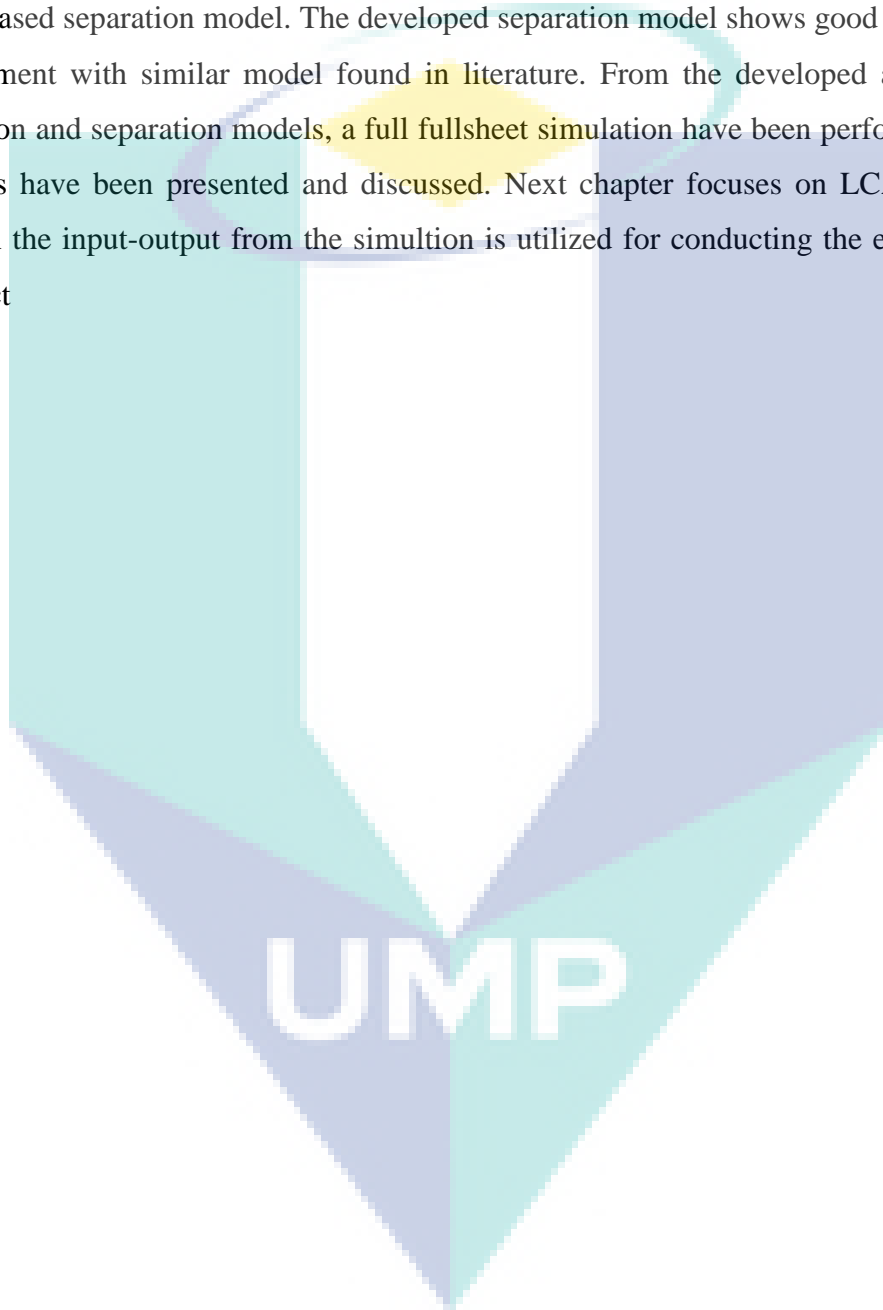
Table 3.12 Summaries stream results for mole flow rate

Stream	ETH	Steam	Leanin	H2	Water	CO2out	Leanout
Molar flowrate, kmol/hr							
MEA	0	0	561.11	9.47E-7	0.0004	7.60E-6	576.59
H ₂ O	0	610.59	11364.5	21.40	27.79	139.31	11437.39
CO ₂	0	0	0.0021	19.96	0.0005	167.89	1.073
CO	0	0	0	6.3	4.65E-6	0.0038	1.28E-26
H ₂	0	0	0	625.12	0.0004	0.40	1.28E-26
ETH	107.45	0	0	0	0	0.02	2.12
Comp							
MEA	0	0	0.04	1.41E-9	1.33E-5	2.47E-8	0.045
H ₂ O	0	1	0.90	0.032	0.99	0.45	0.90
CO ₂	0	0	1.47E-7	0.03	1.8E-5	0.55	8.41E-5
CO	0	0	0	0.009	1.67E-7	1.25E-5	1.00E-3
H ₂	0	0	0	0.93	1.36E-5	0.0013	1.0E-3
Eth	1	0	0	0	0	6.38E-5	0.0002

3.3.4 Concluding Remarks

This chapter explained the modelling effort for methane based hydrogen production (Case 1) and ethanol based hydrogen production (Case 2). The reactor modelling for methane steam reforming (MSR) and water gas shift reactor (WGS) were model using LHHW kinetic reaction whereas ethanol steam reforming (ESR) were model using powerlaw kinetic reaction. Equation modification have been introduced to fit the equations model used in Aspen Plus. Validation results shows good agreement

with results of similar model found in literature. Furthermore, from the validated models, sensitivity analysis were conducted for several parameter such as catalyst weight, pressure, temperature and water feed ratio. Apart from that, rigorous modelling and simulation of the separation section namely absorption column and stripping column have been done that considers the absorption and stripping chemistry as well as rate-based separation model. The developed separation model shows good results and in agreement with similar model found in literature. From the developed and validated reaction and separation models, a full fullsheet simulation have been performed and the results have been presented and discussed. Next chapter focuses on LCA analysis in which the input-output from the simulation is utilized for conducting the environmental impact assessment.



CHAPTER 4

ENVIRONMENTAL AND ECONOMIC ANALYSIS

4.1 Introduction

This chapter discusses the environmental and economic analysis of Case 1 and Case 2 which include environmental assessment of both processes using LCA and also its economic potential. In addition, comparison of both cases will also be highlighted.

4.2 LCA Goal and Scope

In this work, the LCA objective is to evaluate the environmental impact of all processes involved in hydrogen production from methane (Case 1) and ethanol (Case 2). The functional unit (FU) which provide a basis for calculating the inputs and outputs were based on 1 kg of hydrogen production (Galera & Ortiz, 2015; Verma & Kumar, 2015). The system boundaries were based on the cradle to grave approach which starts from methane/ethanol feedstock to hydrogen storage. System boundaries for Case 1 is shown in Figure 4.1 whereas Case 2 in Figure 4.2. Detail explanation is given next.

4.2.1 Case 1 system boundaries

In Figure 4.1, the system boundaries consist of five subsystems namely methane feedstock (SB1-1), hydrogen production (SB1-2), process steam (SB1-3), solvent absorption (SB1-4) and process water plant (SB1-5). Note that, the construction and commissioning phases as well as energy consumptions were excluded from the analysis. For SB1-1, methane is obtained from natural gas processing plant. However, the transportation of natural gas was assumed using pipeline and thus excludes from the analysis. SB1-2 consist of reactions and purification section. The reaction section include MSR and WGS reactors. The separation section on the other hand consists of carbon dioxide removal and a separator. The aim of this section is to purify the

hydrogen especially from CO₂. The system boundary also considers process steam generation section (SB1-3). This section considers the combustion of hydrocarbon fuel in the boiler to generate steam which is used during plant operation. Meanwhile, SB1-4 is the MEA supply subsystem which supply absorbents for CO₂ removal in the separation process. Finally, the water supply for the reforming process and cooling water were included in SB1-5.

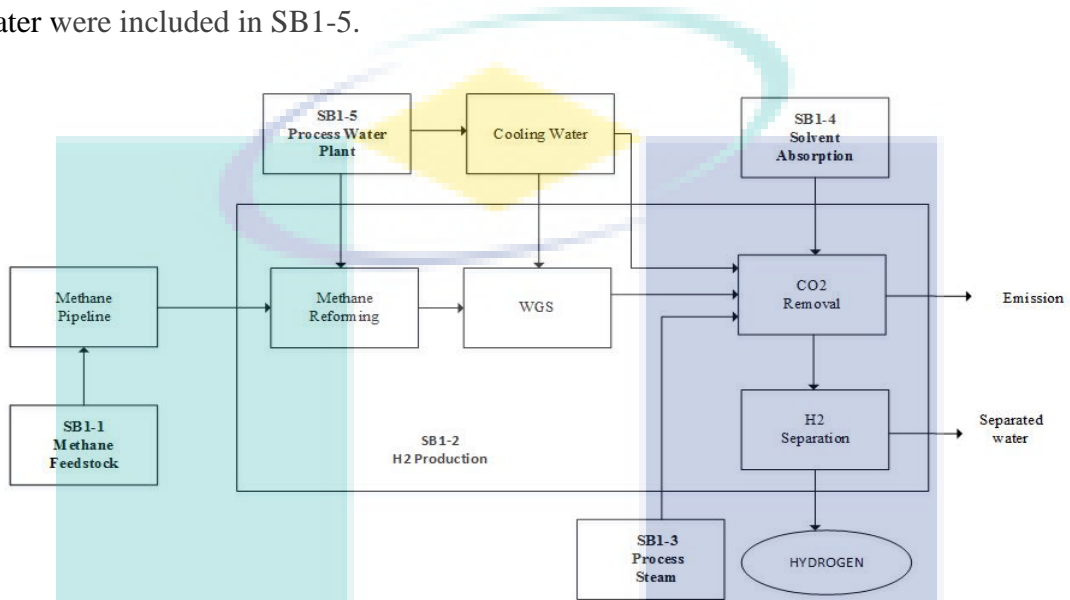


Figure 4.1 System boundaries for Case 1.

UMP

4.2.2 Case 2 system boundaries

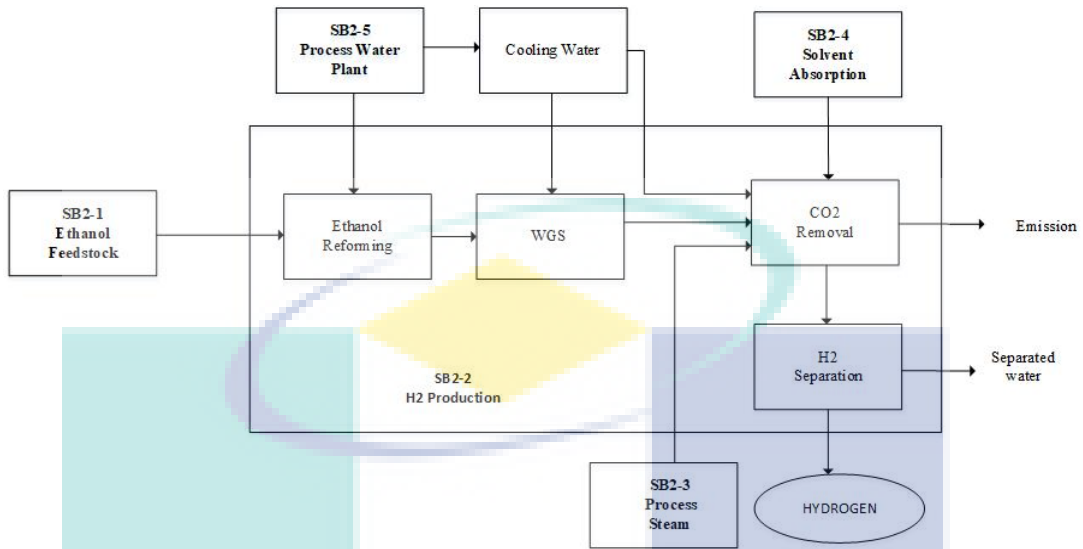


Figure 4.2 System boundaries for Case 2.

Figure 4.2 shows the system boundaries for Case 2. As in Case 1, Case 2 also consists of five subsystems. The first subsystem is the ethanol feedstock from fermentation (SB2-1). SB2-2 on the other hand include the production and the purification of hydrogen which consists of ethanol reforming, water gas shift and CO₂ removal. SB2-3 is the process steam boundary which supply steam as heating medium in stripper to remove CO₂ from MEA solvent. Meanwhile SB2-4 is the solvent (MEA) supply to the absorption tower. Lastly, SB2-5 is the process water plant which supply water for superheated steam generation and cooling water.

4.3 Life Cycle Inventory (LCI)

LCI involves the collection and compilation of the data required to quantify all the relevant inputs and outputs associated with the production of the functional unit (FU). In this study, Aspen Plus software were used to solve the mass and energy balances in hydrogen production for both cases. The modelling and the summary results were discussed in the Chapter 3.

The data obtained from Aspen Plus were used as the main inventory data in GaBi. The stream table results from Aspen Plus (Appendix A-1 and Appendix A-2) obtained were entered in inventory sheet in the Gabi. Then, inventory sheet in gabi were scaled down to the factor of 0.0008 for 1 kg of hydrogen production. The output and input result can be observed in the Table 4.1 and Table 4.2. Table 4.1 summarize the

main inventory data per functional unit (FU) of 1 kg hydrogen for case 1. For every kg of hydrogen produced requires 6.4 kg of steam and 2.04 kg of methane and produced 4.68 kg of carbon dioxide and 0.26 kg of carbon monoxide. In addition, the utilities required for heating and cool down the process gas is 6.81 MJ/FU of steam and 386.43 kg/FU of cooling water.

Table 4.1 Main inventory data for the Case 1

Input	Mass (kg)	Output	Mass (kg)
Flue gas	3.2	Carbon dioxide	4.68
Hydrogen	0	Carbon monoxide	0.2632
Iron (Catalyst)	0.504	Catalysts material	0.632
Monoethanolamine	14.75	Flue gas	3.2
Natural gas (Methane)	2.04	Hydrogen	1.00
Nickel (catalyst)	0.128	Monoethanolamine	14.75
Heating steam (MJ)	6.81	Waste water	0.40
Process steam, kg	6.4	Water (Absorbent)	88.20
Water (Absorbent)	88.20	Cooling water	1545.15
Cooling Water	386.43		

Table 4.2 shows main inventory data for Case 2. With 1 kg hydrogen, the carbon dioxide produced is 5.9 kg and carbon monoxide is 0.14 kg. The cooling water consumed for the cooling medium in process is 2145.65 kg and the net calorific value for the steam used in heating is 50.02 MJ. The ethanol as feedstock used for produced 1 kg of hydrogen is 3.96 kg, meanwhile the steam consumed in the reaction between ethanol with steam is 8.79 kg.

Table 4.2 Main inventory data for Case 2

Input	Mass (kg)	Output	Mass (kg)
Ethanol	3.96	Carbon Dioxide	5.903
Monoethanethanolamine	27.39	Carbon Monoxide	0.1411
Process steam, kg	8.79	Catalyst Material	0.783
Process steam (MJ)	50.02	Flue gas	19.18
Water (Absorbent)	163.58	Hydrogen	1
Cooling water	2145.65	Monoethanolamine	27.39
Flue gas	19.2	Waste water	0.3995
Nickel (catalyst)	0.24	Cooling water	2145.65
Iron (catalyst)	0.543	Water (Absorbent)	163.58

4.4 Life cycle impact assessment

The life cycle impact assessment aims at understanding and evaluating the magnitude and significance of the potential environmental impacts of a product system throughout the life cycle of the product (ISO14040, 2006). The environmental characterization of the process was carried out based on the following categories;

- Climate change
- Terrestrial acidification
- Freshwater eutrophication
- Ozone depletion
- Fossil depletion
- Freshwater ecotoxicity
- Human toxicity
- Ionising radiation
- Marine ecotoxicity
- Marine eutrophication
- Metal depletion
- Particulate matter
- Photochemical oxidant formation
- Water depletion
- Terrestrial ecotoxicity.

The impact potentials were evaluated using ReCipe method whereas the calculation implementation of the inventories was performed in GaBi.

4.5 Life Cycle Results Interpretation

4.5.1 Hydrogen Production from Methane (Case 1)

The overall results for Case 1 is given in the Table 4.3. Figure 4.3 shows the individual contribution of the impact category to each of the boundary analysis whereas Figure 4.4 is focuses on the highest impact category namely climate change, fossil depletion and water depletion.

Overall the most significant impact category is climate change with total of 9.44 kg CO₂ eq (see Figure 4.3). Note that, for climate change the CO₂ equivalance (eq.) is the equivalent amount of CO₂ produced per kilogram of hydrogen in a period of 100 years. The most affected system boundaries with regards to climate change is SB1-2

with 4.68 kg CO₂ eq and it cover 49.48% of the total impact. This is due to the MSR and WGS reactions that produced significant amount of carbon dioxide. This result is in agreement with the work by Galera and Ortiz (2015) and Hajjaji et al. (2013). It is then followed by SB1-3 with 1.99 kg CO₂ eq or 21.08%. SB1-3 is the process steam boundary in which fossil fuel is burned to generate a steam. The SB1-5 and SB1-1 contribute the least with 1.48 kg CO₂ eq and 1.29 kg CO₂ eq respectively.

From Figure 4.3 fossil depletion is the second most significant impact category with total of 4.044 kg oil eq. From Figure 4.3, SB1-1 contributes the most with amount 2.694 kg oil eq or 66.62 %. This is expected since methane is a type of fossil fuel and used as a feedstock in hydrogen production. It is then followed by SB1-3 with amount 0.845 kg oil eq or 20.90 %. In SB1-3, natural gas is used as raw material to generate the steam as shown in Appendix C-1. The third most significant impact category is water depletion with total of 4.01 kg m³ eq (see Figure 4.3). SB1-5 contributed the most with amount of 3.81 m³ eq and covers 95.01% of the total impact. This is obvious since water is used as a raw material to generate steam and cooling water. It is then followed by SB1-3 with amount 0.03 m³ eq or 4.24%.

The other impact categories have a value less than 1 kg eq. Details of the value is shown in Table 4.3. These values presents less environmental impact of the process. This is mainly due the nature of the process which mainly involve chemical processing and combustion.

Table 4.3 Impact categories for each subsystems for case 1

Categories	Unit	SB1-1	SB1-2	SB1-3	SB1-4	SB1-5	Total
Climate Change	kg CO ₂ eq	1.29	4.68	1.99	0	1.48	9.44
Terrestrial acidification	kg SO ₂ eq	0.00177	0	0.0022	0	0.00316	0.0071
Freshwater eutrophication	kg P eq	6.80E-07	0	3.00E-08	0	4.54E-5	4.61E-5
Ozone Depletion	kg CFC-11 eq	3.00E-12	0	1.00E-13	0	2.97E-10	3.001E-10
Fossil depletion	kg oil eq	2.694	0	0.845	0	0.505	4.044
Freshwater ecotoxicity	kg 1,4-DB eq	0	0	2.57E-06	0.075	0.005	0.080
Human toxicity	kg 1,4-DB eq	0.035	0	0.05	0	0.05	0.135
Ionising radiation	kg U235 eq	0.002	0	0	0	0.235	0.235
Marine ecotoxicity	kg 1,4-DB eq	0.000137	0	6.39E-06	4.66E-4	0.004735	0.005
marine eutrophication	kg N eq	0.00093	0	0.001247	0	0.001375	0.004
Metal Depletion	kg Fe eq	0.04	0.504	0.001	0	0.007	0.552
Natural land transformation	m ²	0	0	0	0	0	0
particulate matter formation	kg PM10 eq	0.000671	0	0.000853	0	0.001068	0.003
Photochemical oxidant formation	kg NMVC eq	0.003	0.012	0.004	0	0.003	0.022
Terrestrial ecotoxicity	kg 1,4-DB eq	0	0	0	0.212	0	0.212
Water depletion	m ³	3.00E-02	0	0.17	0	3.81	4.01

UMP

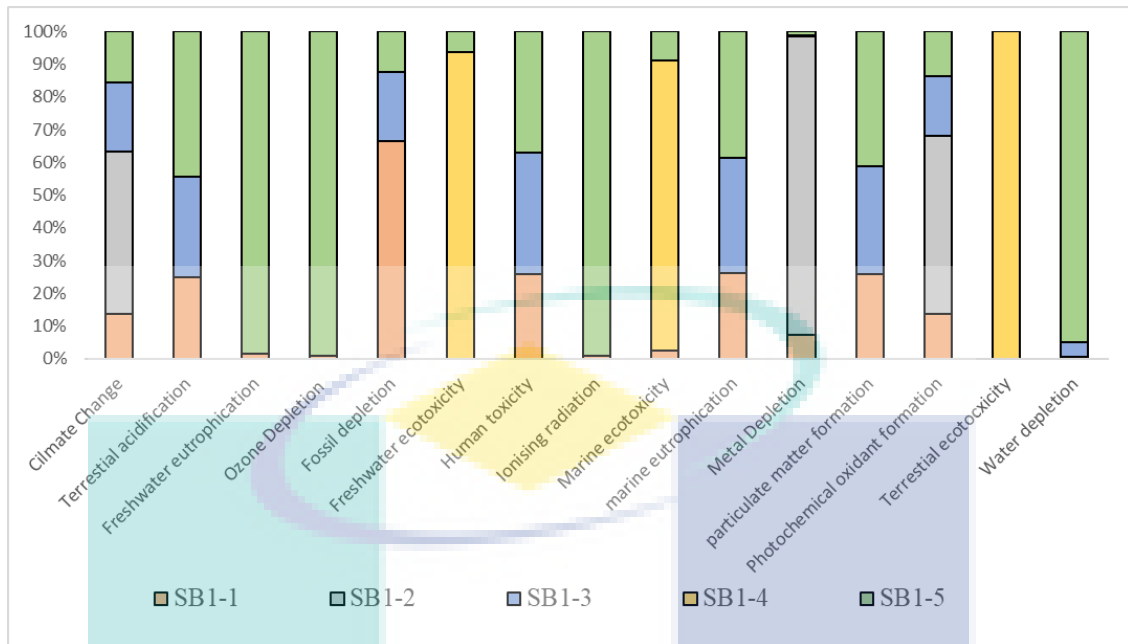


Figure 4.3 Contribution environment impact categories in hydrogen production from methane.

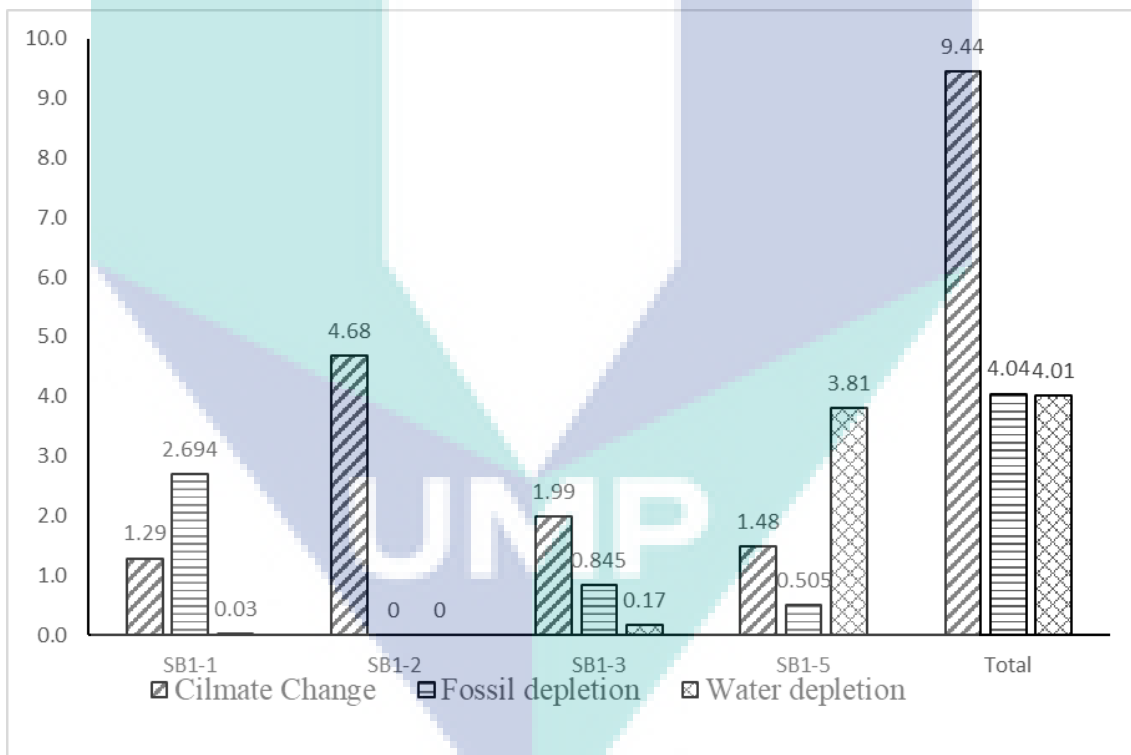


Figure 4.4 Environmental impact results for the most significant impact category in case 1.

4.5.2 Hydrogen Production from Ethanol (Case 2)

The Table 4.4 is shown the overall results for Case 2 and Figure 4.5 is shows the individual contribution of the impact category to each of the boundary analysis. Meanwhile, Figure 4.6 is focusses only the highest impact category namely climate change, fossil depletion and water depletion.

As shown in Figure 4.6, the overall most significant impact category is climate change with total of 26.91 kg CO₂ eq. The SB2-1 is the most affected system boundaries with regards to climate change is SB2-1 with 4.41 kg CO₂ eq and it cover 28.99% of the total impact. The next system boudaries is SB2-5 with 8.1 kg CO₂ eq or 26.26% of the total impact. This is because the utilities used for heating and cooling used is high to produce hydrogen. Then, the SB2-3 and SB2-2- contribute the least with 7.9 kg CO₂ and 5.9 kg CO₂ eq respectively.

The second high impact category is the water depletion with total of 25.51 m³ eq. The result in Figure 4.6 illustrated that SB2-5 contributes the most with amount 20.91 m³ eq and cover with 89.55%. The large amount of water was supplied into the process for the reaction in ESR caused SB2-5 contributes the most water depletion. Then, it is followed by SB2-1 with amount 1.62 m³ eq or 6.94% . Meanwhile, the water was used as utilities for heating in SB2-3. The third most significant impact category is fossil depletion as shown in Figure 4.6 with total of 12.54% kg oil eq. SB2-1 was contributed extensively to fossil depletion compared to the other subsystem in Figure 4.6 with amount 6.42 kg oil eq and covers only 51.17% of the total impact. Then, next system boundary was SB2-3 was 3.36 kg oil eq with only 26.76% of the total impact. The reason is it used fossil fuel as raw material to heat the water become steam.

In the Table 4.4 show the other impact categories that have a value less than 1 kg eq. These values exhibits the minor environmental impact of the process. The reason is mainly due the nature of the process which mainly involve chemical pccessing and combustion.

Table 4.4 Impact categories for each subsystems for case 2

Categories	Unit	SB2-1	SB2-2	SB2-3	SB2-4	SB2-5	Total
Climate Change	kg CO ₂ -eq	4.41	5.9	7.9	0	8.1	26.31
Terrestrial Acidification	kg SO ₂ eq	0.015	0	0.009	0	0.017	0.041
Freshwater Eutrophication	kg P-eq	4.85E-04	0	1.00e-7	0	2.73E-4	7.58E-4
Ozone Depletion	kg CFC-11eq	5.60E-11	0	0	0	1.63E-9	1.69E-9
Fossil Depletion	kg oil eq	0.24	0	3.36	0	2.77	6.36
Freshwater Ecotoxicity	kg 1,4-DB eq	0.074	0	0	0.139	0.027	0.24
Human Toxicity	kg 1,4-DB eq	0.243	0	0.019	0	0.272	0.534
Ionising Radiation	kg U235 eq	0.074	0	0	0	1.28	1.354
Marine Ecotoxicity	kg 1,4-DB eq	0.002	0	0	0.009	0.003	0.014
Marine Eutrophication	kg N-eq	0.004	0	0.005	0	0.008	0.031
Metal Depletion	kg Fe eq	0.018	0.543	0.004	0	0.041	0.703
Particulate Matter Formation	kg PM10 eq	0.004	0	0.003	0	0.006	0.013
Photochemical Oxidant Formation	kg NMVOC	0.007	0.006	0.015	0	0.018	0.046
Terrestrial Ecotoxicity	kg 1,4-DB eq	0	0	0.001	0.394	0	0.395
Water Depletion	m ³	3.78	0.16	0.66	0	20.91	25.51

UMP

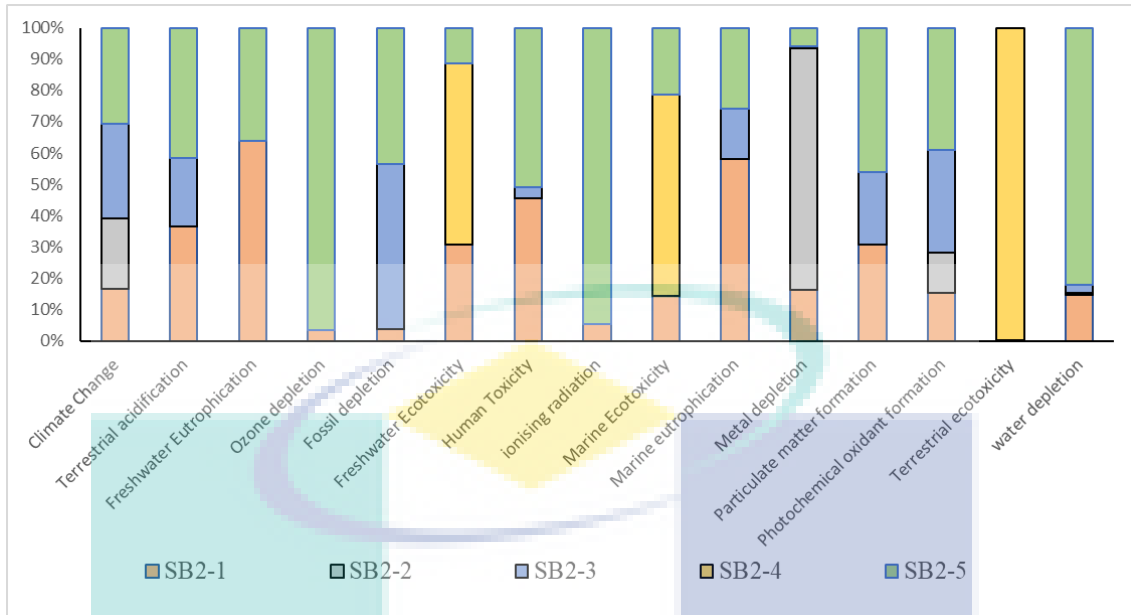


Figure 4.5 Contribution environment impact categories in hydrogen production from ethanol.

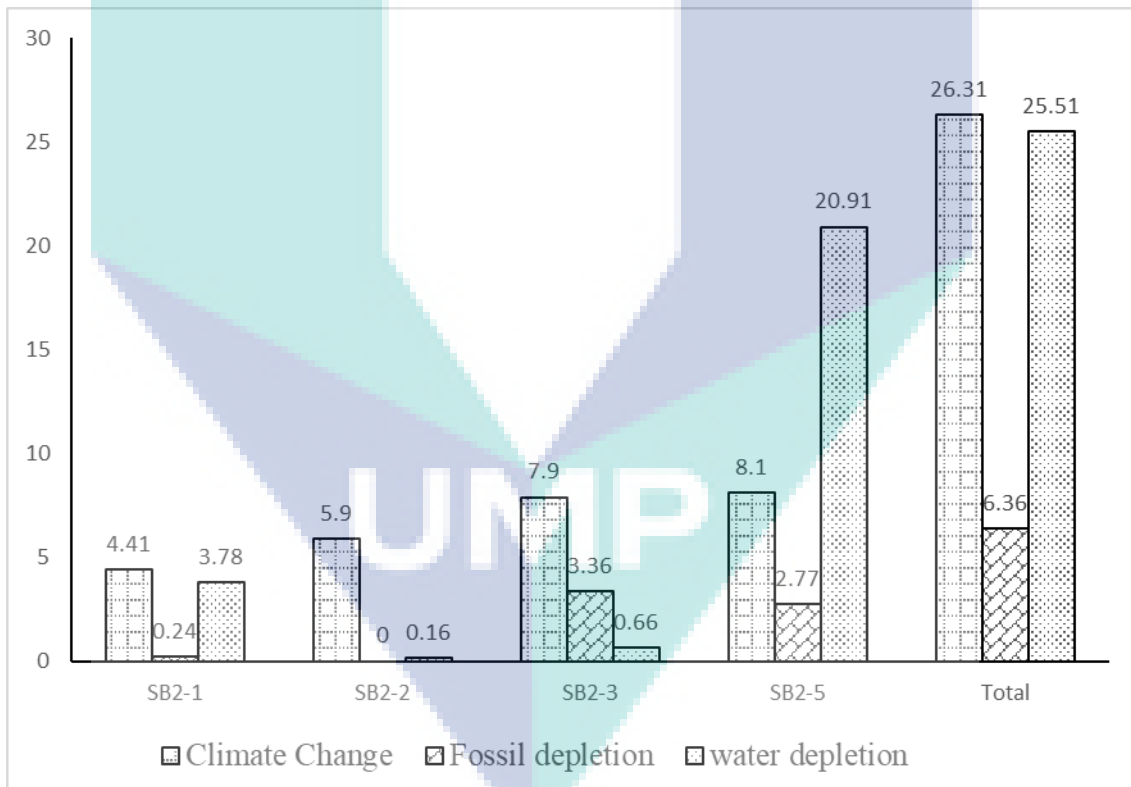


Figure 4.6 Environmental impact results for the most significant impact category in Case 2.

4.6 Comparison Between Hydrogen Production from Methane (Case 1) and Hydrogen Production from Ethanol (Case 2).

The total environment impact comparison between Case 1 and Case 2 for the main impact categories namely global warming potential, fossil depletion and water depletion is shown in Figure 4.7. For climate change category, Case 2 produced the highest impact with 26.31 kg CO₂ eq compared to Case 1 with only 9.44 kg CO₂ eq. This shows the hydrogen pathway from ethanol released higher greenhouse gas emission compared to the hydrogen pathway from methane. This is because the steam required is high compared with Case 1 for the reaction and heating in the process. Because of that, the greenhouse gas emission released is high due to combustion for steam generation.

On the other hand, Case 2 has a higher fossil fuel resource depletion compared to Case 1. The depletion occurred in the Case 2 is 6.36 kg oil eq while Case 1 is only 4.044 kg oil eq. This is because in Case 2, high amount of steam is needed for the reactions and heating which resulted in high amount of fossil fuel consumed. This can be observed in simulation result which the consumption of utilities especially in steam is high compared with Case 1. The evidence also can be observed on SB1-3 and SB2-3 fossil depletion impacted on the table 4.3 and table 4.4. The result shows the consumption of fossil fuel for generation steam Case 2 is higher compared with Case 1. Meanwhile, Case 2 also has a higher water resources depletion impact than Case 1 with total amount of 25.51 m³ and 4.01 m³ respectively. This is due to water supply to the process is high for the steam generation and cooling system in Case 2 as shown in Table 4.7 and Table 4.9.

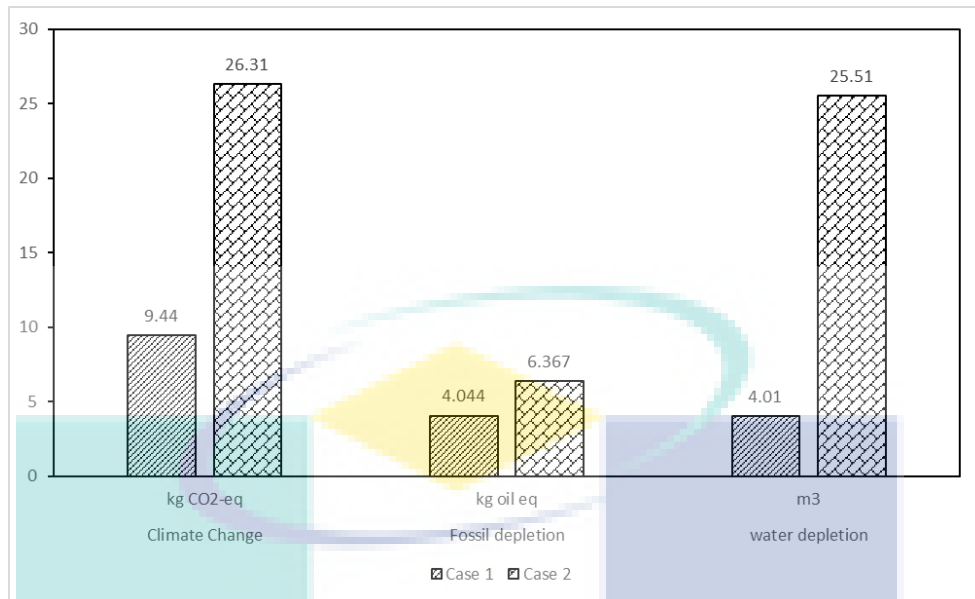


Figure 4.7 Environment impact comparison between Case 1 and Case 2

In climate change, Case 2 has a higher impact compare to Case 1 with respect to SB1 as shown in Figure 4.8. The carbon emission associated from climate change category in Case 2 is three times compared to Case 1 because carbon content for ethanol is higher than methane and moreover ethanol is more volatile compared with methane. In SB2, the carbon emission is higher in Case 2 with amount 5.9 kg CO₂ eq compared to 4.68 kg CO₂ eq in Case 1. For SB3, the difference gap between both cases; 7.9 kg CO₂ eq for Case 2 and 1.99 kg CO₂ eq for Case 1. This is because Case 2 requires larger amount of steam to supply the necessary heat needed in the process. Moreover, for SB5, Case 2 also show a higher carbon emission with amount of 8.1 kg CO₂ eq compared to 1.48 kg CO₂ eq for Case 1 due the higher amount of water required for reactions and cooling process.

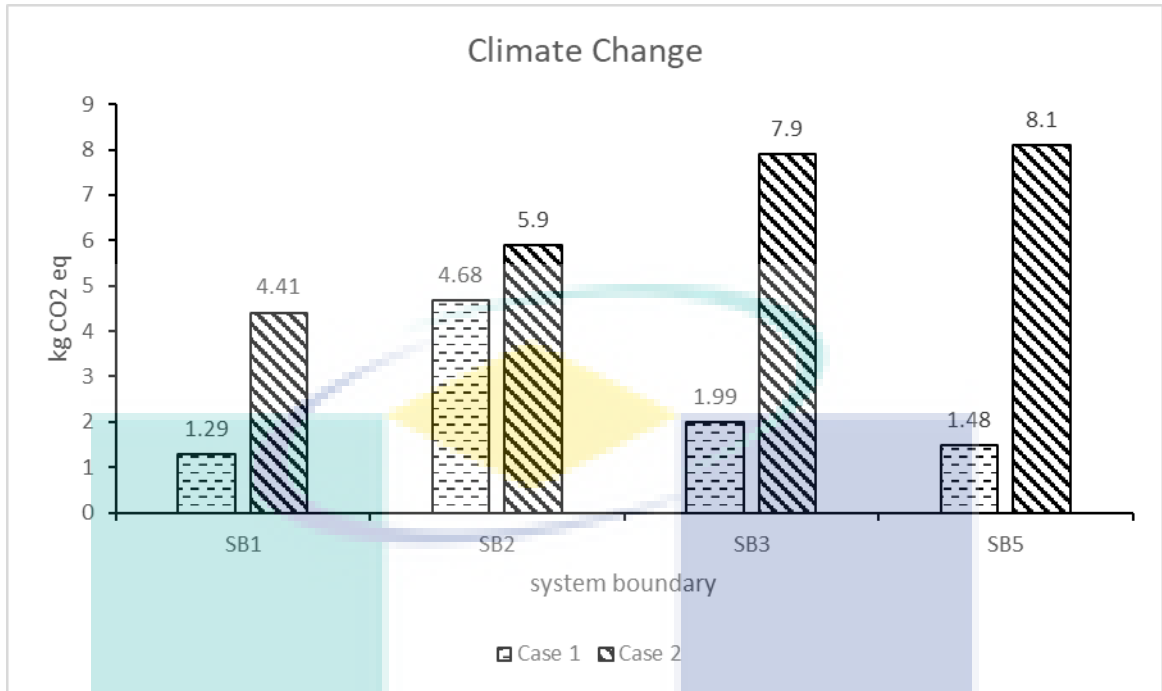
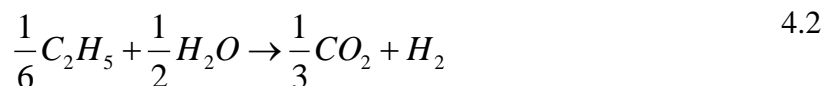
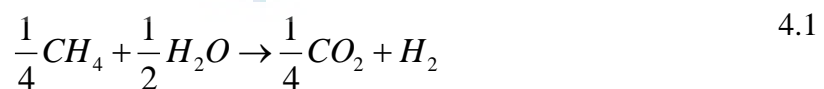


Figure 4.8 Comparison between system boundaries with case study in climate change

Figure 4.9 shows the fossil depletion impact category for each boundary. For SB1, Case 1 contribute extensively compared with Case 2 which are 2.694 kg oil eq and 0.24 kg oil eq respectively. For SB3, the Case 2 is giving more impact on fossil depletion with 3.36 kg oil eq compared with Case 1. This is due high consumption of steam in utility especially in HE-05 located in CO₂ removal. This increasing of usage of absorbent will increasing the usage of steam. The usage of absorbent is related with CO₂ production in the process. The high CO₂ produced during hydrogen production, the usage of asorbent also increased. In this study, Case 2 was produced high CO₂ with 7388.61 kg/hr (Appendix B-1) and Case 1 (Appendix B-1) is 5348.10 kg/hr. This also can refer eq 4.1 (Case 1) and eq 4.2 (Case 2) which shows that eq 4.2 are produced more carbon than with eq 4.1. The fossil fuel was used as combustion in boiler to generate steam as heating medium. So, it is caused the increase the impact on fossil depletion.



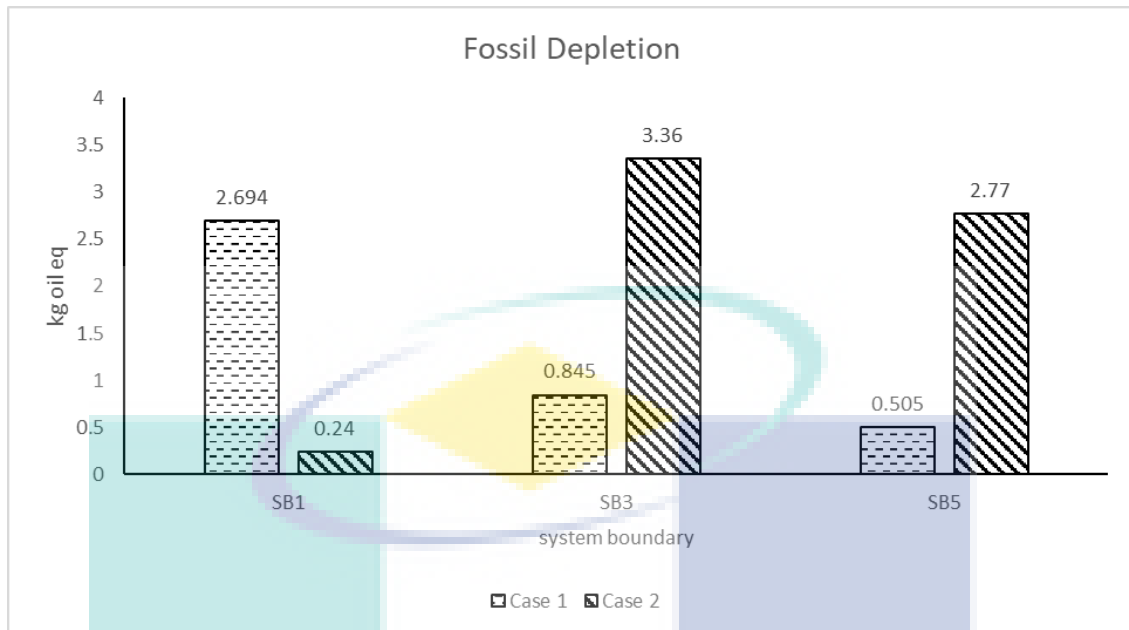


Figure 4.9 Comparison between system boundary with case study in fossil depletion

Figure 4.10 is shows comparison between system boundaries for the water depletion category. Overall, Case 2 shows a higher water depletion compared to Case 1. Case 2 for SB5 recorded the highest amount with 20.91 m³ eq compared to 3.81 m³ eq for Case 1. The reason the water consumption is high because the required exchanger area in Case 2 (Appendix B-2) is much than required exchanger area in Case 1 (Appendix B-1). With larger exchanger area is required high heat transfer. Consequences, the heat transfer is using cooling water as medium to transfer heat from hot medium (process gas) to cool medium (cooling water). With the exchanger area in Case 2 is high caused the usage of cooling water also high than cooling water used in Case 1. So, the water depletion in Case 2 is high compared with Case 1.

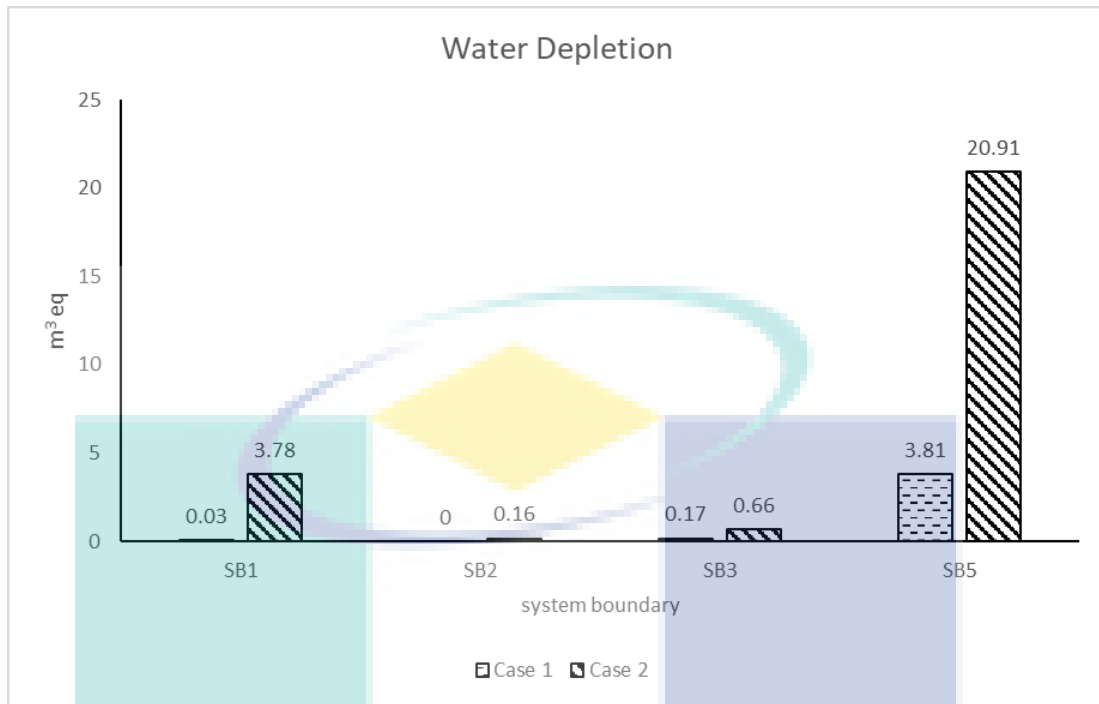


Figure 4.10 Comparison between system boundaries with case study in water depletion.

4.6.1 Concluding Remarks

This subchapter discuss the environment impact and economic analysis of production of hydrogen using methane (Case 1) and hydrogen production using ethanol (Case 2). Environmental impact were assessed using life cycle assessment (LCA) by using GaBi software. For the LCA analysis, overall it is found that Case 2 has a higher environmental impact than Case 1 especially for the total climate change category, fossil depletion and water depletion. In conclusion, Case 1 is an environmental friendlier compared with Case 2 because less environment impact compared with Case 2.

4.7 Economic Assessment

The economic investment of the chemical plants depends largely on capital expenditure (CAPEX). In this work, CAPCOST software (Richard Turton et al. (2013) was used to calculate the capital cost which based on the equipment size, operating condition and and material of construction (MOC). The sizing and operation condition were obtained from the models developed in Aspen Plus. Note that the production is

assumed with capacity of 10 000 Mtonne/annum of hydrogen. Normally, the purchased cost increase yearly due to inflation. The updated purchase costs is calculated using the chemical engineering plant cost index (CEPCI) represented by the following equation. Note that, in this work the CEPCI used is 558.3 for June 2017 obtained from World (June 2017).

$$\text{current cost} = \text{cost year } X \times \frac{\text{CEPCI current}}{\text{CEPCI year } X} \quad 4.3$$

The MOC of equipments were assumed stainless steel. Apart from that, the operating expenditure (OPEX) were also calculated using CAPCOST based on the utilities consumed which include steam, cooling water and electricity. The utilities cost per unit is show in the Table 4.5 below. The utilities consumption data were obtained the simulated model. The details result of the economic analysis can be found in Appendix D-1 and Appendix D-2.

Table 4.5 The utilities cost per unit (Turton et al., 2013)

Utilities	Cost (\$/GJ)
Steam	17.7
Cooling Water	0.354

4.7.1 Economic Analysis of Case 1

The CAPEX results of each equipment results in shown in Table 4.6. Additionally, the table also include purchased equipment cost (C_P), bare module cost (C_{BM}), total module cost (C_{TM}) and grassrootcost (C_{GR}). The grassroots cost (C_{GR}) is the costs for the site development, auxiliary buildings and utilities and this cost is assumed 50% of bare module cost. For Case 1, the total capital cost is estimated to be \$4,282,326.68. Heat exchanger (E-107) which is a kettle reboiler used in the stripper tower has the highest cost because due to large shell size compared with other heat exchanger.

Table 4.6 The summary of capital cost for the hydrogen production from methane

Block ID	C_P (\$)	C_{BM} (\$)	C_{TM} (\$)	C_{GR} (\$)
E-101	3,720.00	22,200.00	26,226.68	32,300.00
E-102	4,810.00	28,700.00	33,900.00	41,800.00

E-103	5,220.00	31,200.00	36,800.00	45,400.00
E-104	31,700.00	195,000.00	230,600.00	283,000.00
E-105	30,900.00	191,000.00	225,000.00	276,000.00
E-106	40,800.00	251,000.00	297,000.00	364,000.00
E-107	193,000.00	1,190,000.00	1,406,000.00	1,720,000.00
R-101	23,500.00	232,000.00	274,000.00	322,000.00
R-102	36,100.00	413,000.00	488,000.00	561,000.00
R-103	36,100.00	413,000.00	488,000.00	561,000.00
T-101	26,000.00	235,000.00	277,000.00	325,000.00
T-102	35,800.00	378,000.00	447,000.00	512,000.00
V-101	5,650.00	44,700.00	52,800.00	64,300.00
Total			4,282,326.68	5,107,800.00

Regarding the utilities cost, Table 4.7 summarize the results. The total annuity utilities cost is estimated to be \$ 12,558,200.

Table 4.7 Summary utilities for hydrogen production from methane

Utilities Used	Actual Usage (MJ/h)	Annuity utility cost (\$)
Steam	84600	12,461,000
Cooling Water	33030	97,200
Total		12,558,200

4.7.2 Economic analysis of Case 2

The CAPEX results of each equipment results in shown in Table 4.8. Additionally, the table also include purchased equipment cost (C_P), bare module cost (C_{BM}), total module cost (C_{TM}) and grassroots cost, (C_{GR}). For Case 1, the total capital cost is estimated to be \$4,504,628.30. Heat exchanger (E-207) which is a kettle reboiler used in the stripper tower has the highest cost because due to large shell size compared with other heat exchanger.

Table 4.8 Summary capital cost for hydrogen production from ethanol

Block ID	C_P , (\$)	C_{BM} , (\$)	C_{TM} , (\$)	C_{GR} , (\$)
E-201	32,400.00	200,000.00	235,628.30	289000
E-202	28,000.00	172,000.00	203,000.00	249000
E-203	26,700.00	164,000.00	194,000.00	238000
E-204	42,000.00	259,000.00	306,000.00	375000
E-205	39,400.00	243,000.00	287,000.00	351000
E-206	29,700.00	183,000.00	216,000.00	265000

E-207	108,000.00	667,000.00	787,000.00	970000
R-201	23,500.00	232,000.00	274,000.00	322000
R-202	36,100.00	413,000.00	488,000.00	561000
R-203	36,100.00	413,000.00	488,000.00	561000
T-201	65,900.00	274,000.00	324,000.00	372000
T-202	117,000.00	536,000.00	633,000.00	712000
V-201	7,210.00	58,500.00	69,000.00	84000
Total			4,504,628.30	5,349,000.00

Regarding the utilities cost, Table 4.9 summarize the results. The total annuity utilities cost is estimated to be \$14,165,200.

Table 4.9 Summary utilities used in hydrogen production from ethanol

Utility Used	Actual Usage (MJ/h)	Annual Utility Cost (\$)
Steam	95000	13,994,000.00
Cooling water	58240	171,200.00
Total		14,165,200.00

4.7.3 Economic Comparison

The comparative economic potential of both cases can be observed in Table 4.10. From the result obtained, the total bare cost of Case 2 is 5.19 % higher than Case 1 with \$ 4,504,628.30 and \$ 4,282,326.68 respectively. Meanwhile, the grassroot cost for the Case 1 was \$5,107,800.00 and it low compared with the case 2 which are \$5,349,000 . The difference between the case 1 and case 2 for the grass root cost was 4.72%.

Table 4.10 The comparison of the capital cost between Case 1 and Case 2

Case Study	Case 1	Case 2	Comparison (%)
C_{TM} (\$)	4,282,326.68	4,504,628.30	5.19
C_{GR} (\$)	5,107,800.00	5,349,000.00	4.72

On the other hand Table 4.11 shows the comparative result for the utilities consumption. The result shows that steam cost in the Case 1 is \$ 12,461,000. Meanwhile, the steam cost for the Case 2 is 12.30% higher with total of \$13,994,000. On the other hand, the cooling water cost for the Case 1 is \$ 97,200 and for Case 2 is \$

171,200 with difference of 76.13%. Overall, the total utilities cost for the Case 2 is higher compared to Case 1 with difference of 12.80%. The high utilities were used in case 2 because the heat duty required for heat transfer in heat exchanger in case 2 is high. In conclusion, Case 1 is more economic in the term capital cost and utilities cost compared with the Case 2.

Table 4.11 The comparison utilities cost for Case 1 and Case 2

Utility	Case 1	Case 2	Differences (%)
Steam	\$ 12,461,000.00	\$ 13,994,000.00	12.30
Cooling water	\$ 97,200.00	\$ 171,200.00	76.13
Total	\$ 12,558,200.00	\$ 14,165,200.00	12.80

4.7.4 Concluding Remarks

This subchapter discuss economic analysis of production of hydrogen using methane (Case 1) and hydrogen production using ethanol (Case 2). The economic analysis were performed using CAPEX and OPEX calculation. From the economic analysis conducted, it is found that Case 2 has a higher CAPEX compared to Case 1 with difference of 5.19% of C_{BM} and 4.72 % of C_{GR} . For OPEX, Case 2 also indicate higher utilities cost compared to Case 1 with difference of 12.80 %. In conclusion, Case 1 is less costing than Case 2.

UMP

CHAPTER 5

CONCLUSION

5.1 Conclusion

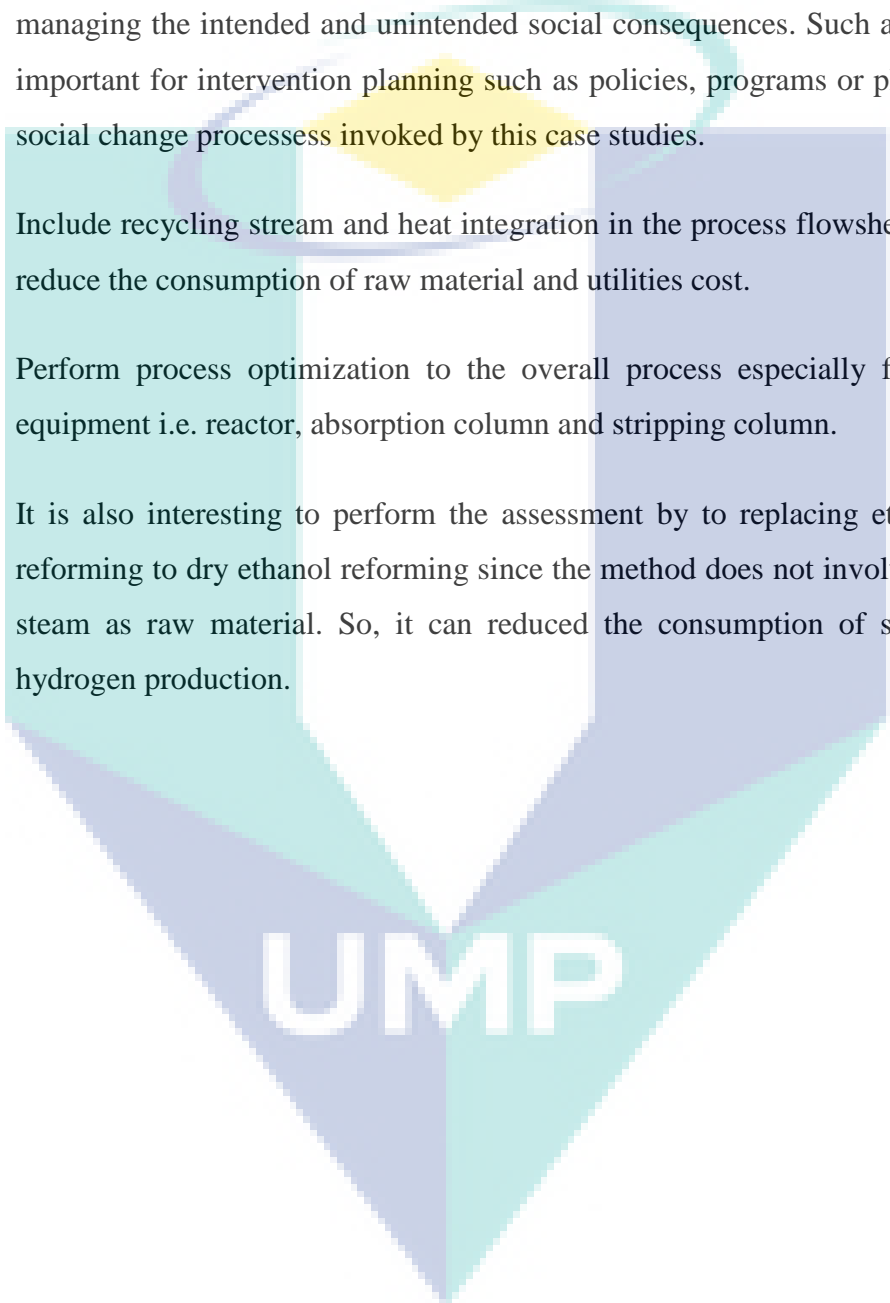
The main objective of this study is to assess and compare environmental impact and economic feasibility of hydrogen production from methane (Case 1) and ethanol (Case 2). The environmental assessment was performed using LCA while economic analysis was based on CAPEX and OPEX calculations. Both case studies were simulated in Aspen Plus 8.6. In the simulation study, a modified kinetic based reaction models were used for MSR, ESR and WGS reactions. The result shows that the modified models show good agreement with results found in literature with error <14% and then the models were utilized for sensitivity analysis. For the separation of CO₂, MEA was used for the absorption process which was modeled using RADFRAC and validated (error <3%) with results found in literature. The data obtained from the simulation were then used for LCA and economic assessment.

LCA analysis of both case studies were done in GaBi software. From the results obtained, all impact categories show that Case 1 is environmentally friendlier than Case 2. It is also found that three categories namely climate change, fossil depletion and water depletion have the most significant environmental impact compared to the other categories. The economic assessment on the other hand, focuses on capital cost, grassroots cost and utilities cost. In all categories, it is found that Case 1 is less costly compared with Case 2. Overall, it is concluded Case 1 is more environmentally friendly and less costly in terms of CAPEX and OPEX than Case 2.

5.2 Recommendation for future works

Several suggestions are made to improve and further expand the research work. Below are some of the suggestions:-

- Perform social impact assessment which include analysing, monitoring and managing the intended and unintended social consequences. Such assessment is important for intervention planning such as policies, programs or plans and any social change processes invoked by this case studies.
- Include recycling stream and heat integration in the process flowsheet. This will reduce the consumption of raw material and utilities cost.
- Perform process optimization to the overall process especially for the main equipment i.e. reactor, absorption column and stripping column.
- It is also interesting to perform the assessment by to replacing ethanol steam reforming to dry ethanol reforming since the method does not involve the use of steam as raw material. So, it can reduced the consumption of steam during hydrogen production.

The logo for UIMP (Universiti Malaysia Perlis) is a large, stylized letter 'V' shape. The left side of the 'V' is light blue, the right side is a darker blue, and the bottom point is a teal color. The letters 'UIMP' are written in white, bold, sans-serif font across the center of the 'V'.

REFERENCES

- Abbasi, T., & Abbasi, S. A. (2011). 'Renewable' hydrogen: Prospects and challenges. *Renewable and Sustainable Energy Reviews*, 15(6), 3034-3040. doi: 10.1016/j.rser.2011.02.026
- Acar, C., & Dincer, I. (2014). Comparative assessment of hydrogen production methods from renewable and non-renewable sources. *International Journal of Hydrogen Energy*, 39(1), 1-12. doi: 10.1016/j.ijhydene.2013.10.060
- Afgan, N. H., & Carvalho, M. G. (2008). Sustainability assessment of a hybrid energy system. *Energy Policy*, 36(8), 2903-2910. doi: 10.1016/j.enpol.2008.03.040
- Akande, A., Aboudheir, A., Idem, R., & Dalai, A. (2006). Kinetic modeling of hydrogen production by the catalytic reforming of crude ethanol over a co-precipitated Ni-Al₂O₃Ni-Al₂O₃ catalyst in a packed bed tubular reactor. *International Journal of Hydrogen Energy*, 31(12), 1707-1715. doi: 10.1016/j.ijhydene.2006.01.001
- Amadeo, N. E., & Laborde, M. A. (1995). Hydrogen production from the low temperature water gas shift reaction: kinetics and simulation of the industrial reactor. *Int. J. Hydrogen Energy*, 20, 949-956.
- Antzara, A., Heracleous, E., Bukur, D. B., & Lemonidou, A. A. (2014). Thermodynamic Analysis of Hydrogen Production via Chemical Looping Steam Methane Reforming Coupled with in Situ CO₂ Capture. *Energy Procedia*, 63, 6576-6589. doi: 10.1016/j.egypro.2014.11.694
- Authayanun, S., Suwanmanee, U., & Arpornwichanop, A. (2015). Enhancement of dilute bio-ethanol steam reforming for a proton exchange membrane fuel cell system by using methane as co-reactant: Performance and life cycle assessment. *International Journal of Hydrogen Energy*, 40(36), 12144-12153. doi: 10.1016/j.ijhydene.2015.07.042
- Balat, M. (2008). Potential importance of hydrogen as a future solution to environmental and transportation problems. *International Journal of Hydrogen Energy*, 33(15), 4013-4029. doi: 10.1016/j.ijhydene.2008.05.047
- Ball, M., & Wietschel, M. (2009). The future of hydrogen – opportunities and challenges☆. *International Journal of Hydrogen Energy*, 34(2), 615-627. doi: 10.1016/j.ijhydene.2008.11.014
- Basile, A., Curcio, S., Bagnato, G., Liguori, S., Jokar, S. M., & Iulianelli, A. (2015). Water gas shift reaction in membrane reactors: Theoretical investigation by artificial neural networks model and experimental validation. *International Journal of Hydrogen Energy*, 40(17), 5897-5906. doi: 10.1016/j.ijhydene.2015.03.039

- Bej, B., Pradhan, N. C., & Neogi, S. (2013). Production of hydrogen by steam reforming of methane over alumina supported nano-NiO/SiO₂ catalyst. *Catalysis Today*, 207, 28-35. doi: 10.1016/j.cattod.2012.04.011
- Bion, N., Duprez, D., & Epron, F. (2012). Design of nanocatalysts for green hydrogen production from bioethanol. *ChemSusChem*, 5(1), 76-84. doi: 10.1002/cssc.201100400
- Boyano, A., Morosuk, T., Blanco-Marigorta, A. M., & Tsatsaronis, G. (2012). Conventional and advanced exergoenvironmental analysis of a steam methane reforming reactor for hydrogen production. *Journal of Cleaner Production*, 20(1), 152-160. doi: 10.1016/j.jclepro.2011.07.027
- Braga, L. B., Silveira, J. L., da Silva, M. E., Tuna, C. E., Machin, E. B., & Pedroso, D. T. (2013). Hydrogen production by biogas steam reforming: A technical, economic and ecological analysis. *Renewable and Sustainable Energy Reviews*, 28, 166-173. doi: 10.1016/j.rser.2013.07.060
- Camero, C., & Sowlati, T. (2014). Assessment and optimization of forest biomass supply chains from economic, social and environmental perspectives – A review of literature. *Renewable and Sustainable Energy Reviews*, 36, 62-73. doi: 10.1016/j.rser.2014.04.041
- Caravaca, A., de Lucas-Consuegra, A., Calcerrada, A. B., Lobato, J., Valverde, J. L., & Dorado, F. (2013). From biomass to pure hydrogen: Electrochemical reforming of bio-ethanol in a PEM electrolyser. *Applied Catalysis B: Environmental*, 134-135, 302-309. doi: 10.1016/j.apcatb.2013.01.033
- Chaubey, R., Sahu, S., James, O. O., & Maity, S. (2013). A review on development of industrial processes and emerging techniques for production of hydrogen from renewable and sustainable sources. *Renewable and Sustainable Energy Reviews*, 23, 443-462. doi: 10.1016/j.rser.2013.02.019
- Chen, W.-H., Jheng, J.-G., & Yu, A. B. (2008). Hydrogen generation from a catalytic water gas shift reaction under microwave irradiation. *International Journal of Hydrogen Energy*, 33(18), 4789-4797. doi: 10.1016/j.ijhydene.2008.06.059
- Chen, Z. X., Prasad, P., Yan, Y. B., & Elnashaie, S. (2003). Simulation for steam reforming of natural gas with oxygen input in a novel membrane reformer. *Fuel Processing Technology*, 83(1-3), 235-252. doi: 10.1016/S0378-3820(03)00072-9
- Christoforou, E. A., & Fokaides, P. A. (2016). Life cycle assessment (LCA) of olive husk torrefaction. *Renewable Energy*, 90, 257-266. doi: 10.1016/j.renene.2016.01.022

Contreras, J. L., Salmones, J., Colín-Luna, J. A., Nuño, L., Quintana, B., Córdova, I., . . . Fuentes, G. A. (2014). Catalysts for H₂ production using the ethanol steam reforming (a review). *International Journal of Hydrogen Energy*, 39(33), 18835-18853. doi: 10.1016/j.ijhydene.2014.08.072

de Lucas-Consuegra, A., Calcerrada, A. B., de la Osa, A. R., & Valverde, J. L. (2014). Electrochemical reforming of ethylene glycol. Influence of the operation parameters, simulation and its optimization. *Fuel Processing Technology*, 127, 13-19. doi: 10.1016/j.fuproc.2014.06.010

Dincer. (2000). Renewable energy and sustainable development: a crucial review. *Renewable & Sustainable Energy Reviews*, 4(2), 157-175. doi: Doi 10.1016/S1364-0321(99)00011-8

Dincer, I., & Zamfirescu, C. (2012). Sustainable hydrogen production options and the role of IAHE. *International Journal of Hydrogen Energy*, 37(21), 16266-16286. doi: 10.1016/j.ijhydene.2012.02.133

Dufour, J., Serrano, D. P., Gálvez, J. L., Moreno, J., & González, A. (2011). Hydrogen Production from Fossil Fuels: Life Cycle Assessment of Technologies with Low Greenhouse Gas Emissions. *Energy & Fuels*, 25(5), 2194-2202. doi: 10.1021/ef200124d

Energy, D. o. (2015). Department of Energy FY 2015 Congressional Budget Request.

Er-rbib, H., & Bouallou, C. (2014). Methanation catalytic reactor. *Comptes Rendus Chimie*, 17(7-8), 701-706. doi: 10.1016/j.crci.2014.01.016

Er-rbib, H., & Bouallou, C. (2014). Modeling and simulation of CO methanation process for renewable electricity storage. *Energy*, 75, 81-88. doi: 10.1016/j.energy.2014.05.115

Fernandes, F. A. N., & Soares, A. B. (2006). Methane steam reforming modeling in a palladium membrane reactor. *Fuel*, 85(4), 569-573. doi: 10.1016/j.fuel.2005.08.002

Galera, S., & Ortiz, F. J. G. (2015). Life cycle assessment of hydrogen and power production by supercritical water reforming of glycerol. *Energy Conversion and Management*, 96, 637-645. doi: 10.1016/j.enconman.2015.03.031

Giraldi, M. R., François, J.-L., & Martin-del-Campo, C. (2015). Life cycle assessment of hydrogen production from a high temperature electrolysis process coupled to a high temperature gas nuclear reactor. *International Journal of Hydrogen Energy*, 40(10), 4019-4033. doi: 10.1016/j.ijhydene.2015.01.093

Gutiérrez-Guerra, N., Jiménez-Vázquez, M., Serrano-Ruiz, J. C., Valverde, J. L., & de Lucas-Consuegra, A. (2015). Electrochemical reforming vs. catalytic reforming of ethanol: A process energy analysis for hydrogen production. *Chemical Engineering and Processing: Process Intensification*, 95, 9-16. doi: 10.1016/j.cep.2015.05.008

Haarlemmer, G. (2015). Simulation study of improved biomass drying efficiency for biomass gasification plants by integration of the water gas shift section in the drying process. *Biomass and Bioenergy*, 81, 129-136. doi: 10.1016/j.biombioe.2015.06.002

Hajjaji, N., Pons, M. N., Renaudin, V., & Houas, A. (2013). Comparative life cycle assessment of eight alternatives for hydrogen production from renewable and fossil feedstock. *Journal of Cleaner Production*, 44, 177-189. doi: 10.1016/j.jclepro.2012.11.043

Han, S. J., Bang, Y., Song, J. H., Yoo, J., Park, S., Kang, K. H., & Song, I. K. (2016). Hydrogen production by steam reforming of ethanol over dual-templated Ni-Al₂O₃ catalyst. *Catalysis Today*, 265, 103-110. doi: 10.1016/j.cattod.2015.07.041

Haseli, Y., Dincer, I., & Naterer, G. F. (2008). Thermodynamic analysis of a combined gas turbine power system with a solid oxide fuel cell through exergy. *Thermochimica Acta*, 480(1-2), 1-9. doi: 10.1016/j.tca.2008.09.007

Hla, S. S., Morpeth, L. D., & Dolan, M. D. (2015). Modelling and experimental studies of a water-gas shift catalytic membrane reactor. *Chemical Engineering Journal*, 276, 289-302. doi: 10.1016/j.cej.2015.04.079

Holladay, J. D., Hu, J., King, D. L., & Wang, Y. (2009). An overview of hydrogen production technologies. *Catalysis Today*, 139(4), 244-260. doi: 10.1016/j.cattod.2008.08.039

Hwang, J., Chang, W., Weng, F., Su, A., & Chen, C. (2008). Development of a small vehicular PEM fuel cell system. *International Journal of Hydrogen Energy*, 33(14), 3801-3807. doi: 10.1016/j.ijhydene.2008.04.043

Hwang, J., Wang, D., & Shih, N. (2005). Development of a lightweight fuel cell vehicle. *Journal of Power Sources*, 141(1), 108-115. doi: 10.1016/j.jpowsour.2004.08.056

Hwang, J. J. (2013). Sustainability study of hydrogen pathways for fuel cell vehicle applications. *Renewable and Sustainable Energy Reviews*, 19, 220-229. doi: 10.1016/j.rser.2012.11.033

Inc, A. T. (2014). Rate-Based Model of the CO₂ Capture Process by MEA using Aspen Plus. Burlington (USA).

ISO14040. (2006). Environmental Management-Life Cycle Assessment-Principles and Framework.

Kadier, A., Simayi, Y., Kalil, M. S., Abdesahian, P., & Hamid, A. A. (2014). A review of the substrates used in microbial electrolysis cells (MECs) for producing sustainable and clean hydrogen gas. *Renewable Energy*, *71*, 466-472. doi: 10.1016/j.renene.2014.05.052

Khila, Z., Hajjaji, N., Pons, M.-N., Renaudin, V., & Houas, A. (2013). A comparative study on energetic and exergetic assessment of hydrogen production from bioethanol via steam reforming, partial oxidation and auto-thermal reforming processes. *Fuel Processing Technology*, *112*, 19-27. doi: 10.1016/j.fuproc.2013.02.013

Koroneos, C. (2004). Life cycle assessment of hydrogen fuel production processes. *International Journal of Hydrogen Energy*, *29*(14), 1443-1450. doi: 10.1016/j.ijhydene.2004.01.016

LeValley, T. L., Richard, A. R., & Fan, M. H. (2014). The progress in water gas shift and steam reforming hydrogen production technologies - A review. *International Journal of Hydrogen Energy*, *39*(30), 16983-17000. doi: 10.1016/j.ijhydene.2014.08.041

Li, B.-H., Zhang, N., & Smith, R. (2016). Simulation and analysis of CO₂ capture process with aqueous monoethanolamine solution. *Applied Energy*, *161*, 707-717. doi: 10.1016/j.apenergy.2015.07.010

Liguras, D. K., Kondarides, D. I., & Verykios, X. E. (2003). Production of hydrogen for fuel cells by steam reforming of ethanol over supported noble metal catalysts. *Applied Catalysis B: Environmental*, *43*(4), 345-354. doi: 10.1016/s0926-3373(02)00327-2

Ling-Chin, J., Heidrich, O., & Roskilly, A. P. (2016). Life cycle assessment (LCA) – from analysing methodology development to introducing an LCA framework for marine photovoltaic (PV) systems. *Renewable and Sustainable Energy Reviews*, *59*, 352-378. doi: 10.1016/j.rser.2015.12.058

Llera, I., Mas, V., Bergamini, M. L., Laborde, M., & Amadeo, N. (2012). Bio-ethanol steam reforming on Ni based catalyst. Kinetic study. *Chemical Engineering Science*, *71*, 356-366. doi: 10.1016/j.ces.2011.12.018

Marbán, G., & Valdés-Solís, T. (2007). Towards the hydrogen economy? *International Journal of Hydrogen Energy*, *32*(12), 1625-1637. doi: 10.1016/j.ijhydene.2006.12.017

Mas, V., Bergamini, M. L., Baronetti, G., Amadeo, N., & Laborde, M. (2008). A Kinetic Study of Ethanol Steam Reforming Using a Nickel Based Catalyst. *Topics in Catalysis*, 51(1-4), 39-48. doi: 10.1007/s11244-008-9123-y

Mathure, P. V., Ganguly, S., Patwardhan, A. V., & Saha, R. K. (2007). Steam reforming of ethanol using a commercial nickel-based catalyst. *Industrial & Engineering Chemistry Research*, 46(25), 8471-8479. doi: 10.1021/ie070321k

Mendes, D., Chibante, V., Mendes, A., & Madeira, L. M. (2010). Determination of the Low-Temperature Water-Gas Shift Reaction Kinetics Using a Cu-Based Catalyst. *Industrial & Engineering Chemistry Research*, 49(22), 11269-11279. doi: 10.1021/ie101137b

Migliardini, F., Veneri, O., & Corbo, P. (2011). Hydrogen and proton exchange membrane fuel cells for clean road transportation. *Journal of Industrial and Engineering Chemistry*, 17(3), 633-641. doi: 10.1016/j.jiec.2011.05.011

Montané, D., Bolshak, E., & Abelló, S. (2011). Thermodynamic analysis of fuel processors based on catalytic-wall reactors and membrane systems for ethanol steam reforming. *Chemical Engineering Journal*, 175, 519-533. doi: 10.1016/j.cej.2011.09.095

Morero, B., Rodriguez, M. B., & Campanella, E. A. (2015). Environmental impact assessment as a complement of life cycle assessment. Case study: Upgrading of biogas. *Bioresour Technol*, 190, 402-407. doi: 10.1016/j.biortech.2015.04.091

Muellerlanger, F., Tzimas, E., Kaltschmitt, M., & Peteves, S. (2007). Techno-economic assessment of hydrogen production processes for the hydrogen economy for the short and medium term. *International Journal of Hydrogen Energy*, 32(16), 3797-3810. doi: 10.1016/j.ijhydene.2007.05.027

Oliveira, E. L. G., Grande, C. A., & Rodrigues, A. E. (2010). Methane steam reforming in large pore catalyst. *Chemical Engineering Science*, 65(5), 1539-1550. doi: 10.1016/j.ces.2009.10.018

Oshima, K., Shinagawa, T., Haraguchi, M., & Sekine, Y. (2013). Low temperature hydrogen production by catalytic steam reforming of methane in an electric field. *International Journal of Hydrogen Energy*, 38(7), 3003-3011. doi: 10.1016/j.ijhydene.2012.12.069

Othman, M. R., Hady, L., Repke, J. U., & Wozny, G. (2012). Introducing sustainability assessment and selection (SAS) into chemical engineering education. *Education for Chemical Engineers*, 7(3), e118-e124. doi: 10.1016/j.ece.2012.05.003

Petrescu, L., & Cormos, C.-C. (2015). Waste reduction algorithm applied for environmental impact assessment of coal gasification with carbon capture and storage. *Journal of Cleaner Production*, 104, 220-235. doi: 10.1016/j.jclepro.2014.08.064

raynolds, M., Fraser, r., & Checkel, D. (2000). The Relative Mass-Energy-Economic (RMEE) Method for System Boundary Selection *Int. J. LCA*, 5(1), 37-46.

Rebitzer, G., Ekvall, T., Frischknecht, R., Hunkeler, D., Norris, G., Rydberg, T., . . . Pennington, D. W. (2004). Life cycle assessment part 1: framework, goal and scope definition, inventory analysis, and applications. *Environ Int*, 30(5), 701-720. doi: 10.1016/j.envint.2003.11.005

Richard Turton, Richard C. Bailie, Wallace B. Whiting, Joseph A. Shaeiwitz, & Debangsu Bhattacharyya. (2013). *Analysis, Synthesis, and Design of Chemical Processes* (Vol. Fourth Edition): Pearson Education Inc.

Roldan, R. (2015). Technical and economic feasibility of adapting an industrial steam reforming unit for production of hydrogen from renewable ethanol. *International Journal of Hydrogen Energy*, 40(4), 2035-2046. doi: 10.1016/j.ijhydene.2014.12.003

Rossetti, I., Compagnoni, M., & Torli, M. (2015a). Process simulation and optimisation of H₂ production from ethanol steam reforming and its use in fuel cells. 1. Thermodynamic and kinetic analysis. *Chemical Engineering Journal*, 281, 1024-1035. doi: 10.1016/j.cej.2015.08.025

Rossetti, I., Compagnoni, M., & Torli, M. (2015b). Process simulation and optimization of H₂ production from ethanol steam reforming and its use in fuel cells. 2. Process analysis and optimization. *Chemical Engineering Journal*, 281, 1036-1044. doi: 10.1016/j.cej.2015.08.045

Rui, Z. B., Zhang, K., Li, Y. D., & Lin, Y. S. (2008). Simulation of methane conversion to syngas in a membrane reactor: Part I A model including product oxidation. *International Journal of Hydrogen Energy*, 33(9), 2246-2253. doi: 10.1016/j.ijhydene.2008.02.047

Saxena, R. C., Seal, D., Kumar, S., & Goyal, H. B. (2008). Thermo-chemical routes for hydrogen rich gas from biomass: A review. *Renewable and Sustainable Energy Reviews*, 12(7), 1909-1927. doi: 10.1016/j.rser.2007.03.005

Simpson, A., & Lutz, A. (2007). Exergy analysis of hydrogen production via steam methane reforming. *International Journal of Hydrogen Energy*, 32(18), 4811-4820. doi: 10.1016/j.ijhydene.2007.08.025

- Singh, A. P., Singh, S., Ganguly, S., & Patwardhan, A. V. (2014). Steam reforming of methane and methanol in simulated macro & micro-scale membrane reactors: Selective separation of hydrogen for optimum conversion. *Journal of Natural Gas Science and Engineering*, 18, 286-295. doi: 10.1016/j.jngse.2014.03.008
- Sobrinho, F. H., Monroy, C. R., & Pérez, J. L. H. (2010). Critical analysis on hydrogen as an alternative to fossil fuels and biofuels for vehicles in Europe. *Renewable and Sustainable Energy Reviews*, 14(2), 772-780. doi: 10.1016/j.rser.2009.10.021
- Suh, S., Lenzen, M., Treloar, G. J., Hondo, H., Horvath, A., Huppes, G., . . . Norris, G. (2004). System Boundary Selection in Life-Cycle Inventories Using Hybrid Approaches. *Environ Sci Technol*, 38(3), 657-664. doi: 10.1021/es0263745
- Susmozas, A., Iribarren, D., Zapp, P., Linßen, J., & Dufour, J. (2016). Life-cycle performance of hydrogen production via indirect biomass gasification with CO₂ capture. *International Journal of Hydrogen Energy*. doi: 10.1016/j.ijhydene.2016.02.053
- Verma, A., & Kumar, A. (2015). Life cycle assessment of hydrogen production from underground coal gasification. *Applied Energy*, 147, 556-568. doi: 10.1016/j.apenergy.2015.03.009
- Vicente, J., Erena, J., Olazar, M., Benito, P. L., Bilbao, J., & Gayubo, A. G. (2014). Kinetic behaviour of commercial catalysts for methane reforming in ethanol steam reforming process. *Journal of Energy Chemistry*, 23(5), 639-644. doi: 10.1016/S2095-4956(14)60195-9
- West, A. H., Posarac, D., & Ellis, N. (2008). Assessment of four biodiesel production processes using HYSYS.Plant. *Bioresour Technol*, 99(14), 6587-6601. doi: 10.1016/j.biortech.2007.11.046
- World, C. E. (June 2017). *Chemical Engineering World CEW*, 52.
- Wurzler, G. T., Rabelo-Neto, R. C., Mattos, L. V., Fraga, M. A., & Noronha, F. B. (2016). Steam reforming of ethanol for hydrogen production over MgO—supported Ni-based catalysts. *Applied Catalysis A: General*, 518, 115-128. doi: 10.1016/j.apcata.2015.11.020
- Ye, C., Mu, D., Horowitz, N., Xue, Z., Chen, J., Xue, M., . . . Zhou, W. (2018). Life cycle assessment of industrial scale production of spirulina tablets. *Algal Research*, 34, 154-163. doi: 10.1016/j.algal.2018.07.013
- Young, D. M., & Cabezas, H. (1999). Designing sustainable processes with simulation the waste reduction WAR algorithm. *computers and chemical engineering*, 23.

APPENDIX A-1
STREAM SUMMARY FROM ASPEN PLUS FOR CASE 1

Stream	NG	STEAM	LEANIN	H2	WATER	CO2OUT	LEANOUT
Mole Flow kmol/hr							
MEA	0	0	301.84	1.49E-06	0.0026	0.0156	285.23
H2O	0	444.07	6119.71	21.38	121.54	737.21	5369.53
CO2	0	0	0.00100	11.43	0.00126	121.52	0.093
H2S	0	0	0	0	0	0	0
H3O+	0	0	4.48E-08	0	2.40E-08	0	8.92E-07
OH-	0	0	0.0240	0	2.79E-06	0	0.02422
HCO3-	0	0	3.64	0	0.068	0	14.93
CO3-2	0	0	4.43	0	0.000575	0	1.40
HS-	0	0	0	0	0	0	0
S-2	0	0	0	0	0	0	0
MEAH+	0	0	195.78	0	0.071	0	206.65
MEACOO-	0	0	183.25	0	0.0016	0	188.90
N2	0	0	0	0	0	0	0
O2	0	0	0	0	0	0	0
CO	0	0	0	11.76	3.80E-05	0.0047	4.75E-27
H2	1.60	0	0	624.69	0.001657	0.2578	4.75E-27
CH4	158.7	0	0	0	0	0	0
ETHYL-01	0	0	0	0	0	0	0
N-HEX-01	0	0	0	0	0	0	0
Mole Frac							
MEA	0	0	0.0443	2.23E-09	2.12E-05	1.81E-05	0.0470
H2O	0	1	0.8988	0.0319	0.9988	0.8582	0.8851
CO2	0	0	1.47E-07	0.0171	1.03E-05	0.1415	1.53E-05
H2S	0	0	0	0	0	0	0
H3O+	0	0	6.58E-12	0	1.97E-10	0	1.47E-10
OH-	0	0	3.53E-06	0	2.29E-08	0	3.99E-06
HCO3-	0	0	0.0005348	0	0.000561	0	0.00246
CO3-2	0	0	0.0006509	0	4.73E-06	0	0.000231
HS-	0	0	0	0	0	0	0
S-2	0	0	0	0	0	0	0
MEAH+	0	0	0.02875	0	0.000583	0	0.03406
MEACOO-	0	0	0.0269	0	1.29E-05	0	0.0311
N2	0	0	0	0	0	0	0
O2	0	0	0	0	0	0	0
CO	0	0	0	0.0176	3.12E-07	5.53E-06	7.82E-31
H2	0.01	0	0	0.9334	1.36E-05	3.00E-04	7.82E-31
CH4	0.99	0	0	0	0	0	0
ETHYL-01	0	0	0	0	0	0	0

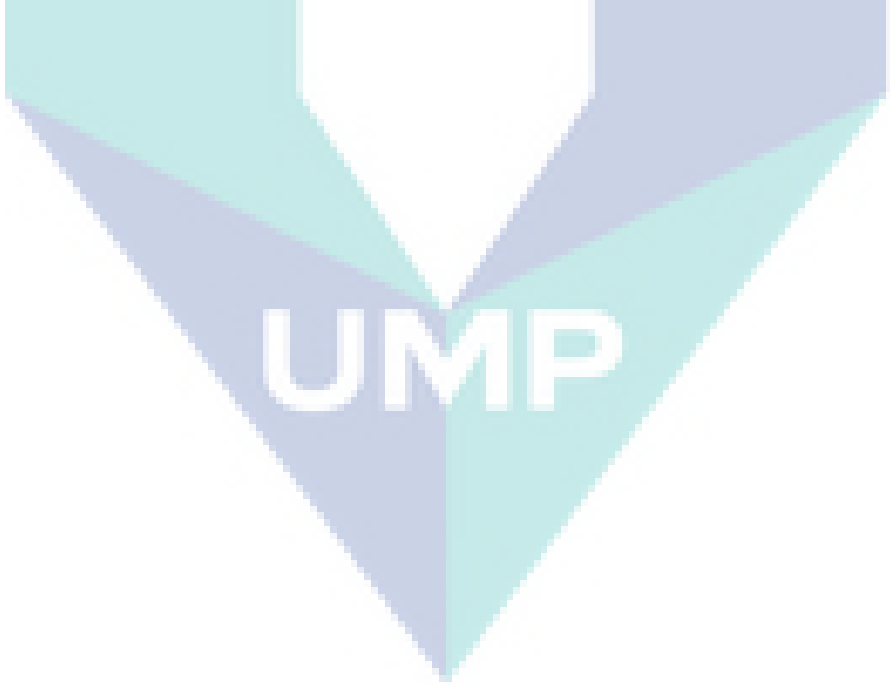
N-HEX-01	0	0	0	0	0	0	0
Mass Flow kg/hr							
MEA	0	0	18437.47	9.13E-05	0.16	0.9523	17423.06
H2O	0	8000	110248.00	385.21	2189.56	13281.12	96733.51
CO2	0	0	0.04416	503.12	0.05541	5348.10	4.07
H2S	0.0000	0.000	0.000	0.0000	0.0000	0.0000	0.0000
H3O+	0	0	8.52E-07	0	4.56E-07	0	1.70E-05
OH-	0	0	0.4086	0	4.75E-05	0	0.4119
HCO3-	0	0	222.19	0	4.1626	0	910.77
CO3-2	0	0	265.96	0	0.03452	0	84.07
HS-	0	0	0	0	0	0	0
S-2	0	0	0	0	0	0	0
MEAH+	0	0	12156.12	0	4.4052	0	12831.03
MEACOO-	0	0	19073.73	0	0.1639	0	19661.45
N2	0	0	0	0	0	0	0
O2	0	0	0	0	0	0	0
CO	0	0	0	329.32	0.001065	0.1330	1.33E-25
H2	3.233	0	0	1259.31	0.00334	0.5196	9.57E-27
CH4	2546.77	0	0	0	0	0	0
ETHYL-01	0	0	0	0	0	0	0
N-HEX-01	0	0	0	0	0	0	0
Mass Frac							
MEA	0	0	0.1149	3.69E-08	7.17E-05	5.11E-05	0.118
H2O	0	1	0.6873	0.1555	0.9959	0.7129	0.6552
CO2	0	0	2.75E-07	0.2031	2.52E-05	0.2871	2.76E-05
H2S	0	0	0	0	0	0	0
H3O+	0	0	5.31E-12	0	2.07E-10	0	1.15E-10
OH-	0	0	2.55E-06	0	2.16E-08	0	2.79E-06
HCO3-	0	0	0.001385	0	0.001893	0	0.006168
CO3-2	0	0	0.001658	0	1.57E-05	0	0.000569
HS-	0	0	0	0	0	0	0
S-2	0	0	0	0	0	0	0
MEAH+	0	0	0.07578	0	0.002004	0	0.08690
MEACOO-	0	0	0.1189	0	7.46E-05	0	0.1332
N2	0	0	0	0	0	0	0
O2	0	0	0	0	0	0	0
CO	0	0	0	0.1330	4.84E-07	7.14E-06	9.00E-31
H2	0.001268	0	0	0.5084	1.52E-06	2.79E-05	6.48E-32
CH4	0.9987	0	0	0	0	0	0
ETHYL-01	0	0	0	0	0	0	0
N-HEX-01	0	0	0	0	0	0	0
Total Flow kmol/hr	160.35	444.07	6808.68	669.27	121.69	859.01	6066.75
Total Flow kg/hr	2550	8000	160404	2476.96	2198.55	18630.82	147648
Total Flow l/min	66128.91	391681	2534.58	276644	36.69	453165	2398.54
Temperature K	298.15	1273.15	313.15	298.15	298.15	367.16	372.80
Pressure atm	0.9869	1.97	1.97	0.9869	0.9869	0.9376	0.9474

APPENDIX A-2

MODEL SUMMARY FROM ASPEN PLUS FOR CASE 1

Name	HeatX					
	E-101	E-102	E-103	E-104	E-105	E-106
Hot side property method	ENRTL-RK	ENRTL-RK	ENRTL-RK	ENRTL-RK	ENRTL-RK	ENRTL-RK
Hot side Henry's component list ID	GLOBAL	GLOBAL	GLOBAL	GLOBAL	GLOBAL	GLOBAL
Hot side electrolyte chemistry ID	MEA-CHEM	MEA-CHEM	MEA-CHEM	MEA-CHEM	MEA-CHEM	MEA-CHEM
Hot side use true species approach for electrolytes	YES	YES	YES	YES	YES	YES
Hot side free-water phase properties method	STEAM-TA	STEAM-TA	STEAM-TA	STEAM-TA	STEAM-TA	STEAM-TA
Hot side water solubility method	3	3	3	3	3	3
Cold side property method	ENRTL-RK	ENRTL-RK	ENRTL-RK	ENRTL-RK	ENRTL-RK	ENRTL-RK
Cold side Henry's component list ID	GLOBAL	GLOBAL	GLOBAL	GLOBAL	GLOBAL	GLOBAL
Cold side electrolyte chemistry ID	MEA-CHEM	MEA-CHEM	MEA-CHEM	MEA-CHEM	MEA-CHEM	MEA-CHEM
Cold side use true species approach for electrolytes	YES	YES	YES	YES	YES	YES
Cold side free-water phase properties method	STEAM-TA	STEAM-TA	STEAM-TA	STEAM-TA	STEAM-TA	STEAM-TA
Cold side water solubility method	3	3	3	3	3	3
Exchanger specification	730	400	210	40	105	25
Units of exchanger specification	C	C	C	C	C	C
Exchanger area [sqm]						
Constant UA [cal/sec-K]						
Minimum temperature approach [K]	1	1	1	10	10	5
Hot side outlet pressure [atm]	0	0	0	0	0	0
Cold side outlet pressure [atm]	0	0	0	0	0	0
EO Model components						
Hot side EO Model components						
Cold side EO Model components						
Inlet hot stream temperature [K]	1273.15	1003.15	790.881604	551.694744	523.15	492.6119
Inlet hot stream pressure [atm]	2	0.986923267	0.986923267	0.986923267	39.2338672	2.86207747
Inlet hot stream vapor fraction	1	1	1	1	1	1
Outlet hot stream temperature [K]	1065.56723	673.15	483.15	313.15	473.15	298.15
Outlet hot stream pressure [atm]	2	0.986923267	0.986923267	0.986923267	15.3439472	2.86207747
Outlet hot stream vapor fraction	1	1	1	0.91856597	0	0.828256882
Inlet cold stream temperature [K]	968.656009	293.15	293.15	293.15	324.922199	293.15
Inlet cold stream pressure [atm]	0.986923267	1	1	1	2.86207747	1
Inlet cold stream vapor fraction	1	0	0	0	0	0
Outlet cold stream temperature [K]	1003.15	313.15	313.15	313.15	378.15	313.15
Outlet cold stream pressure [atm]	0.986923267	1	1	1	2.86207747	1
Outlet cold stream vapor fraction	1	0	0	0	0	0
Heat duty [cal/sec]	68102.543	667551.047	619857.565	685051.07	2031911.09	705600.856
Calculated heat duty [cal/sec]	68102.543	667551.047	619857.565	685051.07	2031911.09	705600.856
Required exchanger area [sqm]	1.98574445	6.32714055	9.7841976	73.8346145	68.2668922	133.697236
Actual exchanger area [sqm]	1.98574445	6.32714055	9.7841976	73.8346145	68.2668922	133.697236
Average U (Dirty) [cal/sec-sqcm-K]	0.020301901	0.020301901	0.020301901	0.020301901	0.020301901	0.020301901
Average U (Clean)						
UA [cal/sec-K]	403.143877	1284.52982	1986.37813	14989.8305	13859.477	27143.0807
LMTD (Corrected) [K]	168.92863	519.685128	312.054163	45.7010551	146.608064	25.9956068
LMTD correction factor	1	1	1	1	1	1
Thermal effectiveness						
Number of transfer units						
Number of shells in series	1	1	1	1	1	1
Number of shells in parallel						
Total feed stream CO2e flow [kg/hr]	65801.8837	0	4191.89038	6470.15673	4.02771875	506.271596
Total product stream CO2e flow [kg/hr]	65801.8837	0	4191.89038	6470.15414	81.0885429	503.03597
Net stream CO2e production [kg/hr]	0	0	0	-0.002585424	77.0608241	-3.23562614
Utility CO2e production [kg/hr]	0	0	0	0	2013.74342	0
Total CO2e production [kg/hr]	0	0	0	-0.002585424	2090.80424	-3.23562614
Utility usage [kg/hr]		120405.09	111802.695	123561.541	15723.089	127268.072
Utility cost [\$/hr]		2.13306976	1.98067164	2.18898873	76.5648482	2.25465281
Hot utility ID					U-1	
Cold utility ID		COOL	COOL	COOL		COOL

Name	RPlug		
	R-102	R-103	R-101
Process stream property method	RKSMHV2	RKSMHV2	RKSMHV2
Process stream Henry's component list ID	GLOBAL	GLOBAL	GLOBAL
Process stream electrolyte chemistry ID	MEA-CHEM	MEA-CHEM	MEA-CHEM
Process stream use true species approach for electrolytes	YES	YES	YES
Process stream free-water phase properties method	STEAM-TA	STEAM-TA	STEAM-TA
Process stream water solubility method	3	3	3
Thermal fluid property method	ENRTL-RK	ENRTL-RK	ENRTL-RK
Thermal fluid Henry's component list ID	GLOBAL	GLOBAL	GLOBAL
Thermal fluid electrolyte chemistry ID	MEA-CHEM	MEA-CHEM	MEA-CHEM
Thermal fluid use true species approach for electrolytes	YES	YES	YES
Thermal fluid free-water phase properties method	STEAM-TA	STEAM-TA	STEAM-TA
Thermal fluid water solubility method	3	3	3
Number of tubes	10	10	40
Reactor dimensions length [meter]	10	10	10
Reactor dimensions diameter [meter]	2	2	1.5
Pressure at reactor inlet: process stream [atm]	0	0	0
EO Model components			
Heat duty [cal/sec]	-2.41E-07	-1.41E-06	2366284.3
Minimum reactor temperature [K]	673.240471	483.285519	973.15
Maximum reactor temperature [K]	790.877856	551.637917	973.15
Residence time [hr]	0.002334498	0.002987961	0.005089524
Thermal fluid inlet temperature			
Thermal fluid inlet vapor fraction			
Total feed stream CO2e flow [kg/hr]	37.7729514	4228.84972	63669.1873
Total product stream CO2e flow [kg/hr]	4228.84972	6504.42848	37.7729514
Net stream CO2e production [kg/hr]	4191.07677	2275.57876	-63631.4143



UMP

Flash2	
Name	V-101
Property method	ENRTL-RK
Henry's component list ID	GLOBAL
Electrolyte chemistry ID	MEA-CHEM
Use true species approach for electrolytes	YES
Free-water phase properties method	STEAM-TA
Water solubility method	3
Temperature [K]	298.15
Pressure [atm]	0.986923267
Specified vapor fraction	
Specified heat duty [cal/sec]	
EO Model components	
Outlet temperature [K]	298.15
Outlet pressure [atm]	0.986923267
Vapor fraction	0.846152598
Heat duty [cal/sec]	41151.6921
Net duty [cal/sec]	41151.6921
First liquid / total liquid	1
Total feed stream CO2e flow [kg/hr]	503.03597
Total product stream CO2e flow [kg/hr]	503.174673
Net stream CO2e production [kg/hr]	0.138703437
Utility CO2e production [kg/hr]	0
Total CO2e production [kg/hr]	0.138703437
Utility usage	
Utility cost	
Utility ID	

UMP

RadFrac		
Name	T-101	T-102
Property method	ENRTL-RK	ENRTL-RK
Henry's component list ID	GLOBAL	GLOBAL
Electrolyte chemistry ID	MEA-CHEM	MEA-CHEM
Use true species approach for electrolytes	YES	YES
Free-water phase properties method	STEAM-TA	STEAM-TA
Water solubility method	3	3
Number of stages	20	20
Condenser	NONE	PARTIAL-V
Reboiler	NONE	KETTLE
Number of phases	2	2
Free-water	NO	NO
Top stage pressure [atm]	0.957315569	0.937577103
Specified reflux ratio		0.5
Specified bottoms rate [kmol/hr]		
Specified boilup rate [kmol/hr]		
Specified distillate rate [kmol/hr]		
EO Model components		
Calculated molar reflux ratio	8.8587053	0.5
Calculated bottoms rate [kmol/hr]	6804.57968	6066.74667
Calculated boilup rate [kmol/hr]	903.027387	1249.42185
Calculated distillate rate [kmol/hr]	791.022594	859.012922
Condenser / top stage temperature [K]	332.084895	367.164582
Condenser / top stage pressure [atm]	0.957315569	0.937577103
Condenser / top stage heat duty [cal/sec]	0	-1176931.85
Condenser / top stage subcooled duty		
Condenser / top stage reflux rate [kmol/hr]	7007.43604	429.506461
Condenser / top stage free water reflux ratio		
Reboiler pressure [atm]	0.957315569	0.947446336
Reboiler temperature [K]	325.840059	372.795565
Reboiler heat duty [cal/sec]	0	3582688.45
Total feed stream CO2e flow [kg/hr]	6470.1983	81.0885429
Total product stream CO2e flow [kg/hr]	525.340864	5352.17317
Net stream CO2e production [kg/hr]	-5944.85743	5271.08463
Utility CO2e production [kg/hr]	0	0
Total CO2e production [kg/hr]	-5944.85743	5271.08463
Condenser utility usage		
Condenser utility cost		
Condenser utility ID		
Reboiler utility usage		
Reboiler utility cost		
Reboiler utility ID		
Basis for specified distillate to feed ratio	MOLE	MOLE
Specified distillate to feed ratio		
Basis for specified bottoms to feed ratio	MOLE	MOLE
Specified bottoms to feed ratio		
Basis for specified boilup ratio	MOLE	MOLE
Specified boilup ratio		
Calculated molar boilup ratio		0.20594594
Calculated mass boilup ratio	0.06079891	0.165298061

APPENDIX B-1
STREAM SUMMARY FROM ASPEN PLUS FOR CASE 2

Stream	ETH	H2O	LEANIN	H2	WATER	CO2OUT	LEANOUT
Mole Flow kmol/hr							
MEA	0	0	561.11	9.47E-07	0.000371	7.60E-06	576.59
H2O	0	610.59	11364.5	21.40	27.79	139.31	11437.39
CO2	0	0	0.002162	19.96	0.0005	167.89	1.073
H2S	0	0	0	0	0	0	0
H3O+	0	0	9.02E-08	0	9.06E-09	0	4.90E-06
OH-	0	0	0.04156	0	3.89E-07	0	0.03589
HCO3-	0	0	7.307	0	0.01650	0	53.54
CO3-2	0	0	8.368	0	8.51E-05	0	1.710
HS-	0	0	0	0	0	0	0
S-2	0	0	0	0	0	0	0
MEAH+	0	0	363.72	0	0.01691	0	372.43
MEACOO-	0	0	339.64	0	0.00024	0	315.43
N2	0	0	0	0	0	0	0
O2	0	0	0	0	0	0	0
CO	0	0	0	6.301	4.65E-06	0.003846	1.28E-26
H2	0	0	0	625.12	0.000378	0.3983	1.28E-26
CH4	0	0	0	0	0	0	0
ETHYL-01	0	0	0	0	0	0	0
N-HEX-01	0	0	0	0	0	0	0
ETHANOL	107.45	0	0	0	0	0.01962	2.124
Mole Frac							
MEA	0	0	0.04437	1.41E-09	1.33E-05	2.47E-08	0.04519
H2O	0	1	0.8988	0.03181	0.9987	0.4529	0.8963
CO2	0	0	1.71E-07	0.02967	1.80E-05	0.5458	8.41E-05
H2S	0	0	0	0	0	0	0
H3O+	0	0	7.13E-12	0	3.25E-10	0	3.84E-10
OH-	0	0	3.29E-06	0	1.40E-08	0	2.81E-06
HCO3-	0	0	0.000578	0	0.000593	0	0.004196
CO3-2	0	0	0.000662	0	3.06E-06	0	0.000134
HS-	0	0	0	0	0	0	0
S-2	0	0	0	0	0	0	0
MEAH+	0	0	0.02876	0	0.000608	0	0.02919
MEACOO-	0	0	0.02686	0	8.63E-06	0	0.02472
N2	0	0	0	0	0	0	0
O2	0	0	0	0	0	0	0
CO	0	0	0	0.009365	1.67E-07	1.25E-05	1.00E-30
H2	0	0	0	0.9292	1.36E-05	0.001295	1.00E-30
CH4	0	0	0	0	0	0	0
ETHYL-01	0	0	0	0	0	0	0
N-HEX-01	0	0	0	0	0	0	0

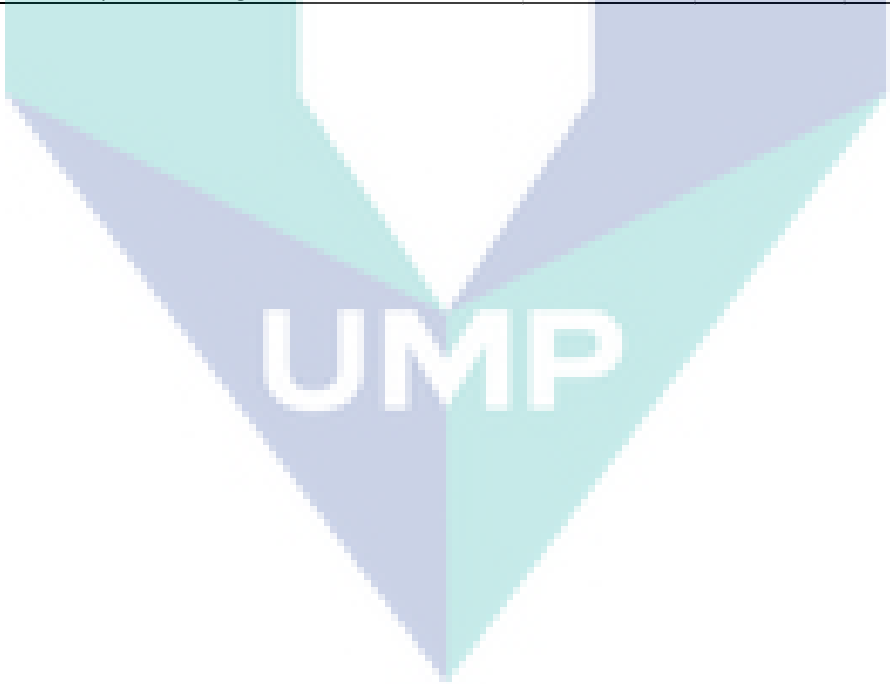
ETHANOL	1	0	0	0	0	6.38E-05	0.000166
Mass Flow kg/hr							
MEA	0	0	34274.49	5.79E-05	0.02266	0.000464	35220.45
H2O	0	11000	204735	385.56	500.73	2509.70	206048
CO2	0	0	0.09513	878.59	0.02201	7388.61	47.23
H2S	0	0	0	0	0	0	0
H3O+	0	0	1.72E-06	0	1.72E-07	0	9.32E-05
OH-	0	0	0.7068	0	6.61E-06	0	0.610387
HCO3-	0	0	445.85	0	1.007	0	3266.75
CO3-2	0	0	502.15	0	0.005108	0	102.61
HS-	0	0	0	0	0	0	0
S-2	0	0	0	0	0	0	0
MEAH+	0	0	22583.95	0	1.050	0	23124.32
MEACOO-	0	0	35351.7	0	0.02499	0	32832.13
N2	0	0	0	0	0	0	0
O2	0	0	0	0	0	0	0
CO	0	0	0	176.48	0.00013	0.1077	3.57E-25
H2	0	0	0	1260.17	0.000762	0.8029	2.57E-26
CH4	0	0	0	0	0	0	0
ETHYL-01	0	0	0	0	0	0	0
N-HEX-01	0	0	0	0	0	0	0
ETHANOL	4950	0	0	0	0	0.9041	97.84
Mass Frac							
MEA	0	0	0.1151	2.14E-08	4.51E-05	4.69E-08	0.1171
H2O	0	1	0.6873	0.1428	0.99576	0.2535	0.6851
CO2	0	0	3.19E-07	0.3253	4.38E-05	0.7463	0.000157
H2S	0	0	0	0	0	0	0
H3O+	0	0	5.76E-12	0	3.43E-10	0	3.10E-10
OH-	0	0	2.37E-06	0	1.31E-08	0	2.03E-06
HCO3-	0	0	0.001497	0	0.002002	0	0.01086
CO3-2	0	0	0.001686	0	1.02E-05	0	0.000341
HS-	0	0	0	0	0	0	0
S-2	0	0	0	0	0	0	0
MEAH+	0	0	0.07581	0	0.002088	0	0.07689
MEACOO-	0	0	0.1187	0	4.97E-05	0	0.1092
N2	0	0	0	0	0	0	0
O2	0	0	0	0	0	0	0
CO	0	0	0	0.06534	2.59E-07	1.09E-05	1.19E-30
H2	0	0	0	0.4666	1.52E-06	8.11E-05	8.55E-32
CH4	0	0	0	0	0	0	0
ETHYL-01	0	0	0	0	0	0	0
N-HEX-01	0	0	0	0	0	0	0
ETHANOL	1	0	0	0	0	9.13E-05	0.000325
Total Flow kmol/hr	107.45	610.59	12644.69	672.79	27.83	307.62	12760.33
Total Flow kg/hr	4950	11000	297894	2700.81	502.86	9900.13	300740
Total Flow cum/hr	6.299	64630.51	282.41	16685.8	0.5034	4670.46	299.55
Temperature C	25	1000	40	25	25	96.56	117.46
Pressure bar	1	1	2	1	1	2.00	2.01

APPENDIX B-2
MODEL SUMMARY FROM ASPEN PLUS FOR CASE 2

Name	HeatX					
	E-201	E-202	E-203	E-204	E-205	E-206
Hot side property method	ENRTL-RK	ENRTL-RK	ENRTL-RK	ENRTL-RK	ENRTL-RK	ENRTL-RK
Hot side Henry's component list ID	GLOBAL	GLOBAL	GLOBAL	GLOBAL	GLOBAL	GLOBAL
Hot side electrolyte chemistry ID	MEA-CHEM	MEA-CHEM	MEA-CHEM	MEA-CHEM	MEA-CHEM	MEA-CHEM
Hot side use true species approach for electrolytes	YES	YES	YES	YES	YES	YES
Hot side free-water phase properties method	STEAM-TA	STEAM-TA	STEAM-TA	STEAM-TA	STEAM-TA	STEAM-TA
Hot side water solubility method	3	3	3	3	3	3
Cold side property method	ENRTL-RK	ENRTL-RK	ENRTL-RK	ENRTL-RK	ENRTL-RK	ENRTL-RK
Cold side Henry's component list ID	GLOBAL	GLOBAL	GLOBAL	GLOBAL	GLOBAL	GLOBAL
Cold side electrolyte chemistry ID	MEA-CHEM	MEA-CHEM	MEA-CHEM	MEA-CHEM	MEA-CHEM	MEA-CHEM
Cold side use true species approach for electrolytes	YES	YES	YES	YES	YES	YES
Cold side free-water phase properties method	STEAM-TA	STEAM-TA	STEAM-TA	STEAM-TA	STEAM-TA	STEAM-TA
Cold side water solubility method	3	3	3	3	3	3
Exchanger specification	873	400	210	40	112	25
Units of exchanger specification	C	C	C	C	C	C
Exchanger area [sqm]						
Constant UA [kJ/sec-K]						
Minimum temperature approach [C]	1	1	1	1	1	5
Hot side outlet pressure [bar]	0	0	0	0	0	0
Cold side outlet pressure [bar]	0	0	0	0	0	0
EO Model components						
Hot side EO Model components						
Cold side EO Model components						
Inlet hot stream temperature [C]	1000	873	541.502521	267.484779	250	194.330101
Inlet hot stream pressure [bar]	2.0265	1	1	1	39.7537159	2.9
Inlet hot stream vapor fraction	1	1	1	1	1	1
Outlet hot stream temperature [C]	593.192294	400	210	40	249	25
Outlet hot stream pressure [bar]	2.0265	1	1	1	39.0875964	2.9
Outlet hot stream vapor fraction	1	1	1	0.79339497	0	0.940069094
Inlet cold stream temperature [C]	580.758045	20	20	20	55.5637077	20
Inlet cold stream pressure [bar]	1	1.01325	1.01325	1.01325	2.9	1.01325
Inlet cold stream vapor fraction	1	0	0	0	0	0
Outlet cold stream temperature [C]	873	40	40	40	112	40
Outlet cold stream pressure [bar]	1	1.01325	1.01325	1.01325	2.9	1.01325
Outlet cold stream vapor fraction	1	0	0	0	0.000115539	0
Heat duty [kW]	3288.57708	5260.57891	3615.93845	5216.95824	17391.4374	1496.06152
Calculated heat duty [kW]	3288.57708	5260.57891	3615.93845	5216.95824	17391.4374	1496.06152
Required exchanger area [sqm]	78.4730269	10.7228426	13.2548225	161.528822	124.692657	67.9644365
Actual exchanger area [sqm]	78.4730269	10.7228426	13.2548225	161.528822	124.692657	67.9644365
Average U (Dirty) [kW/sqm-K]	0.85	0.85	0.85	0.85	0.85	0.85
Average U (Clean)						
UA [kJ/sec-K]	66.7020728	9.11441618	11.2665991	137.299499	105.988759	57.769771
LMTD (Corrected) [C]	49.3024721	577.171242	320.943206	37.9969212	164.087566	25.8969612
LMTD correction factor	1	1	1	1	1	1
Thermal effectiveness						
Number of transfer units						
Number of shells in series	1	1	1	1	1	1
Number of shells in parallel						
Total feed stream CO2e flow [kg/hr]	12796.1785	0	6545.10825	8991.36757	3.66138354	879.355728
Total product stream CO2e flow [kg/hr]	12796.1785	0	6545.10825	8991.35673	185.380806	878.591637
Net stream CO2e production [kg/hr]	0	0	0	-0.010845965	181.719422	-0.764090709
Utility CO2e production [kg/hr]	0	0	0	0	4116.73738	0
Total CO2e production [kg/hr]	0	0	0	-0.010845965	4298.45681	-0.764090709
Utility usage [kg/hr]		226627.021	155775.509	224747.832	36415.0351	64450.6947
Utility cost [\$/sec]		0.001115243	0.000766579	0.001105995	0.043478594	0.000317165
Hot utility ID					STEAMHP	
Cold utility ID		COOL	COOL	COOL		COOL

RadFrac		
Name	T-201	T-202
Property method	ENRTL-RK	ENRTL-RK
Henry's component list ID	GLOBAL	GLOBAL
Electrolyte chemistry ID	MEA-CHEM	MEA-CHEM
Use true species approach for electrolytes	YES	YES
Free-water phase properties method	STEAM-TA	STEAM-TA
Water solubility method	3	3
Number of stages	20	20
Condenser	NONE	PARTIAL-V
Reboiler	NONE	KETTLE
Number of phases	2	2
Free-water	NO	NO
Top stage pressure [bar]	0.97708	1.99914225
Specified reflux ratio		0.5
Specified bottoms rate [kmol/hr]		
Specified boilup rate [kmol/hr]		
Specified distillate rate [kmol/hr]		
EO Model components		
Calculated molar reflux ratio	18.050175	0.5
Calculated bottoms rate [kmol/hr]	12899.9964	12760.3259
Calculated boilup rate [kmol/hr]	978.875886	657.227634
Calculated distillate rate [kmol/hr]	700.633745	307.616948
Condenser / top stage temperature [C]	40.3170107	96.5583408
Condenser / top stage pressure [bar]	0.97708	1.99914225
Condenser / top stage heat duty [kW]	0	-1777.63336
Condenser / top stage subcooled duty		
Condenser / top stage reflux rate [kmol/hr]	12646.5617	153.808474
Condenser / top stage free water reflux ratio		
Reboiler pressure [bar]	0.98708	2.00914225
Reboiler temperature [C]	56.1068051	117.455488
Reboiler heat duty [kW]	0	9000
Total feed stream CO2e flow [kg/hr]	8991.45185	185.380806
Total product stream CO2e flow [kg/hr]	923.899172	7435.83623
Net stream CO2e production [kg/hr]	-8067.55268	7250.45543
Utility CO2e production [kg/hr]	0	0
Total CO2e production [kg/hr]	-8067.55268	7250.45543
Condenser utility usage		
Condenser utility cost		
Condenser utility ID		
Reboiler utility usage		
Reboiler utility cost		
Reboiler utility ID		
Basis for specified distillate to feed ratio	MOLE	MOLE
Specified distillate to feed ratio		
Basis for specified bottoms to feed ratio	MOLE	MOLE
Specified bottoms to feed ratio		
Basis for specified boilup ratio	MOLE	MOLE
Specified boilup ratio		
Calculated molar boilup ratio	97	0.051505552
Calculated mass boilup ratio	0.040943524	0.048972975

RPlug			
Name	R-201	R-202	R-203
Process stream property method	ENRTL-RK	ENRTL-RK	ENRTL-RK
Process stream Henry's component list ID	GLOBAL	GLOBAL	GLOBAL
Process stream electrolyte chemistry ID	MEA-CHEM	MEA-CHEM	MEA-CHEM
Process stream use true species approach for electrolytes	YES	YES	YES
Process stream free-water phase properties method	STEAM-TA	STEAM-TA	STEAM-TA
Process stream water solubility method	3	3	3
Thermal fluid property method	ENRTL-RK	ENRTL-RK	ENRTL-RK
Thermal fluid Henry's component list ID	GLOBAL	GLOBAL	GLOBAL
Thermal fluid electrolyte chemistry ID	MEA-CHEM	MEA-CHEM	MEA-CHEM
Thermal fluid use true species approach for electrolytes	YES	YES	YES
Thermal fluid free-water phase properties method	STEAM-TA	STEAM-TA	STEAM-TA
Thermal fluid water solubility method	3	3	3
Number of tubes	40	10	10
Reactor dimensions length [meter]	10	10	10
Reactor dimensions diameter [meter]	1.5	2	2
Pressure at reactor inlet: process stream [bar]	0	0	0
EO Model components			
Heat duty [kW]	8168.3758	-1.55E-07	1.04E-07
Minimum reactor temperature [C]	800	400	210
Maximum reactor temperature [C]	800	541.659335	267.765869
Residence time [sec]	10.8308073	5.8621115	8.83022571
Thermal fluid inlet temperature			
Thermal fluid inlet vapor fraction			
Total feed stream CO2e flow [kg/hr]	0	0	6553.46908
Total product stream CO2e flow [kg/hr]	0	6553.46908	9012.46892
Net stream CO2e production [kg/hr]	0	6553.46908	2458.99984

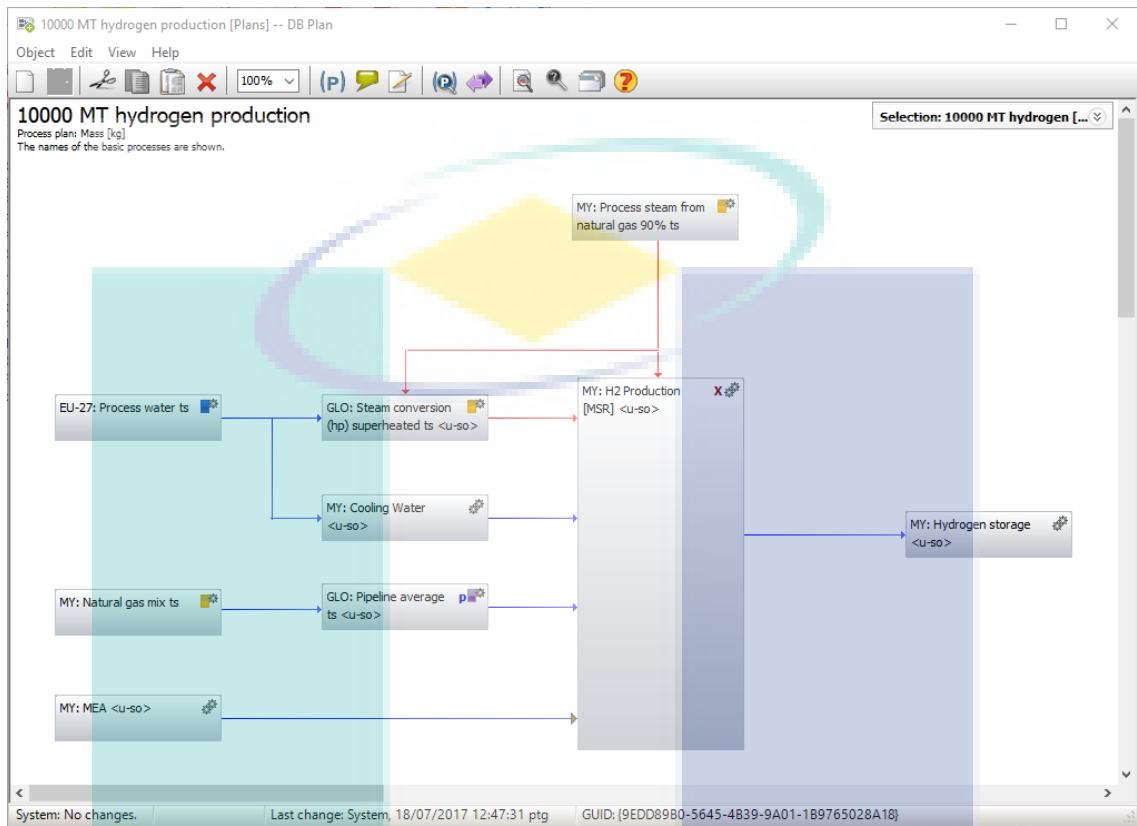


UMP

Flash2	
Name	V-201
Property method	ENRTL-RK
Henry's component list ID	GLOBAL
Electrolyte chemistry ID	MEA-CHEM
Use true species approach for electrolytes	YES
Free-water phase properties method	STEAM-TA
Water solubility method	3
Temperature [C]	25
Pressure [bar]	1
Specified vapor fraction	
Specified heat duty [kW]	
EO Model components	
Outlet temperature [C]	25
Outlet pressure [bar]	1
Vapor fraction	0.960278647
Heat duty [kW]	172.377439
Net duty [kW]	172.377439
First liquid / total liquid	1
Total feed stream CO2e flow [kg/hr]	878.591637
Total product stream CO2e flow [kg/hr]	878.615393
Net stream CO2e production [kg/hr]	0.023756229
Utility CO2e production [kg/hr]	0
Total CO2e production [kg/hr]	0.023756229
Utility usage	
Utility cost	
Utility ID	

UMP

APPENDIX C-1 DETAILS FROM THE GABI FOR CASE 1



UMP

MY: H2 Production [MSR] <u-so> [inorganics] -- DB Process

Object Edit View Help

Name: MY H2 Production [MSR] Source: u-so - Unit process, single operat

Parameter

Parameter	Formula	Value	Minimum	Maximum	Standard	Commer
Parameter						

LCA LCC: 0 EUR LCWE Documentation

Completeness: No statement

Inputs

Flow	Quantity	Amount	Unit	Tr2	Standar	Origin	Comment
Cooling water [Waste for recove	Mass	4.83E005	kg	X	0 %	(No statement)	
Flue gas (for treatment) [Waste	Mass	4E003	kg	X	0 %	(No statement)	
Hydrogen [Inorganic intermedia	Mass	0	kg	X	0 %	(No statement)	
Monoethanolamine [Organic em	Mass	1.84E004	kg	X	0 %	(No statement)	
Natural gas Malaysia [Natural ga	Mass	2.55E003	kg	X	0 %	(No statement)	
Process steam from natural gas	Energy (net ca	8.51E003	MJ	X	0 %	(No statement)	
Steam superheated (hp) [steam	Mass	8E003	kg	X	0 %	(No statement)	
Iron [Non renewable elements]	Mass	630	kg	*	0 %	(No statement)	
Nickel [Metals]	Mass	160	kg	*	0 %	(No statement)	
Water [Water]	Mass	1.1E005	kg	*	0 %	(No statement)	

Outputs

Flow	Quantity	Amount	Unit	Tr2	Standar	Origin	Comment
Hydrogen [Inorganic intermedia	Mass	1.26E003	kg	X	0 %	(No statement)	
Carbon dioxide [Inorganic emissio	Mass	5.85E003	kg	*	0 %	(No statement)	
Carbon monoxide [Inorganic emissio	Mass	329	kg	*	0 %	(No statement)	
Catalysts material [Hazardous waste]	Mass	790	kg	*	0 %	(No statement)	
Cooling water [Waste for recovery]	Mass	1.93E006	kg	*	0 %	(No statement)	
Flue gas [Other emissions to air]	Mass	4E003	kg	*	0 %	(No statement)	
Monoethanolamine [Organic emissio	Mass	1.84E004	kg	*	0 %	(No statement)	
Waste water [Other emissions to fres	Mass	503	kg	*	0 %	(No statement)	
Water [Water]	Mass	1.1E005	kg	*	0 %	(No statement)	

System: No changes. Last change: System, 18/07/2017 1:11:47 ptg GUID: {C1F3E845-71F6-495E-B47C-51B099...

MY: H2 Production [MSR] <u-so> -- Process instance

Local name: MY: H2 Production [MSR] <u-so>

Local settings LCC

Scaling factor: 0.0008 Fixed Allocation: (no allocation)

Free parameters

Fixed parameters

Inputs					Outputs				
ParametFlow	Quantity	Amount	Unit	Tr2	ParametFlow	Quantity	Amount	Unit	Tr2
Flue gas (for treatment) [Waste	Mass	3.2	kg	X	Carbon dioxide [Inorganic emis	Mass	4.68	kg	X
Hydrogen [Inorganic intermedia	Mass	0	kg	X	Carbon monoxide [Inorganic en	Mass	0.263	kg	X
Iron [Non renewable elements]	Mass	0.504	kg	X	Catalysts material [Hazardous	Mass	0.632	kg	X
Monoethanolamine [Group NMV	Mass	14.7	kg	X	Flue gas [Other emissions to air	Mass	3.2	kg	X
Natural gas, at consumer USA	Mass	2.04	kg	X	Hydrogen [Inorganic intermedia	Mass	1.01	kg	X
Nickel [Metals]	Mass	0.128	kg	X	Monoethanolamine [Group NMV	Mass	14.7	kg	X
Steam (MJ) [steam]	Energy (net	6.81	MJ	X	Waste water [Other emissions	Mass	0.402	kg	X
Steam superheated (hp) [stea	Mass	6.4	kg	X	Water [Water]	Mass	88.2	kg	X
Water [Water]	Mass	88.2	kg	X	Water (cooling water) [Operati	Mass	1.55E003	kg	X
Water (cooling water) [Operati	Mass	386	kg	X					

Data quality

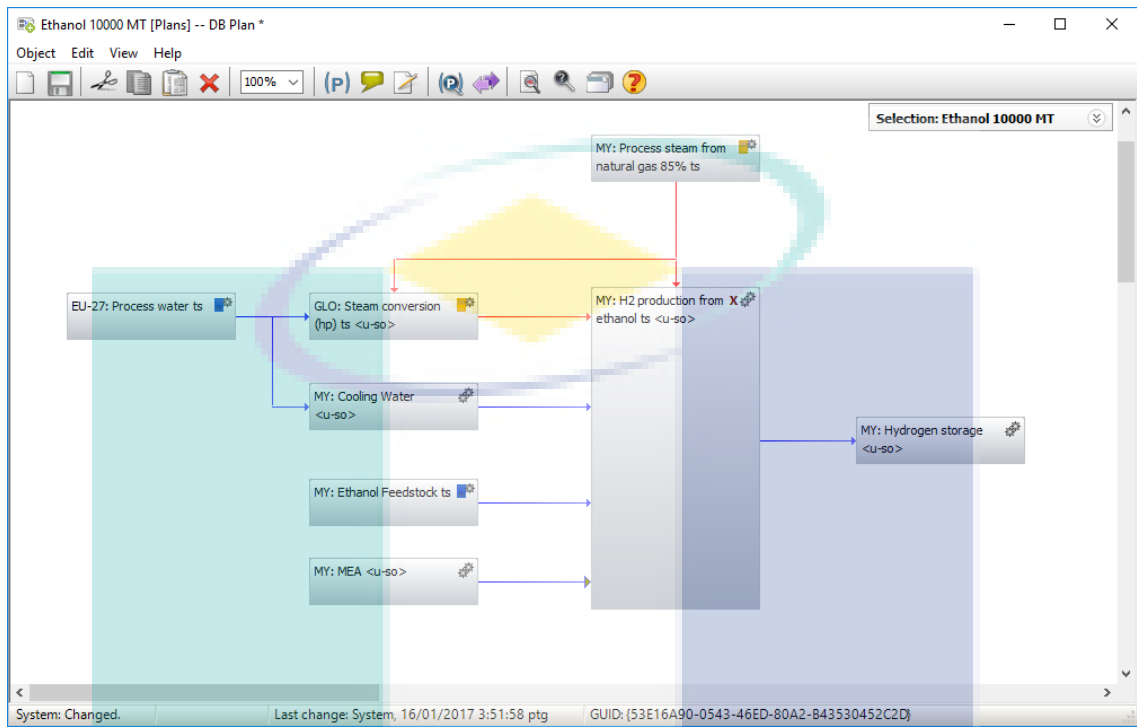
Technique: No statement Location: No statement Time: No statement

Grouping

Nation: Type: Ecoinvent Enterprise: external User defined

Cancel OK

APPENDIX C-2 DETAILS FROM GABI FOR CASE 2



UMP

MY: H2 production from ethanol ts <u-so> [inorganics] -- DB Process

Object Edit View Help

Name MY H2 production from ethanol ts u-so - Unit process, single operat

Parameter

Parameter	Formula	Value	Minimum	Maximum	Standard	Comment
Parameter						

LCA LCC: 0 EUR LCWE Documentation

Completeness No statement

Inputs

Flow	Quantity	Amount	Unit	Tr	Standard	Origin	Comment
Cooling water [Waste for recovery]	Mass	2.69E006	kg	X	0 %	(No statement)	
Ethanol (96%) [Organic intermediate]	Mass	4.95E003	kg	X	0 %	(No statement)	
Monoethanolamine [Organic emissions]	Mass	3.43E004	kg	X	0 %	(No statement)	
Process steam from natural gas	Energy (net calorific value)	9.5E004	MJ	X	0 %	(No statement)	
Steam superheated (hp) [steam]	Mass	1.1E004	kg	X	0 %	(No statement)	
Water [Water]	Mass	2.05E005	kg	X	0 %	(No statement)	
Flue gas (for treatment) [Waste for recovery]	Mass	2.4E004	kg	*	0 %	(No statement)	
Hydrogen [Inorganic intermediate product]	Mass	0	kg	*	0 %	(No statement)	
Iron [Non renewable elements]	Mass	680	kg	*	0 %	(No statement)	
Nickel [Metals]	Mass	300	kg	*	0 %	(No statement)	

Outputs

Flow	Quantity	Amount	Unit	Tr	Standard	Origin	Comment
Hydrogen [Inorganic intermediate product]	Mass	1.26E003	kg	X	0 %	(No statement)	
Carbon dioxide [Inorganic emissions to air]	Mass	7.39E003	kg	*	0 %	(No statement)	
Carbon monoxide [Inorganic emissions to air]	Mass	177	kg	*	0 %	(No statement)	
Catalysts material [Hazardous waste]	Mass	980	kg	*	0 %	(No statement)	
Cooling water [Waste for recovery]	Mass	2.69E006	kg	*	0 %	(No statement)	
Flue gas [Other emissions to air]	Mass	2.4E004	kg	*	0 %	(No statement)	
Monoethanolamine [Organic emissions to air]	Mass	3.43E004	kg	*	0 %	(No statement)	
Waste water [Other emissions to freshwater]	Mass	500	kg	*	0 %	(No statement)	

System: No changes. Last change: System, 18/07/2017 1:05:53 ptg GUID: {549ED95C-566A-4E08-AEDA-F09449...}

MY: H2 production from ethanol ts <u-so> -- Process instance

Local name MY: H2 production from ethanol ts <u-so> No image

Local settings LCC

Scaling factor: 0.000799 Fixed Allocation: (no allocation)

Free parameters

Fixed parameters

Inputs	Outputs																																																																																																						
<table border="1"> <thead> <tr> <th>Paramet</th> <th>Flow</th> <th>Quantity</th> <th>Amount</th> <th>Unit</th> <th>Tr</th> </tr> </thead> <tbody> <tr> <td>Ethanol (96%) [Organic intermediate]</td> <td>Mass</td> <td>3.96</td> <td>kg</td> <td>X</td> </tr> <tr> <td>Flue gas (for treatment) [Waste for recovery]</td> <td>Mass</td> <td>19.2</td> <td>kg</td> <td>X</td> </tr> <tr> <td>Hydrogen [Inorganic intermediate product]</td> <td>Mass</td> <td>0</td> <td>kg</td> <td>X</td> </tr> <tr> <td>Iron [Non renewable elements]</td> <td>Mass</td> <td>0.543</td> <td>kg</td> <td>X</td> </tr> <tr> <td>Monoethanolamine [Group NMV]</td> <td>Mass</td> <td>27.4</td> <td>kg</td> <td>X</td> </tr> <tr> <td>Nickel [Metals]</td> <td>Mass</td> <td>0.24</td> <td>kg</td> <td>X</td> </tr> <tr> <td>Steam (hp) [steam]</td> <td>Mass</td> <td>8.79</td> <td>kg</td> <td>X</td> </tr> <tr> <td>Steam (MJ) [steam]</td> <td>Energy (net calorific value)</td> <td>75.9</td> <td>MJ</td> <td>X</td> </tr> <tr> <td>Water [Water]</td> <td>Mass</td> <td>164</td> <td>kg</td> <td>X</td> </tr> <tr> <td>Water (cooling water) [Operational]</td> <td>Mass</td> <td>2.15E003</td> <td>kg</td> <td>X</td> </tr> </tbody> </table>	Paramet	Flow	Quantity	Amount	Unit	Tr	Ethanol (96%) [Organic intermediate]	Mass	3.96	kg	X	Flue gas (for treatment) [Waste for recovery]	Mass	19.2	kg	X	Hydrogen [Inorganic intermediate product]	Mass	0	kg	X	Iron [Non renewable elements]	Mass	0.543	kg	X	Monoethanolamine [Group NMV]	Mass	27.4	kg	X	Nickel [Metals]	Mass	0.24	kg	X	Steam (hp) [steam]	Mass	8.79	kg	X	Steam (MJ) [steam]	Energy (net calorific value)	75.9	MJ	X	Water [Water]	Mass	164	kg	X	Water (cooling water) [Operational]	Mass	2.15E003	kg	X	<table border="1"> <thead> <tr> <th>Paramet</th> <th>Flow</th> <th>Quantity</th> <th>Amount</th> <th>Unit</th> <th>Tr</th> </tr> </thead> <tbody> <tr> <td>Carbon dioxide [Inorganic emissions to air]</td> <td>Mass</td> <td>5.9</td> <td>kg</td> <td>X</td> </tr> <tr> <td>Carbon monoxide [Inorganic emissions to air]</td> <td>Mass</td> <td>0.141</td> <td>kg</td> <td>X</td> </tr> <tr> <td>Catalysts material [Hazardous waste]</td> <td>Mass</td> <td>0.783</td> <td>kg</td> <td>X</td> </tr> <tr> <td>Flue gas [Other emissions to air]</td> <td>Mass</td> <td>19.2</td> <td>kg</td> <td>X</td> </tr> <tr> <td>Hydrogen [Inorganic intermediate product]</td> <td>Mass</td> <td>1.01</td> <td>kg</td> <td>X</td> </tr> <tr> <td>Monoethanolamine [Group NMV]</td> <td>Mass</td> <td>27.4</td> <td>kg</td> <td>X</td> </tr> <tr> <td>Waste water [Other emissions to freshwater]</td> <td>Mass</td> <td>0.4</td> <td>kg</td> <td>X</td> </tr> <tr> <td>Water (cooling water) [Operational]</td> <td>Mass</td> <td>2.15E003</td> <td>kg</td> <td>X</td> </tr> </tbody> </table>	Paramet	Flow	Quantity	Amount	Unit	Tr	Carbon dioxide [Inorganic emissions to air]	Mass	5.9	kg	X	Carbon monoxide [Inorganic emissions to air]	Mass	0.141	kg	X	Catalysts material [Hazardous waste]	Mass	0.783	kg	X	Flue gas [Other emissions to air]	Mass	19.2	kg	X	Hydrogen [Inorganic intermediate product]	Mass	1.01	kg	X	Monoethanolamine [Group NMV]	Mass	27.4	kg	X	Waste water [Other emissions to freshwater]	Mass	0.4	kg	X	Water (cooling water) [Operational]	Mass	2.15E003	kg	X
Paramet	Flow	Quantity	Amount	Unit	Tr																																																																																																		
Ethanol (96%) [Organic intermediate]	Mass	3.96	kg	X																																																																																																			
Flue gas (for treatment) [Waste for recovery]	Mass	19.2	kg	X																																																																																																			
Hydrogen [Inorganic intermediate product]	Mass	0	kg	X																																																																																																			
Iron [Non renewable elements]	Mass	0.543	kg	X																																																																																																			
Monoethanolamine [Group NMV]	Mass	27.4	kg	X																																																																																																			
Nickel [Metals]	Mass	0.24	kg	X																																																																																																			
Steam (hp) [steam]	Mass	8.79	kg	X																																																																																																			
Steam (MJ) [steam]	Energy (net calorific value)	75.9	MJ	X																																																																																																			
Water [Water]	Mass	164	kg	X																																																																																																			
Water (cooling water) [Operational]	Mass	2.15E003	kg	X																																																																																																			
Paramet	Flow	Quantity	Amount	Unit	Tr																																																																																																		
Carbon dioxide [Inorganic emissions to air]	Mass	5.9	kg	X																																																																																																			
Carbon monoxide [Inorganic emissions to air]	Mass	0.141	kg	X																																																																																																			
Catalysts material [Hazardous waste]	Mass	0.783	kg	X																																																																																																			
Flue gas [Other emissions to air]	Mass	19.2	kg	X																																																																																																			
Hydrogen [Inorganic intermediate product]	Mass	1.01	kg	X																																																																																																			
Monoethanolamine [Group NMV]	Mass	27.4	kg	X																																																																																																			
Waste water [Other emissions to freshwater]	Mass	0.4	kg	X																																																																																																			
Water (cooling water) [Operational]	Mass	2.15E003	kg	X																																																																																																			

Data quality

Technique Location Time

No statement No statement No statement

Grouping

Nation Type Enterprise User defined

Cancel OK

**APPENDIX D-1
CAPCOST DETAILS FOR CASE 1**

<input type="button" value="Add Equipment"/>		<input type="text" value="Unit Number"/> 100	
<input type="button" value="Edit Equipment"/>		<input type="text" value="CEPCI"/> 558.3	
<input type="button" value="Remove All Equipment"/>		June 2017	

User Added Equipment

Exchangers	Exchanger Type	Shell Pressure (barg)	Tube Pressure (barg)	MOC	Area (square meters)	Purchased Equipment Cost	Bare Module Cost
E-101	Double Pipe		5	Stainless Steel / Stainless Steel	2	\$ 3,720.00	\$ 22,200.00
E-102	Double Pipe		5	Stainless Steel / Stainless Steel	6.33	\$ 4,810.00	\$ 28,700.00
E-103	Double Pipe		5	Stainless Steel / Stainless Steel	9.78	\$ 5,220.00	\$ 31,200.00
E-104	Floating Head	5	5	Stainless Steel / Stainless Steel	73.8	\$ 31,700.00	\$ 195,000.00
E-105	Floating Head	5	5	Stainless Steel / Stainless Steel	68.3	\$ 30,900.00	\$ 191,000.00
E-106	Floating Head	5	5	Stainless Steel / Stainless Steel	134	\$ 40,800.00	\$ 251,000.00
E-107	Kettle Reboiler	5	5	Stainless Steel / Stainless Steel	140	\$ 193,000.00	\$ 1,190,000.00

Towers	Tower Description	Height (meters)	Diameter (meters)	Tower MOC	Demister MOC	Pressure (barg)	Purchased Equipment Cost	Bare Module Cost
T-101	0.5 meters of 304 Stainless	10	1.5	Stainless Steel		5	\$ 26,000.00	\$ 235,000.00
T-102	0.4 meters of 304 Stainless	8	2.07	Stainless Steel		5	\$ 35,800.00	\$ 378,000.00

Vessels	Orientation	Length/Height (meters)	Diameter (meters)	MOC	Demister MOC	Pressure (barg)	Purchased Equipment Cost	Bare Module Cost
V-101	Vertical	3.35	0.8	Stainles Steel		5	\$ 5,650.00	\$ 44,700.00
R-101	Vertical	10	1.5	Stainles Steel		5	\$ 23,500.00	\$ 232,000.00
R-102	Vertical	10	2	Stainles Steel		5	\$ 36,100.00	\$ 413,000.00
R-103	Vertical	10	2	Stainles Steel		5	\$ 36,100.00	\$ 413,000.00

Total Bare Module Cost							\$	3,624,800
-------------------------------	--	--	--	--	--	--	----	-----------

**APPENDIX D-2
CAPCOST DETAILS FOR CASE 2**

<input type="button" value="Add Equipment"/>		<input type="text" value="Unit Number"/> 100						
<input type="button" value="Edit Equipment"/>		<input type="text" value="CEPCI"/> 558.3						
<input type="button" value="Remove All Equipment"/>		June 2017						
User Added Equipment								
Exchangers	Exchanger Type	Shell Pressure (barg)	Tube Pressure (barg)	MOC	Area (square meters)	Purchased Equipment Cost	Bare Module Cost	
E-101	Floating Head	5	5	Stainless Steel / Stainless Steel	78.5	\$ 32,400.00	\$ 200,000.00	
E-102	Floating Head	5	5	Stainless Steel / Stainless Steel	10	\$ 28,000.00	\$ 172,000.00	
E-103	Floating Head	5	5	Stainless Steel / Stainless Steel	13	\$ 26,700.00	\$ 164,000.00	
E-104	Floating Head	5	5	Stainless Steel / Stainless Steel	142	\$ 42,000.00	\$ 259,000.00	
E-105	Floating Head	5	5	Stainless Steel / Stainless Steel	125	\$ 39,400.00	\$ 243,000.00	
E-106	Floating Head	5	5	Stainless Steel / Stainless Steel	59.7	\$ 29,700.00	\$ 183,000.00	
E-107	Kettle Reboiler	5	5	Stainless Steel / Stainless Steel	78.8	\$ 108,000.00	\$ 667,000.00	
Towers	Tower Description	Height (meters)	Diameter (meters)	Tower MOC	Demister MOC	Pressure (barg)	Purchased Equipment Cost	Bare Module Cost
T-101	9 meters of 304 Stainless	10	1.5	Stainless Steel		5	\$ 65,900.00	\$ 274,000.00
T-102	8.5 meters of 304 Stainless	10	2.1	Stainless Steel		5	\$ 117,000.00	\$ 536,000.00
Vessels	Orientation	Length/Height (meters)	Diameter (meters)	MOC	Demister MOC	Pressure (barg)	Purchased Equipment Cost	Bare Module Cost
V-101	Vertical	3.8	0.95	Stainless Steel		5	\$ 7,210.00	\$ 58,500.00
R-101	Vertical	10	1.5	Stainless Steel		5	\$ 23,500.00	\$ 232,000.00
R-102	Vertical	10	2	Stainless Steel		5	\$ 36,100.00	\$ 413,000.00
R-103	Vertical	10	2	Stainless Steel		5	\$ 36,100.00	\$ 413,000.00
Total Bare Module Cost							\$	3,814,500

APPENDIX E-1
LIST OF PUBLICATIONS AND CONFERENCES

Publication

1. Amran U.I., Ahmad, A., & Othman, M. R. (2017). Kinetic Based Simulation of Methane Steam Reforming and Water Gas Shift for Hydrogen Production using Aspen Plus. *Chemical Engineering Transactions*, 56, 1681-1686
2. Amran U.I., Ahmad, A., & Othman, M. R (2017). Life Cycle Assessment of Simulated Hydrogen Production by Methane Steam Reforming. *Australian Journal of Basic and Applied Science*, 11(3), 43-50

Conference

3. U.I. Amran, A. Ahmad & M.R. Othman. 2016. "Life Cycle Assessment Of Hydrogen Production By Methane Steam Reforming". 3rd International Conference of Chemical Engineering & Industrial Biotechnology (ICCEIB 2016). 28-30 November 2016. Melaka. Malaysia. ORAL
4. U.I. Amran, A. Ahmad & M.R. Othman. 2016. "Kinetic Based Simulation of Methane Steam Reforming and Water Gas Shift for Hydrogen Production using Aspen Plus". 9th. Regional Conference on Chemical Engineering (RCChE 2016). 21 – 22 November 2016. UTM Kuala Lumpur. ORAL
5. U.I. Amran, A. Ahmad & M.R. Othman. 2015. "Kinetic based simulation of methane steam reforming and water gas shift for hydrogen production using Aspen Plus". 4th Conference on Emerging Energy and Process Technology (CONCEPT) 2015. 15-16 December 2015. A' Famosa Resort. Melaka. ORAL



Kinetic Based Simulation of Methane Steam Reforming and Water Gas Shift for Hydrogen Production Using Aspen Plus

Umarul Imran Amran^a, Arshad Ahmad^b, Mohamad Rizza Othman^{*,a}

^a Department of Chemical Engineering, Universiti Malaysia Pahang, Lebuhraya Tun Razak, 26300 Gambang, Pahang, Malaysia.

^b Department of Chemical Engineering, , Universiti Teknologi Malaysia, 81310 Johor Bharu, Johor, Malaysia.
rizza@ump.edu.my

This paper presents the kinetic-based simulation of methane steam reforming (MSR) from natural gas and water gas shift (WGS) reaction for hydrogen production. It is found that most simulations of these reactions were either done as balance or equilibrium based. Although it provides simplicity, such approach has limitations, especially for sensitivity analysis, control and optimisation. In order to improve and optimise the reactor performance, kinetic-based simulation is necessary. The kinetic data for MSR and WGS reactions were obtained from literature. The simulation was performed in Aspen Plus using RPLUG model blocks with rearranged Langmuir-Hinshelwood-Hougen-Watson (LHHW) kinetic model. The results of the simulation show good agreement with results found in the literature. Apart from that, sensitivity analysis was carried out to observe the effect of several parameters such as temperature, pressure, catalyst weight and ratio feed to the reactor performance.

1. Introduction

Hydrogen is recognised as a capable energy carrier in the future. Hydrogen energy has the potential to become energy resource and can reduce the dependency on fossil fuel in the future. The product of hydrogen combustion is mainly water with less amount of nitrogen oxide or sulphur oxide. Hydrogen combustion has high energy content, approximately 143 MJ/kg lower heating value (LHV), triple to that of petroleum (Chu et al., 2015). In 2002, 48 % of hydrogen is produced from natural gas, 30 % from heavy oil and naphtha, 18 % from coal and 4 % from electrolysis (Logan, 2004). Methane steam reforming (MSR) is one of the important processes in the production of hydrogen and syngas. MSR is comprehensively used and is a matured technology in hydrogen production industries, but it has a high carbon product released at almost 7 kg CO₂/kg H₂. A commonly MSR system consists of four sequential units, namely desulfuriser, reformer, shift reactor and separation units (Soltani et al., 2014). Desulfuriser can be removed if the natural gas feed is pure methane. Shift reactor involves a WGS reaction in which carbon monoxide react with steam to produce carbon dioxide and hydrogen gas (Choi and Stenger, 2003). The purpose of water gas shift (WGS) on the other hand, is to reduce the carbon monoxide production and optimise the production of hydrogen (Antzara et al., 2014). Mostly in previous study simulation of these reactions were based on stoichiometry or equilibrium model (Boyano et al., 2012). Although it provides simplicity, the results obtained are very limited as such could not offer insights on the process characteristics. There is a need to simulate the reactions using kinetic-based model which particularly useful for reactor sizing, costing, sensitivity analysis as well as control and optimisation. In this study, our objective is to simulate MSR and WGS reactions using kinetic expression model in RPLUG reactor block with LHHW reaction model in Aspen Plus. The kinetic data for both reactions were based on literature for performance and validation purposes and therefore could predict the performance of the reactor at high accuracy with low maximum relative error (Er-rbib and Bouallou, 2014). Apart from that, sensitivity analysis will be carried out to provide insights on the process characteristics.

2. Reaction Kinetics for Methane Steam Reforming (MSR) and Water Gas Shift (WGS)

Hydrogen production via MSR involves reaction between methane with steam to produce hydrogen and carbon monoxide in a catalytic fixed-bed reactor with a molar ratio CH₄ and H₂O of 1 : 3 based on the following reaction formula:



For fast reaction, Ni-based catalyst supported on alumina is commonly used in industry (Fernandes and Soares, 2006). The rate expression for the MSR reaction, R_{MSR} based on Langmuir-Hinshelwood (LHHW) reaction mechanism on Nickel catalyst is as follows:

$$R_{MSR} = \frac{\frac{k_1}{P_{H_2}^{2.5}} [P_{CH_4} P_{CO} - \frac{P_{H_2}^3 P_{CO}}{K_1}]}{DEN^2} \quad (2)$$

$$\text{Where } DEN = 1 + K_{CO} P_{CO} + K_{H_2} P_{H_2} + K_{CH_4} P_{CH_4} + \frac{K_{H_2O} P_{H_2O}}{P_{H_2}}$$

K_1 and K_1 are the rate constant and equilibrium constant for MSR. P_i and K_i are the partial pressure and adsorption equilibrium constant of component i . The rate expression above cannot be used directly in Aspen Plus as the general equation for LHHW used the following equations:

$$R = \frac{(\text{kinetic factor})(\text{driving force})}{\text{adsorption term}} \quad (3)$$

Where,

$$\text{kinetic factor} = k \left(\frac{T}{T_0}\right)^n e^{-\left(\frac{E}{R}\right)\left(\frac{1}{T} - \frac{1}{T_0}\right)} \quad (4)$$

$$\text{driving force} = K_1 \prod_{i=1}^N C_i^\alpha - K_2 \prod_{j=1}^N C_j^\beta \quad (5)$$

$$\text{adsorption term} = \left[\sum_{i=1}^M K_i \left(\prod_{j=1}^N C_j^M \right) \right]^m \quad (6)$$

In Aspen Plus, the pre-exponential constant, adsorption constant used the following equation:

$$K = A \exp\left(\frac{B}{T}\right) T^c \exp(DT) \quad (7)$$

The equation does not fit Eq(3) and need to be rearranged. Using natural logarithm (Ln) and some rearrangements, the newly rearranged equation is shown below:

$$R_{MSR} = \frac{k_1 K_1 \left[K_1 \frac{P_{CH_4} P_{CO}}{P_{H_2}^{2.5}} - P_{H_2}^{0.5} P_{CO} \right]}{DEN^2} \quad (8)$$

The kinetic coefficient and equilibrium constant in Eq(8) are shown in Table 1. The modelling parameters can now describe in Aspen Plus using RPLUG block based on LHHW kinetics model. Note that, hydrogen was added in the feed stream to avoid division by zero in Eq(8).

The WGS reaction is normally used after reforming or gasification process to reduce carbon monoxide and increase hydrogen yield. The reaction formula is shown in Eq(9). It is a reversible and exothermic reaction and involves two reactors in series, namely high temperature and low temperature, which operated at 400 °C and 210 °C (Amadeo and Laborde, 1995). Iron-based catalyst and the copper-based catalyst is commonly used in industry for this reaction (Amadeo and Laborde, 1995).



The kinetic model for reaction in Eq(9) is based on a LHHW reaction mechanism. The rate reaction, RWGS is given by:

$$R_{WGS} = \frac{k_0 P_{CO} P_{H_2O} (1 - \beta)}{(1 + K_1 P_{CO} + K_2 P_{H_2O} + K_3 P_{CO_2} + K_4 P_{H_2})^2} \quad (10)$$

Where,

$$\beta = \frac{P_{CO_2} P_{H_2}}{P_{CO} P_{H_2O} K_e} \quad (11)$$

k_o and K_e are the rate and equilibrium constant for WGS reaction. The kinetic coefficient and equilibrium constants in Eq(10) are shown in Table 1. As for MSR, the rate expression above need to be rearranged to fit Aspen Plus RPLUG block based on LHHW kinetics model input requirements as shown below:

$$R2 = \frac{k_o(P_{CO}P_{H2O} - \frac{P_{CO2}P_{H2}}{K_e})}{(1 + K1P_{CO} + K2P_{H2O} + K3P_{CO2} + K4P_{H2})^2} \quad (12)$$

Table 1: Kinetic parameter for methane steam reforming and water gas shift

Parameter	MSR (Singh et al., 2014)			WGS(Amadeo and Laborde, 1995)		
	Pre-exponential factor	Ea or ΔH (J/mol)	Ln K	Parameter	Ea or ΔH (J/mol)	Ln K
k1	4.2248×10^{15} (mol atm ^{0.5} /g h)	240,100		ko	0.92 (mmol/g s atm ²)	4,080
K1	7.846×10^{12} (atm ²)	220,200	29.69	K1	2.21	-910
K _{CH4}	6.65×10^{-4} (atm ⁻¹)	-38,280	-7.31	K2	0.4	-1,420
K _{H2O}	1.77×10^5 (atm ⁻¹)	88,680	12.08	K3	0.0047	-24,720
K _{H2}	6.12×10^{-5} (atm ⁻¹)	-82,900	-9.70	K4	0.052	-14,400
K _{CO}	8.23×10^{-3} (atm ⁻¹)	-70,650	-9.41			

3. Process Simulation and Modelling

The hydrogen production process was modelled in Aspen Plus V8.6. The components involved were water, methane, carbon dioxide, carbon monoxide and hydrogen. The thermodynamic method used is RKSMHV2 based on the Redlich-Kwong-Soave equation of state with modified Huron-Vidal mixing rules (Er-rbib and Bouallou, 2014). This model is suitable for non-polar and polar compounds in combinations with light gases (Technology, July 2010). Figure 1 shows the process flowsheet. At this stage, the recycle stream is not considered. The feed stream to the MSR reactor was natural gas and steam. The natural gas does not contain hydrogen sulphide and carbon dioxide. Both of these streams were mixed in MIX-01 before heated up to 700 °C. The diameter of the MSR reactor was 0.2 m and the length was 10 m. The output streams from the heater were then introduced to the MSR reactor using RPLUG model block which operated isothermally. The output stream from the WSR reactor were then fed to a WSG reactor at 400 °C which operated adiabatically with a pressure of 1 bar. The WSG reactor was modelled using RPLUG model block. RPLUG is a rigorous model for plug flow reactors which assumes perfect mixing in the radial direction and it can model for three-phase reactors. The WGS reactor diameter was 5 m and the length was 0.3 m. Both reactors involved single reaction and the side reaction is neglected.

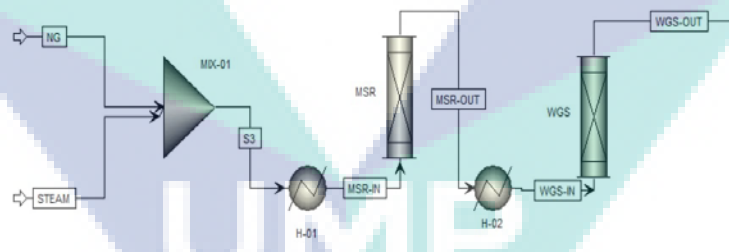


Figure 1: Aspen Plus process flow diagram for MSR and WGS reaction

4. Model Validation

The modelling approach in this work is validated with the same operating conditions from previous experiment by Singh et al. (2014) for MSR and Amadeo and Laborde (1995) for WGS. In the work by Singh et al. (2014), it can be seen in Figure 2(a) that the conversion of methane for conventional reactor increased rapidly at the first meter of the reactor length. After that, the conversion started to resolve. The same trend is found in the simulation work as shown in Figure 2(b). It was found that the highest error was at 1 m with 11.71 % while the smallest error is at 2 m with 0.53 %. Overall the mean error is 3.27 % as such it can be concluded that the

modelling approach for MSR is valid. The same approach is considered for WGS modelling. Figure 3(a) shows the experimental results by Amadeo and Laborde (1995). It shows the relationship between the partial pressure of feed water into the reactor with the conversion of carbon monoxide. The RPLUG block model was set to have the same design parameters as in the experimental work which includes the operating condition, catalyst specification and component flow rate. The hydrogen feed is 0.003604 L/s and carbon monoxide flow rate is 0.000983 L/s. The result from the simulation shows an agreement with the experimental data which indicate that with increased partial pressure of water the conversion of carbon monoxide to carbon dioxide will also increase. It can be concluded that the modelling approach for WGS reaction is valid.

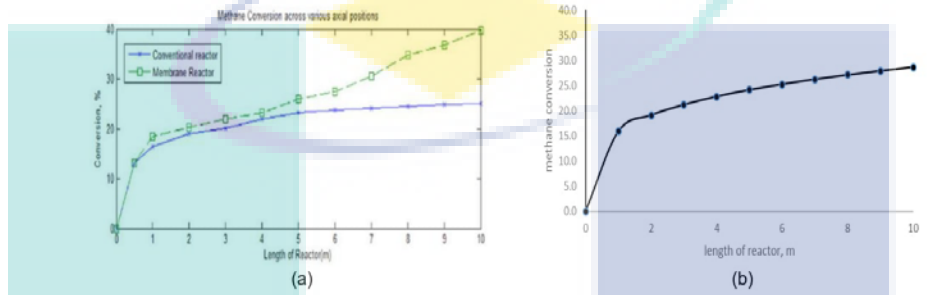


Figure 2: The conversion of MSR (a) from (Singh et al., 2014) (b) from simulation using Aspen Plus.

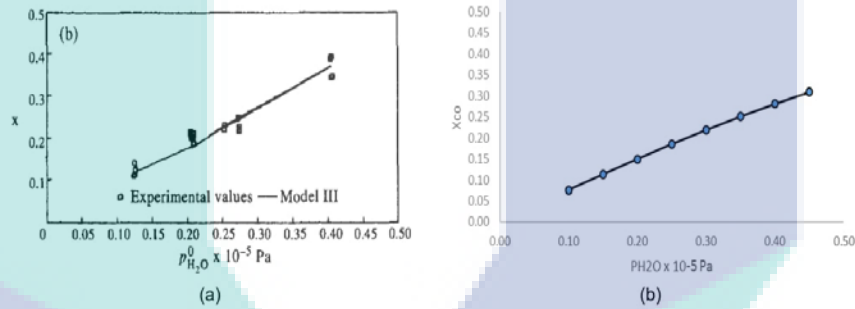


Figure 3: Carbon monoxide conversion with partial pressure (a) from (Amadeo and Laborde 1995) (b) from simulation

5. Sensitivity Analysis

Sensitivity analysis of the reactor performance was done by changing several operation variables, namely catalyst weight, reactor temperature and pressure and steam-to-methane feed ratio into the reactor. During sensitivity analysis, the manipulated variables were varied while the other design parameters remain unchanged. Figure 4 shows the result of the sensitivity analysis. In Figure 4(a), it can be seen that with increased catalyst weight in the reformer, the hydrogen flow rate also increased especially at the first 100 kg. However, at 300 kg the hydrogen flow rate starts to become constant. The same increment is observed for the shift reactor as the increment in catalyst weight increase the carbon dioxide flow rate. The rapid increment is observed at the first 50 kg before the carbon dioxide flow rate started to be constant. At this point, almost all carbon monoxide had been converted to carbon dioxide.

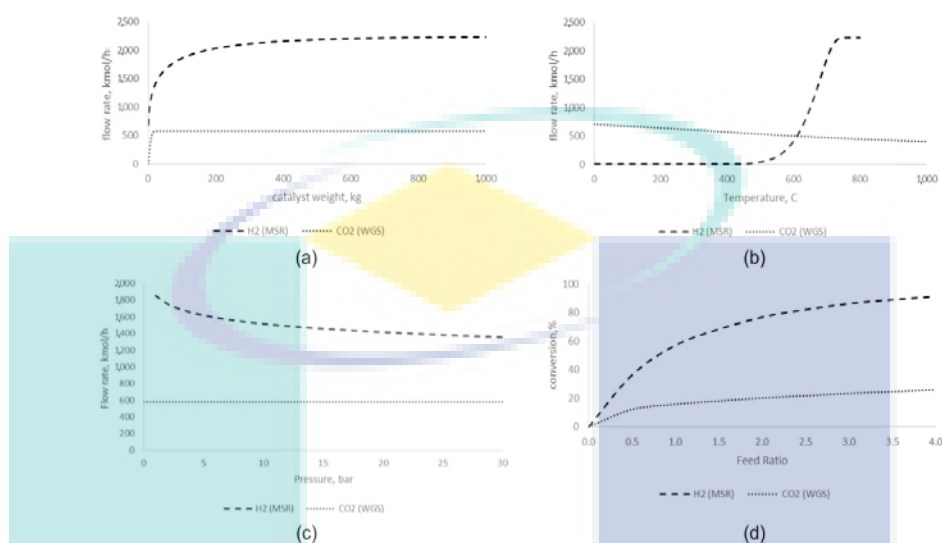


Figure 4: Sensitivity analysis on MSR and WGS (a) weight catalyst (b) temperature feed to reactor (c) pressure feed to the reactor (d) ratio feed for water steam and methane.

As shown in Figure 4 (b) is the response of the hydrogen molar flow rate to reactor temperature increment. For the reformer, hydrogen started to produce at 500 °C and increased drastically until 700 °C. After that, hydrogen flow rate started to become constant. At this point, all the methane had been converted into hydrogen. This trend shows that for MSR reaction, the hydrogen produced depends on a certain range, which is 500 °C to 700 °C in this case. For WGS reaction, it is found that as the feed temperature increased, there was a drop in the carbon dioxide molar flow rate. This is because the equilibrium constant decreases with an increase in temperatures thus lower down the conversion of carbon monoxide at the higher temperature.

Figure 4 (c) shows the effect of pressure on hydrogen flow rate. For MSR, it is found that when the pressure is increased, the hydrogen molar flow rate shows the inverse response. The highest hydrogen produced is at 1 bar. For WGS, the result shows that the effect of pressure to carbon dioxide molar flow rate is insignificant. Figure 4 (d) shows the effect of hydrogen flow rate towards change in steam to methane feed ratio. When the steam feed flow rate is increased, the percentage of methane conversion also increased. This shows that the feed ratio is important to ensure the reaction is pushed to the right side thus increase hydrogen flow rate. For WGS reaction, it is found that the conversion of carbon monoxide is higher when the steam ratio is increased. From the figure conversion of 90 % can be achieved when the ratio steam to carbon monoxide is four.

6. Conclusion

This study successfully model and simulate kinetic based MSR and WGS reaction using modified LHHW model in Aspen Plus. Both reaction model have been validated and show very good agreement with existing experimental data. Upon validation, the sensitivity analysis was conducted. It is found that for both reactions, catalyst weight, reactor temperature and steam : methane feed ratio greatly affect the reactor performance production. However, pressure seems to have low effect to these reactions. The successful modelling and simulation of the kinetic-based hydrogen production set an important basis in our work. Further significance analysis can be done which include work on optimisation, operability and controllability study and sustainability assessment.

Acknowledgement

Financial support for this work was provided by LRGS 4L817 for which the authors are thankful.

References

- Amadeo N., Laborde M.A., 1995, Hydrogen production from the low temperature water gas shift reaction: kinetics and simulation of the industrial reactor, *International Journal of Hydrogen Energy* 20, 949-956.
- Antzara A., Heracleous E., Bukur D.B., Lemonidou A.A., 2014, Thermodynamic analysis of hydrogen production via chemical looping steam methane reforming coupled with in situ CO₂ capture, *Energy Procedia* 63, 6576-6589.
- Boyano A., Morosuk T., Blanco-Marigorta A.M., Tsatsaronis G., 2012, Conventional and advanced exergoenvironmental analysis of a steam methane reforming reactor for hydrogen production, *Journal of Cleaner Production* 20, 152-160.
- Choi Y., Stenger H.G., 2003, Water gas shift reaction kinetics and reactor modeling for fuel cell grade hydrogen, *Journal of Power Sources* 124, 432-439.
- Chu H., Li Q., Meng A., Zhang Y., 2015, Investigation of hydrogen production from model bio-syngas with high CO₂ content by water-gas shift reaction, *International Journal of Hydrogen Energy* 40, 4092-4100.
- Er-rbib H., Bouallou C., 2014, Modeling and simulation of CO methanation process for renewable electricity storage, *Energy* 75, 81-88.
- Fernandes F.A.N., Soares A.B., 2006, Methane steam reforming modeling in a palladium membrane reactor, *Fuel* 85, 569-573.
- Logan B.E., 2004, Extracting hydrogen and electricity from renewable resources, *Environmental Science & Technology* 38, 160A-167A.
- Singh A.P., Singh S., Ganguly S., Patwardhan A.V., 2014, Steam reforming of methane and methanol in simulated macro & micro-scale membrane reactors: Selective separation of hydrogen for optimum conversion, *Journal of Natural Gas Science and Engineering* 18, 286-295.
- Soltani R., Rosen M.A., Dincer I., 2014, Assessment of CO₂ capture options from various points in steam methane reforming for hydrogen production, *International Journal of Hydrogen Energy* 39, 20266-20275.
- Technology A., 2010, Physical Property Methods version 7.2 Aspen Physical Property System, Burlington, USA.



AUSTRALIAN JOURNAL OF BASIC AND APPLIED SCIENCES

ISSN:1991-8178 EISSN: 2309-8414
Journal home page: www.ajbasweb.com



Life Cycle Assessment of Simulated Hydrogen Production by Methane Steam Reforming

¹Umarul Imran Amran, ^{2,3}Arshad Ahmad, ¹Mohamad Rizza Othman

¹Dep. of Chemical Engineering, Universiti Malaysia Pahang, Lebuhraya Tun Abdul Razak, 26300 Gambang, Pahang, Malaysia.

²Dep. of Chemical Engineering, Universiti Teknologi Malaysia, 81310 Johor Bharu, Malaysia

³Centre of hydrogen Energy, Universiti Teknologi Malaysia, 81310 Johor Bharu, Malaysia

Address For Correspondence:

Umarul Imran Amran, Dep. of Chemical Engineering, Universiti Malaysia Pahang, Lebuhraya Tun Abdul Razak, 26300 Gambang, Pahang, Malaysia.
Tel: +609-5492820; E-mail: umarulimran.amran@gmail.com.

ARTICLE INFO

Article history:

Received 18 September 2016

Accepted 21 January 2017

Available online 26 January 2017

Keywords:

Hydrogen, life cycle assessment, methane reforming, Simulation, Aspen Plus, GaBi.

ABSTRACT

Hydrogen has attracted global attention as alternative energy carrier in the future. Typically, hydrogen is produced through methane steam reforming (MSR) followed by water gas shift (WGS) reaction. Although considered as clean energy, it is essential to assess the environmental impact of hydrogen production process which could help to compare and improve existing technology. Thus, the objective of this study is to conduct a life cycle assessment (LCA) of hydrogen production from natural gas (NG) as feedstock. In order to gain detail and extensive process inventory, a rigorous flowsheet simulation of hydrogen production was developed in Aspen Plus 8.6. The goal of LCA is to evaluate the environmental impact of all processes involved in hydrogen production from natural gas. The environmental assessment was carried out using GaBi based on ReCiPe method. The system boundaries considered for this assessment were natural gas feedstock, hydrogen production, process steam, process water plant and solvent absorption. The LCA system function is the production of hydrogen from methane while the functional unit chosen is 1 kg of hydrogen. Overall, ten life cycle impact assessment categories were carried out. Our findings show that the most contributing impact categories were climate change and resource depletion which include fossil and water.

INTRODUCTION

Energy resources is important to satisfy human needs. However, excessive exploitation of energy resources could lead to crucial environmental consequences. Worldwide uncertainty in energy supply, the increasing oil price and the level of greenhouse gas emission have motivated the researcher to find new energy source to reduce dependence on non-renewable sources such as fossil fuels (Lee *et al.*, 2010). In many countries, proactive actions have been taken to reduce the greenhouse gas (GHG) emissions in the energy sector (Tonini & Astrup, 2012). Hydrogen has been proposed as one of the future energy carriers because its high yields, clean combustion and feasible storage (Javier Dufour *et al.*, 2011). Hydrogen mostly produced from natural gas via methane steam reforming (MSR) followed by water gas shift (WGS). It is the most widely method used in industries for the last 20 years (Tugnoli *et al.*, 2008). While energy demand increases with increasing world population, hydrogen although considered as clean combustion gas could cause significant environmental impact due to increase greenhouse gas released during its production stage. In order, to assess the environmental impact, life cycle assessment (LCA) is a suitable tool to assess and compare the environmental impact of

Open Access Journal

Published BY AENSI Publication

© 2017 AENSI Publisher All rights reserved

This work is licensed under the Creative Commons Attribution International License (CC BY).

<http://creativecommons.org/licenses/by/4.0/>



Open Access

To Cite This Article: Umarul Imran Amran, Arshad Ahmad, Mohamad Rizza Othman., Life Cycle Assessment of Simulated Hydrogen Production by Methane Steam Reforming. *Aust. J. Basic & Appl. Sci.*, 11(3): 43-50, 2017

hydrogen production as it able fully evaluate the environmental impact from initial raw material until the final product.

LCA represents a systematic set of procedures for compiling and inspecting the inputs and outputs of materials and energy and the related environmental impacts and directly attributable to a product or service throughout its life cycle (Kalinci *et al.*, 2012). LCA have been widely used in various industries such as paper production, car manufacturing and many more. For hydrogen production, several researchers adopted LCA at different stage of its product life cycle such as production, storage, transport and usage (J. Dufour *et al.*, 2012). Dufour *et al.* (2012) for example perform LCA of various hydrogen production technology to determine which has the lower amount of greenhouse gas and total impact on the environment. In another work, Hajjaji *et al.* (2013) performed LCA on various alternatives of hydrogen production from numerous feedstock. In the same study, the reactor models used to simulate the hydrogen production in the Aspen Plus was the equilibrium reactor. In this work, a rigorous model was used to simulate the hydrogen production in Aspen Plus 8.6 which include reaction kinetics, separation equilibrium models, production capacity and utility consumptions. Based on the simulated model, LCA analysis were performed which will ensure a detail and extensive life cycle inventory for an accurate LCA results. The latest LCA method have been adopted in this work known as Recipe, which is an improvement from CML2000 and Eco-Indicator-99 (Consultants, 2016). The boundary of analysis considered in this work was gate to cradle which involve natural gas feedstock, hydrogen production, process steam, process water plant and solvent absorption. LCA analysis was done by using GaBi software for data collection, analyse and monitor the environmental performance of the process.

Methodology:

Hydrogen Production from Methane:

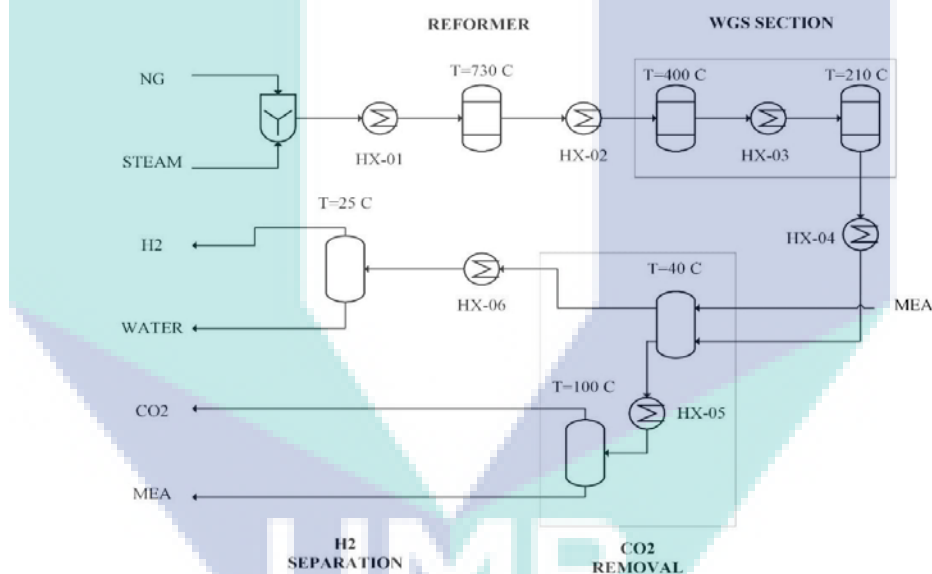
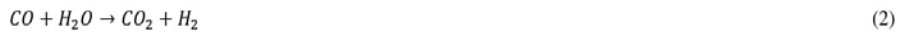


Fig. 1: The simplified flow sheet of hydrogen production by MSR.

Figure 1 shows a simplified flow sheet of hydrogen production by MSR reaction in the reformer followed by WGS reaction. The feed streams contain steam and methane from natural gas. Before entering the reformer, both streams were preheated to 730 C using heat exchanger. The MSR reaction products from the reformer was a mixture of CO, H₂, CH₄ and H₂O according to the following reaction:-



Then, the reaction products enters two adiabatic WGS reactors connected in series to increase the hydrogen yield. The first WGS reactor operated at high temperature around 400 C while the latter operated at low temperature around 210 C. The reaction occurred based on the following equation:-



In order to obtain high purity of hydrogen, CO₂ need to be removed from the system. Absorption column is commonly used using MEA as the absorbent with efficiency up to 99%. Then, hydrogen were separated from water using a separator at temperature 25 C to achieve up to 93% purity. The pure hydrogen were then stored in a pressurized tank.

LCA Goal and Scope:

In LCA goal and scope step it is important to define the objective of the analysis, functional unit (FU) and system boundary. The goal of this study is to evaluate the environmental impact of all processes involved in hydrogen production from natural gas. The functional unit (FU) provide a basis for calculating the inputs and outputs. In this work, a common FU of 1 kg of hydrogen produced was selected (Galera & Gutiérrez Ortiz, 2015; Verma & Kumar, 2015). The system boundaries on the other hand, determined the process units to be included within the evaluated system. The system boundaries for this system is shown in Figure 2. It is a cradle-to-grave approach which starts from methane feedstock until hydrogen storage. In detail, the system boundaries consist of five subsystems namely methane feedstock (SB1), hydrogen production (SB2), process steam (SB3), solvent absorption (SB4) and process water plant (SB5). Note that, the construction and commissioning phases as well as energy consumptions were excluded from the analysis and will be our future work.

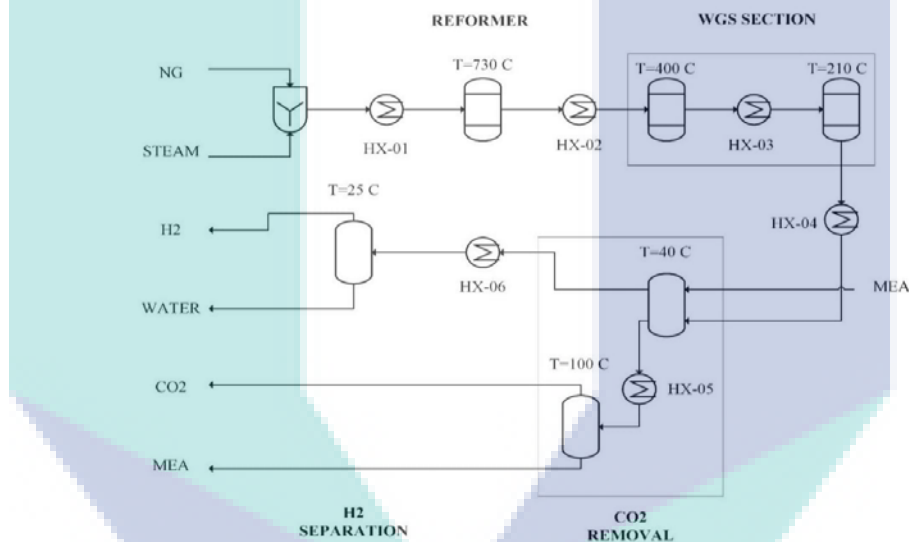


Fig. 1: The simplified flow sheet of hydrogen production by MSR.

For SB, the methane is a product of natural gas processing plant, its associated environmental impact was included in the analysis. However, the transportation of natural gas was assumed using pipeline and thus excludes from the analysis. SB2 consist of reactions and purification section. The reactions system includes a MSR and WGS reactor. In this section, methane reacts with steam to produce hydrogen in a MSR reactor while the gas produced then enters a WGS reactor to convert CO to CO₂ and increase hydrogen yield. The separation section on the other hand, consists of carbon dioxide removal and a separator. The aim of this section is to purify the hydrogen especially from carbon dioxide. The system boundary also considers process steam generation section (SB3). This section considers the combustion of hydrocarbon fuel in the boiler to generate steam which it used during plant operation. Meanwhile, SB4 is the MEA supply subsystem which supply absorbents for CO₂ removal in the separation process. Finally, the water supply for the reforming process and cooling water were came from the process water plant (SB5).

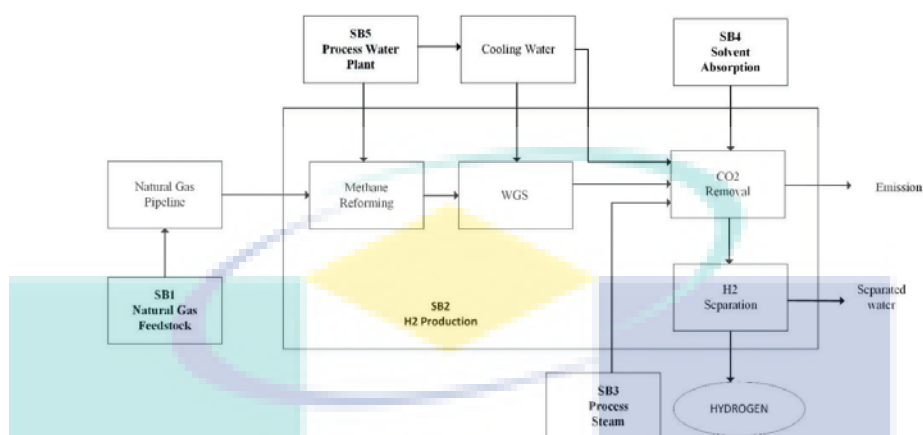


Fig. 2: System boundaries

Life cycle inventory (LCI):

LCI involves the collection and compilation of the data required to quantify all of the relevant inputs and outputs associated with the production of the functional unit (FU). In this study, Aspen Plus software were used to solve the mass and energy balances in hydrogen production from natural gas. The compounds used in this simulation includes hydrogen, carbon dioxide, carbon monoxide, methane, water and monoethanolamine (MEA). Figure 3 shows the flowsheet developed in Aspen Plus 8.6. The global thermodynamic method used in this simulation is electrolyte non-random two-liquid model Redlich Kwong (ENTRL-RK). Whereas, for MSR and WGS reactions the Redlich-Kwong-Soave Modified-Huron-Vidal mixing rule (RKSMHV2) were selected. This method is suitable for the mixture of non-polar and polar compound in combination with light gases. The process flowsheet is shown in Figure 3. For modelling the MSR and WGS reactions, RPLUG reactor block based on LHHW kinetics were selected. Whereas for the separation unit RADFRAC block model were selected for both absorption and stripper unit. Table 1 shows the specification of the models used in the simulation. The stream result summary is shown in the Table 2.

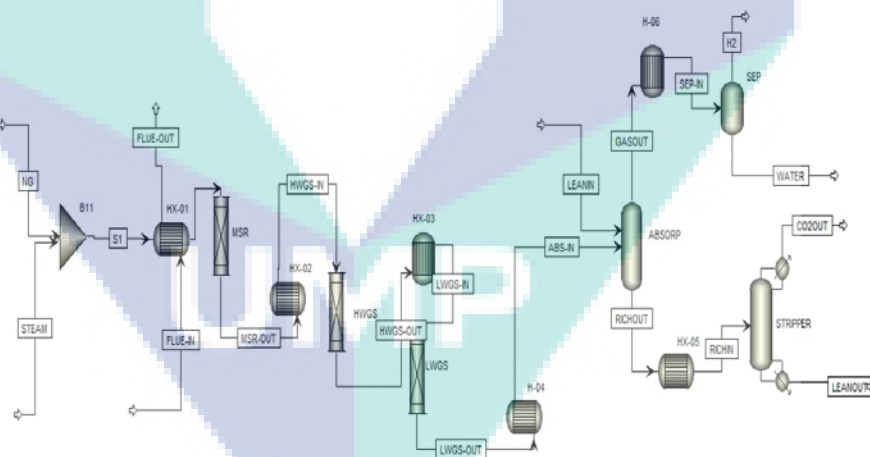


Fig. 3: Hydrogen production from methane flow-sheet in Aspen Plus.

Table 1: Summary of models and utilities used in the simulation.

Code	Equipment	Specification
HX-01	Heat exchanger (Heating)	Cold stream outlet temperature: 730 C Utility: Flue Gas
HX-02	Heat exchanger (Cooling)	Hot stream outlet temperature: 400 C Utility: Cooling water
HX-03	Heat exchanger (Cooling)	Hot stream outlet temperature: 210 C Utility: Cooling water
HX-04	Heat exchanger (Cooling)	Hot stream outlet temperature: 40 C Utility: Cooling water
HX-05	Heat exchanger (Heating)	Cold stream outlet temperature: 105 C Utility: Steam
HX-06	Heat exchanger (Cooling)	Hot stream outlet temperature: 28 C Utility: cooling water
MSR	reforming reactor	Operating temperature: 730 C Isothermal reactor
HWGS	water gas shift reactor	Operating temperature: 400 C RPLUG model block Adiabatic reactor
LWGS	water gas shift reactor	Operating temperature: 210 C RPLUG model block Adiabatic reactor
ABSORP	Absorption column	Number of stages:20 RADFRAC model block Packing size: 4X Packing material: Metal
STRIPPER	Stripper column	Number of stages: 20 RADFRAC model block Reboiler duty :5500 kW
SEP	Separator	Operating temperature: 25 C
Cooling water	Utility	Tin: 20 C / Tout: 40 C Pin: 1 atm / Pout: 1 atm
HP Steam	Utility	Tin: 250 C / Tout: 200 C Pin: 39 bar / Pin: 29 bar
Flue gas	Utility	Tin:1000 C / Tout: 792C Pin: 2 bar / Pout: 2 bar

Life cycle impact assessment (LCIA):

The life cycle impact assessment aims at understanding and evaluating the magnitude and significance of the potential environmental impacts of a product system throughout the life cycle of the product (ISO, 2006). The environmental characterization of the process was carried out based on the following categories; climate change, terrestrial acidification, fossil depletion, freshwater ecotoxicity, marine ecotoxicity, metal depletion, particulate matter, photochemical oxidant formation, water depletion and terrestrial ecotoxicity. The impact potentials were evaluated using ReCiPe whereas the calculation implementation of the inventories was performed in GaBi.

Life Cycle Results Interpretation:

The data obtained from Aspen Plus were used as the main inventory data in GaBi. Table 3 summarize the main inventory data per functional unit of 1 kg hydrogen. Data for background processes such as natural gas or methane, steam and cooling water were taken from the GaBi database. The considered set of environmental impacts potential according to the latest LCIA method, ReCiPe were climate change, terrestrial acidification, fossil depletion, freshwater ecotoxicity, marine ecotoxicity, metal depletion, particulate matter, photochemical oxidant formation, water depletion and terrestrial ecotoxicity. The results offers insights of the subsystems contributions to the environment impacts.

Table 2: Summary of stream results from Aspen Plus.

Mass (kg/hr)	Flow	NG	STEAM	H2	CO2OUT	LEANIN	HWGS-OUT	WATER
MEA	0	0	0	9.13E-05	0.9523	18437.47	0	0.157741
H2O	0	8000	385.21	13281.12	1.10E+05	3423.63	2189.56	
CO2	0	0	503.12	5348.10	0.0441563	4191.89	0.05541	
OH-	0	0	0	0	0.4086	0	4.75E-05	
HCO3-	0	0	0	0	222.19	0	4.1626	
CO3-2	0	0	0	0	265.96	0	0.0345	
MEAH+	0	0	0	0	12156.12	0	4.4052	
MEACOO-	0	0	0	0	19073.73	0	0.1639	
CO	0	0	329.32	0.1330	0	1779.48	1.07E-03	
H2	3.23	0	1259.31	0.5196	0	1155.48	3.34E-03	
CH4	2546.77	0	0	0	0	0	0	

Total Flow	2550.00	8000.00	2476.96	18630.82	160404.00	10550.47	2198.55
------------	---------	---------	---------	----------	-----------	----------	---------

Table 3: Main inventory data for the MSR system per functional unit

INPUT	Value	Unit
Flue gas	2.4	kg
Hydrogen	0	kg
Iron	0.504	kg
Monoethanolamine	14.75	kg
Natural gas	2.04	kg
Nickel	0.128	kg
Steam (MJ)	24.50	MJ
Steam superheated (hp)	6.4	kg
Water	88.20	kg
Water (cooling water)	386	kg
OUTPUT	Value	Unit
Carbon dioxide	5.18	kg
Carbon monoxide	0.2632	kg
Catalysts material	0.632	kg
Flue gas	2.4	kg
Hydrogen	1.00	kg
Monoethanolamine	14.75	kg
Waste water	90.07	kg

RESULTS AND DISCUSSIONS

The result for all environmental impacts potential for each subsystem is shown in the Table 4. Table 4 also shows the specific contribution of each subsystem for all impact categories impacts. Based on Table 4, the climate change category impact is the most significant impact to the environment followed by fossil depletion and water depletion. The other categories have minor environmental impact. The climate change also known as global warming potential (GWP) and resources depletion be worthy of discussions. The climate change quantifies the contribution of gaseous emission from the system to the environmental which include combination of CO₂, CH₄ and N₂O emissions. Figure 4 shows the variation of CO₂ emission in different system boundary. Hydrogen production subsystem contributed the most to climate change with 5.18 kg CO₂-eq per FU. This is because CO₂ was produced in the reactors as a side product. The CO₂ was removed by absorption column and emitted to the atmospheric. This is an agreement with the work by (Galera & Gutiérrez Ortiz, 2015; Hajjaji *et al.*, 2013). Storing the CO₂ into liquid form is an option to reduce the greenhouse emission however it requires extensive energy for CO₂ liquification. Next after hydrogen production system is the process steam subsystem with 3.3 kg CO₂-eq per FU. This comes from burning of fossil fuels to generate high temperature steam. The effect of methane feedstock on climate change impact is low because the methane feedstock comes from natural gas, it contains high purity of methane and no carbon dioxide.

Table 4: Impact categories for each subsystems the hydrogen production from methane

Category	Unit	NG feedstock	Hydrogen production	Process steam	solvent absorption	Process plant	water
Climate change	kg CO ₂ -eq	1.29	5.18	3.3	0	1.48	
Terrestrial Acidification	kg SO ₂ -eq	1.77E-03	0	3.66E-03	0	3.16E-03	
Fossil depletion	kg oil eq	2.694	0	1.403	0	0.505	
freshwater ecotoxicity	kg 1,4-DB eq	0	0	0	0.075	0.005	
marine ecotoxicity	kg N eq	9.30E-04	0	2.07E-03	0	4.66E-04	
metal depletion	kg Fe eq	0.04	0.504	0.002	0	0.007	
Particulate matter	kg PM10	0.000671	0	0.001416	0	1.07E03	
Photochemical oxidant formation	kg NMVOC	0.003	0.012	0.006	0	0.003	
Water depletion	m ³	0.03	0.09	0.28	0	3.81	
Terrestrial ecotoxicity	kg 1,4-DB eq	0	0	0	0.212	0	

Water depletion is defined as the net reduction in the availability of freshwater in a watershed for a given time period. Water depletion also reduces the water availability for current users and generating competition for the water resources. The water depletion can reduce resources availability for future generation and the intensity of the competition for freshwater will potentially increase. Based on water depletion impact in Figure 4, the process water plant subsystem contributes the most to water depletion impact categories compared to the other subsystem. This is obvious since water were used as a raw material to generate steam and also used as cooling water.

For consumption of fossil resources from Figure 4, it shows the natural gas feedstock contributes the most for fossil depletion impact category followed by steam production. This is expected since natural gas is a type of fossil fuel. The natural gas was used as feedstock in hydrogen production to react with steam and produce the

hydrogen. In process steam, the natural gas was used as raw material to generate the steam to transfer the heat energy for heating in the system. So, the used fossil fuel as a raw material is giving the impact to fossil resources and it possible to happened the reduction of availability of fossil resource in the future. The future generation will be competing to get the fossil resource caused by the fossil depletion.

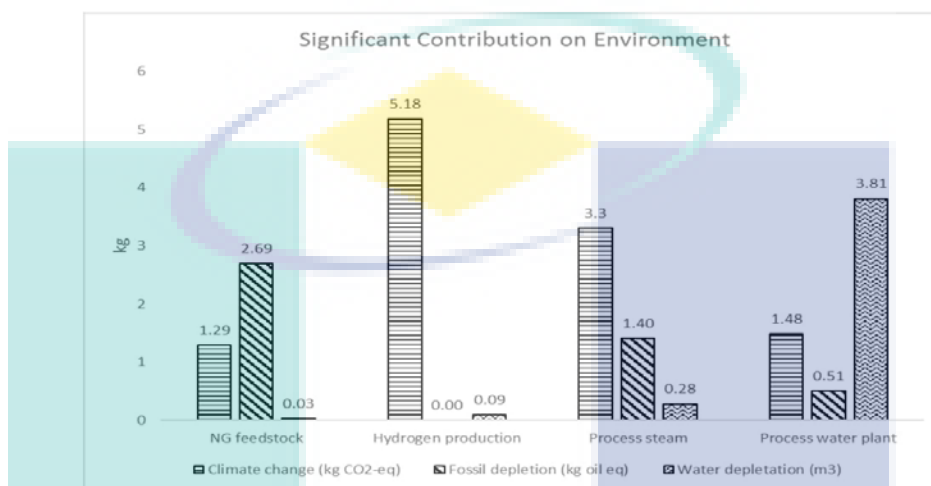


Fig. 4: Environmental impact results for the most significant impact category

Conclusion:

This work presents a life cycle assessment of a simulated hydrogen production from natural gas. Simulated model provide a detail and extensive data for conducting life cycle impact assessment. From the results obtained, the hydrogen production subsystem contributes the most to climate change impact category. Meanwhile, process water plant subsystem and natural gas feedstock subsystem contributes the most to water depletion and natural fossil depletion impact category respectively. The other impact categories just the minor significant in the environment impact. The life cycle approach is an excellent tool which can help identifying subsystems that contribute to the potential impacts attributes. Moreover, LCA could help to make decisions and improve process in reducing its impact to the environment.

ACKNOWLEDGEMENT

Financial support for this work was in part provided by LRGS 4L817 for which the authors are thankful.

REFERENCES

- Consultants, P., 2016. Contribution to impact assessment research. from www.pre-sustainability.com/contribution-to-impact-assessment-research
- Dufour, J., D.P. Serrano, J.L. Galvez, A. Gonzalez, E. Soria and J.L.G. Fierro, 2012. Life cycle assessment of alternatives for hydrogen production from renewable and fossil sources. *International Journal of Hydrogen Energy*, 37(2): 1173-1183, doi: 10.1016/j.ijhydene.2011.09.135
- Dufour, J., D.P. Serrano, J.L. Gálvez, J. Moreno and A. González, 2011. Hydrogen Production from Fossil Fuels: Life Cycle Assessment of Technologies with Low Greenhouse Gas Emissions. *Energy & Fuels*, 25(5): 2194-2202. doi: 10.1021/ef200124d
- Galera, S., and F.J. Gutiérrez Ortiz, 2015. Life cycle assessment of hydrogen and power production by supercritical water reforming of glycerol. *Energy Conversion and Management*, 96: 637-645. doi: 10.1016/j.enconman.2015.03.031
- Hajjaji, N., M.N. Pons, V. Renaudin and A. Houas, 2013. Comparative life cycle assessment of eight alternatives for hydrogen production from renewable and fossil feedstock. *Journal of Cleaner Production*, 44: 177-189. doi: 10.1016/j.jclepro.2012.11.043
- ISO., 2006. Environmental Management-life cycle assessment-requirements and guidelines. Geneva: International Organization for Standardization.

Kalinci, Y., A. Hepbasli and I. Dincer, 2012. Life cycle assessment of hydrogen production from biomass gasification systems. *International Journal of Hydrogen Energy*, 37(19): 14026-14039. doi: 10.1016/j.ijhydene.2012.06.015

Lee, J.-Y., S. An, K. Cha and T. Hur, 2010. Life cycle environmental and economic analyses of a hydrogen station with wind energy. *International Journal of Hydrogen Energy*, 35(6): 2213-2225. doi: 10.1016/j.ijhydene.2009.12.082

Tonini, D. and T. Astrup, 2012. LCA of biomass-based energy systems: A case study for Denmark. *Applied Energy*, 99: 234-246. doi: 10.1016/j.apenergy.2012.03.006

Tugnoli, A., G. Landucci and V. Cozzani, 2008. Sustainability assessment of hydrogen production by steam reforming. *International Journal of Hydrogen Energy*, 33(16): 4345-4357. doi: 10.1016/j.ijhydene.2008.06.011

Verma, A. and A. Kumar, 2015. Life cycle assessment of hydrogen production from underground coal gasification. *Applied Energy*, 147: 556-568. doi: 10.1016/j.apenergy.2015.03.009

